

**Detection of Cyanox®53 within surface sediments
and the microplastic biomonitor, *Nuttallia obscurata*,
dwelling in Burrard Inlet, British Columbia:
implications for toxicity**

by
Stephanie Renkers

B. Sc. (Biology), University of the Fraser Valley, 2019

Project Submitted in Partial Fulfillment of the
Requirements for the Degree of
Master of Environmental Toxicology

in the
Department of Biological Sciences
Faculty of Science

© Stephanie Renkers 2022
SIMON FRASER UNIVERSITY
Summer 2022

Copyright in this work is held by the author. Please ensure that any reproduction or re-use is done in accordance with the relevant national copyright legislation.

Declaration of Committee

Name: **Stephanie Renkers**
Degree: **Master of Environmental Toxicology**
Title: **Detection of Cyanox®53 within surface sediments and the microplastic biomonitor, *Nuttallia obscurata*, dwelling in Burrard Inlet, British Columbia: implications for toxicity**

Committee: **Chair: Gerhard Gries**
Professor, Biological Sciences

Leah Bendell
Supervisor
Professor, Biological Sciences

Isabelle Côté
Committee Member
Professor, Biological Sciences

Curtis Eickhoff
Committee Member
Adjunct Professor, Biological Sciences

Juan José Alava
Examiner
Adjunct Professor, Resource & Environmental Management

Abstract

The minuscule nature of microplastics results in their uptake in many aquatic species, leading to the risk of physiological damage and exposure to toxic additives and anthropogenic pollutants not irreversibly bound to the polymer matrix. Cyanox®53 presents a unique case as it not only can function as an additive but also as a physical particle. Though recent surveys have documented its presence in the environment, significant gaps in knowledge concerning Cyanox®53 remain in the literature. Hence, the purpose of this study was to investigate the abundance and distribution of Cyanox®53 from seven beaches throughout Burrard Inlet, British Columbia, and to explore its toxicological implications via QSAR modelling. Particle concentrations of Cyanox®53 and microplastics were recovered following survey samplings of surface sediments and varnish clams. Model simulation based on a feasible structure predicted Cyanox®53 to be a persistent chemical unlikely to bioaccumulate; however, it was inconclusive if it could elicit toxicity.

Keywords: Cyanox®53; microplastics; Burrard Inlet; varnish clams; sediment; QSAR modelling

Dedication

I dedicate this thesis to my Dad.

Not a day goes by that I don't miss you and wish you were here. I treasure the memories I shared with you and will be forever grateful for the life you provided me. The sacrifices you made and the lessons you instilled in me will never be forgotten.

Love you always

Acknowledgements

The completion of this MET project could not have been possible without the support, assistance, or contribution of so many people. First and foremost, I want to thank my supervisor Dr. Leah Bendell for giving me the opportunity to work on such an interesting project. I am so grateful for all the supportive encouragement, reassurance, and guidance you provided me throughout this research experience. To Dr. Isabelle Côté and Dr. Curtis Eickhoff, your professional insights, approachability, and constant encouragement kept me motivated and gave me reassurance whenever doubt surfaced. I am very grateful to have had both of your support. It was such a pleasure and honour to have had all of you as my mentors.

I am also thankful to Wen Zhou for his great contribution and advisement in the FTIR analysis, and to Eric Ye and Shane Hamype who performed the nuclear magnetic resonance spectroscopy and mass spectrometry testing for this research. Moreover, I would like to acknowledge the funding support of the Natural Sciences and Engineering Research Council of Canada.

To my fellow MET cohorts, thank you all for being supportive and positive, and for all the good memories during this wild academic journey. The friendships I have made with each of you will be lasting and I look forward to working with you in the future.

Finally, I would like to thank my Mom and siblings, Hailee and Ryan, for supporting me with love and understanding in the best and worst times. Their endless patience and unwavering encouragement throughout this entire process kept me motivated and balanced when I truly needed it. Without them, I would not be the person I am today nor would I have accomplished what I have thus far, and for those reasons they have played a pivotal role in both my personal growth and academic achievements.

Table of Contents

| | |
|--|-----------|
| Declaration of Committee | ii |
| Abstract | iii |
| Dedication | iv |
| Acknowledgements | v |
| Table of Contents | vi |
| List of Tables | viii |
| List of Figures | ix |
| List of Acronyms | xii |
| 1. Introduction | 0 |
| 1.1. Plastics | 0 |
| 1.2. Environmental Impact of Plastics | 0 |
| 1.3. Microplastics | 3 |
| 1.4. Adverse Effects of Microplastics on Aquatic Wildlife | 4 |
| 1.5. Cyanox®53 | 6 |
| 1.6. Polymer Analysis Techniques | 7 |
| 1.7. Research Objectives | 9 |
| 2. Materials & Methods | 11 |
| 2.1. Study Sites | 11 |
| 2.2. Sediment Analysis | 13 |
| 2.2.1. Sample Collection and Preparation | 13 |
| 2.2.2. Nile Red Fluorescent Tagging of Particles | 13 |
| 2.2.3. Density Separation of Particles | 14 |
| 2.3. Bivalve Analysis | 14 |
| 2.3.1. Sample Collection and Preparation | 14 |
| 2.3.2. Staining and Isolation of Particles | 14 |
| 2.4. Filtrate Inspection and ATR-FTIR | 15 |
| 2.5. Statistical Analyses | 16 |
| 2.6. Molecular Structure Identification of Cyanox®53 Particles | 17 |
| 2.6.1. Single-Batch Equilibrium Leaching | 17 |
| 2.6.2. ¹ H-NMR and ESI-LC/MS | 17 |
| 2.7. QSAR Modelling | 18 |
| 2.8. Quality Assurance and Contamination Control | 19 |
| 3. Results | 20 |
| 3.1. Abundance and Distribution of Particles | 20 |
| 3.1.1. Microplastics in Sediment | 20 |
| 3.1.2. Cyanox®53 in Sediment | 22 |
| 3.1.3. Bivalve Biometric Data | 24 |
| 3.1.4. Microplastics in Bivalves | 26 |
| 3.1.5. Cyanox®53 in Bivalves | 28 |

| | | |
|-----------|---|-----------|
| 3.1.6. | Biota-Sediment Accumulation Factor Ratios | 30 |
| 3.2. | ATR-FTIR, ESI-LC/MS, and ¹ H-NMR..... | 30 |
| 3.2.1. | ATR-FTIR..... | 30 |
| 3.2.2. | ESI-LC/MS..... | 32 |
| 3.2.3. | ¹ H-NMR..... | 34 |
| 3.3. | Structure and QSAR Modelling..... | 37 |
| 3.3.1. | Proposed Molecular Structure | 37 |
| 3.3.2. | EPI Suite™..... | 38 |
| 3.3.3. | Toxtree..... | 39 |
| 4. | Discussion | 42 |
| 4.1. | Environmental Survey and Potential Sources | 42 |
| 4.1.1. | Cyanox®53 Concentrations | 42 |
| 4.1.2. | Potential Source(s) of Cyanox®53 | 44 |
| 4.1.3. | Microplastic Concentrations | 45 |
| 4.2. | Compound Identification | 46 |
| 4.3. | Persistence, Bioaccumulation, and Toxicity Predictions..... | 48 |
| 4.3.1. | Persistence | 48 |
| 4.3.2. | Bioaccumulation and Biomagnification | 49 |
| 4.3.3. | Toxicity..... | 50 |
| 4.3.4. | EPI Suite™ and Toxtree Model Limitations | 52 |
| 4.4. | Conclusions..... | 54 |
| | References..... | 56 |
| | Appendix A | 72 |
| | Sediment Analysis Data | 72 |
| | Appendix B | 73 |
| | Bivalve Analysis Data..... | 73 |
| | Appendix C | 76 |
| | Reference Spectra for Comparison | 76 |

List of Tables

| | | |
|-------------------|---|-----------|
| Table 2.1. | Characteristics and GPS coordinates for the seven intertidal study sites found in Burrard Inlet. | 12 |
| Table 3.1 | Biota-Sediment Accumulation Factor ratios based on mean microplastic and Cyanox®53 concentrations recovered from bivalves and sediment sampled at seven intertidal regions in Burrard Inlet. | 30 |
| Table 3.2 | ATR-FTIR sorption peaks of Cyanox®53 based on leached Cyanox®53 and Cyanox®53-PVDF samples. | 32 |
| Table 3.3 | ¹H-NMR measurements and structural assignment of Bisphenol A, Cyanox®2246, Cyanox®425, and Cyanox®53. For each chemical, the notation, shift (ppm), integral label, hydrogen type and visual assignments are provided. | 36 |
| Table 3.4 | Comprehensive summary of estimated physiochemical, ecotoxicity and relative hazard properties of Cyanox®53 via QSAR modelling. | 40 |

List of Figures

- Figure 2.1.** Locations of seven designated sampling sites in Burrard Inlet, BC involved in surface sediment and varnish clam (*Nutallia obscurata*) collections for environmental survey. Purple markers indicate sampling sites at Ambleside Park Beach (AP), Barnet Marine Park Beach (BMP), Cates Park Beach (CP), English Bay Beach (EB), Jericho Beach (J), Spanish Banks Beach (SB), and Third Beach (TB). Map courtesy of the U.S. Geological Survey (USGS, 2022)..... 11
- Figure 3.1** Microplastic concentrations recovered from surface sediment sampled at seven intertidal sites in Burrard Inlet. Boxplots demonstrating the median values (thick horizontal black line within box) and the lower and upper 25th and 75th percentiles (upper and lower boundaries of box) are presented. A total of N = 21 replicates were analyzed (n = 3 sample size per site). Sites (left to right): Ambleside Park (AP), Barnet Marine Park (BMP), Cates Park (CP), English Bay (EB), Jericho Beach (J), Spanish Banks (SB), and Third Beach (TB). A One-Way ANOVA followed by Tukey’s HSD post-hoc analysis was used to determine significant difference between particles concentrations (particles/kg dw) across the sites. No significant difference between the sites (p = 0.124) was observed. 21
- Figure 3.2** Cyanox®53 concentrations recovered from surface sediment sampled at seven intertidal sites in Burrard Inlet. Boxplots demonstrating the median values (thick horizontal black line within box), and the lower and upper 25th and 75th percentiles (upper and lower boundaries of box) are presented. A total of N = 21 replicates were analyzed (n = 3 sample size per site). Sites (left to right): Ambleside Park (AP), Barnet Marine Park (BMP), Cates Park (CP), English Bay (EB), Jericho Beach (J), Spanish Banks (SB), and Third Beach (TB). A Kruskal-Wallis followed by Steel-Dwass post-hoc analysis was used to determine significant difference between particles concentrations (particles/kg dw) across the sites. No significant difference between the sites (*chi-squared* = 5.84, df = 6, p = 0.442) was observed..... 23
- Figure 3.3** Relationship of wet tissue weight (g) to shell volume (cm³) of *Nutallia obscurata* sampled at seven intertidal sites in Burrard Inlet. Linear mixed-effects model demonstrating linear regressions (coloured lines), fitted confidence regions (transparent shading beneath regression lines), and plotted individuals (colourful dots) from each site are presented. A total of N = 175 bivalves were collected at a sample size of n = 25 per site. Sites: AP (pink), BMP (orange), CP (green), EB (blue), J (purple), SB (gold), and TB (red). The following linear equations and r² values were obtained for each site: AP (wet tissue weight = 0.027*shell volume + 0.050, r² = 0.89); BMP (wet tissue weight = 0.025*shell volume + 1.4, r² = 0.75); CP (wet tissue weight =

0.035*shell volume - 0.90, $r^2 = 0.91$); EB (wet tissue weight = 0.025*shell volume + 0.93, $r^2 = 0.87$); J (wet tissue weight = 0.028*shell volume + 0.69, $r^2 = 0.96$); SB (wet tissue weight = 0.0092*shell volume + 4.7, $r^2 = 0.09$); and TB (wet tissue weight = 0.024*shell volume + 0.98, $r^2 = 0.84$). 25

Figure 3.4 Microplastic concentrations recovered from *Nutallia obscurata* sampled at seven intertidal sites in Burrard Inlet. Boxplots demonstrating the median values (thick horizontal black line within box), the lower and upper 25th and 75th percentiles (upper and lower boundaries of box), the minimum and maximum values (whiskers) and any outliers (black dots) are presented. A total of N = 175 bivalves were collected at a sample size of n = 25 per site. Sites (left to right): Ambleside Park (AP), Barnet Marine Park (BMP), Cates Park (CP), English Bay (EB), Jericho Beach (J), Spanish Banks (SB), and Third Beach (TB). A Kruskal-Wallis followed by Steel-Dwass post-hoc analysis was used to determine significant difference between particles concentrations (particles/g ww) across the sites. A significant effect between the sites (*chi-squared* = 35.8, df = 6, p < 0.0001) was observed. Different superscript letters indicate significant differences (p < 0.05). 27

Figure 3.5 Cyanox®53 concentrations recovered from *Nutallia obscurata* sampled at seven intertidal sites in Burrard Inlet. Boxplots demonstrating the median values (thick horizontal black line within box), the lower and upper 25th and 75th percentiles (upper and lower boundaries of box), the minimum and maximum values (whiskers) and any outliers (black dots) are presented. Note the break indicated by slashed lines on the y axis. A total of N = 175 bivalves were collected at a sample size of n = 25 per site. Sites (left to right): Ambleside Park (AP), Barnet Marine Park (BMP), Cates Park (CP), English Bay (EB), Jericho Beach (J), Spanish Banks (SB), and Third Beach (TB). A Kruskal-Wallis followed by Steel-Dwass post-hoc analysis was used to determine significant difference between particles concentrations (particles/g ww) across the sites. A significant effect between the sites (*chi-squared* = 40.7, df = 6, p < 0.0001) was observed. Different superscript letters indicate significant differences (p < 0.05). 29

Figure 3.6 Fragments recovered from Burrard Inlet along with their matching ATR-FTIR spectra. (a) Cyanox®53, (b) Cyanox®53-PVDF, and (c) Cyanox®53-PE. Absorption band intensities in the ATR-FTIR spectra were measured based on transmittance (%) against wavenumbers (cm^{-1}) between 4000 cm^{-1} to 450 cm^{-1} 31

Figure 3.7 ESI-LC/MS spectra of leached Cyanox®53 fragments. (a) Cyanox®53 and (b) Cyanox®53-PVDF. ESI-LC/MS intensities were measured in positive ion mode against retention time (min) and m/z values (Da). Most relevant ion intensities are shown at retention times 7.14 for (a) Cyanox®53, and 7.16 for (b) Cyanox®53-PVDF. 33

Figure 3.8 $^1\text{H-NMR}$ spectra of leached Cyanox®53 fragments. (a) Cyanox®53 and (b) Cyanox®53-PVDF. Proton peaks are measured based on intensity (ranging from 0 to 380) against chemical shift values (ppm) between 0.5 and 8.75 ppm. 35

Figure 3.9 Proposed molecular structure of Cyanox®53. Two-dimensional (top) and three-dimensional (bottom). 37

List of Acronyms

| | |
|------------------|--|
| ABS | Acrylonitrile Butadiene Styrene |
| ANOVA | Analysis of Variance |
| AP | Ambleside Park Beach |
| ATR-FTIR | Attenuated Total Reflectance-Fourier Transform Infrared Spectroscopy |
| BAF | Bioaccumulation Factor |
| BC | British Columbia |
| BCF | Bioconcentration Factor |
| BMP | Barnet Marine Park Beach |
| BPA | Bisphenol A |
| BSAF | Biota-Sediment Accumulation Factor |
| CP | Cates Park Beach |
| EB | English Bay Beach |
| EC ₅₀ | Effective Concentration (50%) |
| ECOSAR | Ecological Structure Activity Relationships |
| EPI Suite | Estimation Program Interface Suite |
| ESI-LC/MS | Electrospray Ionization-Liquid Chromatography/Mass Spectrometry |
| FTIR | Fourier Transform Infrared Spectroscopy |
| HDPE | High Density Polyethylene |
| HSD | Honesty Significance Difference |
| J | Jericho Beach |
| LC ₅₀ | Lethal Concentration (50%) |
| LDPE | Low Density Polyethylene |
| K _{oc} | Organic Carbon to Water Partition coefficient |
| K _{ow} | Octanol-Water Partition Coefficient |
| MOA | Mode of Action |
| MS | Mass Spectrometry |
| NES | No Effects at Saturation |
| NMR | Nuclear Magnetic Resonance |
| PE | Polyethylene |

| | |
|--------------------|--|
| PETE | Polyethylene Terephthalate |
| POPs | Persistent Organic Pollutants |
| PP | Polypropylene |
| PS | Polystyrene |
| PVC | Polyvinyl Chloride |
| PVDF | Polyvinylidene Fluoride |
| ¹ H-NMR | Proton Nuclear Magnetic Resonance |
| QSAR | Quantitative Structure-Activity Relationship |
| SB | Spanish Banks Beach |
| SMILE | Simplified Molecular Input Line Entry System |
| TB | Third Beach |
| TTC | Threshold of Toxicological Concern |
| XPS | Extruded Polystyrene |

1. Introduction

1.1. Plastics

Synthetic organic polymers, commonly known as plastics, have become a ubiquitous and integral part of modern society, replacing many conventional materials such as wood, glass, and metal (Bridson et al., 2021, Crawford & Quinn, 2019). The dramatic rise in plastics as a manufacturing material undoubtedly stems from their performance characteristics, namely the chemical properties within. By design, plastics are lightweight, strong, durable, biochemically inert, resistant to corrosion, and provide high thermal/electrical insulation (Andrady & Neal, 2009; Andrady, 2011; American Chemistry Council, 2021). In addition, their high versatility and ability to be moulded into specific constructs reduces manufacturing time and costs by many orders of magnitude, making plastics more desirable over traditional materials (Crawford & Quinn, 2019). It is because of these qualities that plastics are used in a variety of industries and applications, including packaging, textiles and clothing, household and consumer products, electrical goods and electronics, building and construction, automotive, aerospace and marine transportation, agriculture, medical and healthcare equipment, in the military, and in sport and leisure activities (American Chemistry Council, 2021; Crawford & Quinn, 2019; British Plastic Federation, 2021). Clearly, plastics constitute as a keystone component in almost all aspects of daily life. Some examples of commonly used plastics include polyethylene (PE), polypropylene (PP), polystyrene (PS), polyvinyl chloride (PVC), acrylonitrile butadiene styrene (ABS) and polyethylene terephthalate (PETE) (Geyer et al., 2017; UNEP, 2018; Gibb, 2019)

1.2. Environmental Impact of Plastics

Despite offering many benefits to society, plastics also possess a considerable number of drawbacks. For one, ironically the very physiochemical properties that make plastics an ideal manufacturing material, such as high strength and durability, also impede their degradation process and consequently extend their persistence in the environment (Crawford & Quinn, 2019). Indeed, while some plastics are soft and brittle (e.g., PE) and deteriorate readily over time, others are naturally strong (e.g., PETE) and have a lower likelihood of degrading, thereby causing them to persist longer in the

environment (Crawford & Quinn, 2019). It is because of this inability to degrade readily that plastics have become archeological markers of the anthropogenic footprint on Earth at unparalleled levels, and part of the pervasive burden of global pollutants affecting the planet's ocean (Reed, 2015; Haram et al., 2020; UNEP, 2021). Global plastic production currently exceeds 290 million tons annually and is anticipated to reach 33 billion tons by 2050 at the present rate (Luan et al., 2019; Crawford & Quinn, 2019). This increase in production and use of non-reusable plastics is unavoidably accompanied by an increase in waste, and deductively creates a challenge for waste management (Rochman, 2015). In fact, of all municipal waste generated globally, approximately 16% is made up of plastic materials alone (Crawford & Quinn, 2019). To combat this issue, many countries have adopted recycling practices as a waste management strategy. Ideally, high levels of recycling, along with repurposing and less use, help reduce plastic pollution and natural resource depletion, ease the demand on fossil fuel consumption, and decreases the energy and material usage per unit of output to ultimately yield improved eco-efficiency (Hopewell et al., 2009; Lawson, 2018). Advancements in waste management technology have also made it relatively easy to collect and control the amount of plastic waste being released into the environment, yet only a small proportion of plastics are properly recycled as it proves rather difficult to maintain efficient collection schemes and proper waste management facilities in municipalities (Gallo et al., 2018). Even in Canada, which is one of the wealthiest nations with a relatively small population, only about 9% of plastic waste is recycled (Young, 2021). To make matters worse, in some countries legislation for recycling plastics is not even enforced, in which case plastic waste is primarily handled through incineration. This method is unfavourable, however, as burning plastic materials releases highly toxic chemicals, such as furans and dioxins, that are detrimental to both humans and the environment alike (Crawford & Quinn, 2019). Alternatively, less destructive processes like bioremediation, which uses microorganisms to enzymatically convert plastics into a comparably less toxic or nontoxic product, have been employed to counteract the growing abundance of plastic waste (Sharma et al., 2017). Unlike incineration, bioremediation is significantly safer, less labour-intensive, requires minimal equipment, can be implemented as an in-situ or ex-situ method, and overall, more economical (Aliotta & Colley, 2013; Bose, 2021). All the same, bioremediation tends to be a sensitive process easily influenced by its environmental conditions. That is, for bioremediation to function effectively, no growth inhibitors can be present and optimal conditions (i.e., nutrients, enzymes, temperature,

pH, and pressure) must be met to promote microorganism growth and biological activity (Sheth et al., 2019; Evode et al., 2021). Consideration of which bacteria or fungi are most suitable to break down the targeted plastic waste must also be taken since the biotic degradation rate of the polymer, and therefore its final fate, is determined by the chemical composition within the plastic (Sheth et al., 2019; Ali et al., 2021). For these reasons, landfills have become the preferred “dumping grounds” for most plastics due to being a cheaper and easier choice than other methods. Canada has regrettably succumbed to this form of disposal where it is estimated that around 86% of plastic wastes are carelessly dumped into landfills nationwide (Young, 2021).

The presence of plastics in terrestrial and aquatic ecosystems is inevitable, fueled by mismanagement and insufficient plastic waste collection schemes, and the continued high demands for plastics production to satisfy consumer needs. Around 80-90% of land-based plastic wastes are transported to the ocean by wind, water currents, urban run-offs, improper disposal (i.e., dumping or littering) and/or insufficient waste management (Espinosa et al., 2016; Gallo et al., 2018; Crawford & Quinn, 2019; UNEP, 2021). In fact, it is estimated that over 8 million tons enters the ocean every year (Jambeck et al., 2015; Gallo et al., 2018). Besides land-based sources, a significant contribution of marine debris can be attributed to the fishery and aquaculture industries (Andrady, 2011; Gallo et al., 2018). Each year more than 640,000 tons of plastic nets, lines, pots and traps used in commercial fishing fleets are invariably lost or discarded into the sea (Laville, 2019). Coupled with the marine litter released by recreational and commercial ships and vessels, as well as changing demographics favouring immigration to coastal regions, it is unsurprising that an increase in the influx of plastic waste entering the ocean has occurred over recent decades (Andrady, 2011). Some seabirds, such as fulmars (*Fulmarus glacialis*), have even been observed to reshape and redistribute microplastics unintentionally via egestion, and thus contribute to the load of plastic waste released into the marine environment (van Franeker & Meijboom, 2002; Gallo et al., 2018). Examples of common plastic debris dispersed in the ocean and nearby shorelines include fishing gear, agricultural plastics, bottles, bags, food packaging, lids, straws, cigarette butts, virgin resin pellets, macroplastics and microplastics (Gallo et al., 2018). Ultimately these landfilled or discarded plastic materials end up either sinking into the subtidal sediments and/or deep seabed, floating along the ocean currents and upper water column surface, or washing up on coastline

beaches and becoming embedded in the surface sediments. Consequently, plastic debris now can be found in all major oceanic gyres, polar seas and ice, and even in the deepest parts of the ocean like the Mariana Trench (Erni-Cassola et al., 2019; Zhang et al., 2019).

1.3. Microplastics

Microplastics are characterized as any plastic particle < 5 mm in diameter (Hermabessiere et al., 2017; Thompson, 2015; Crawford & Quinn, 2019; National Geographic Society, 2019; Bendell et al., 2020). In the aquatic environment, microplastics present in all manners of shapes, sizes, and colours with some possessing a bead-like appearance, while others manifest in a fibrous, foam or a fragmented form. Indeed, it is because of their minuscule size and varying colours that microplastics are also colloquially referred to as 'mermaid tears' (Costa et al., 2017). Depending on their source, microplastics are classified either as primary or secondary. Primary microplastics, which correspond to particles purposely manufactured to be microscopic in size and used to produce macroplastics, are found in industrial abrasives (e.g., sand-blasting media), preproduction plastic pellets, household items (e.g., cleaning agents), textiles, personal hygiene products (e.g., toothpaste) and dermal exfoliants (e.g., facial cleansers), cosmetics (e.g., microbeads), and, to an extent not yet realized, in medicine, namely as drug vectors (Baztan et al., 2017; Costa et al., 2017; Hermabessiere et al., 2017). Conventionally, primary microplastics will have a manufactured appearance and therefore exhibit a spherical or fibrous shape with a smooth exterior (Crawford & Quinn, 2019). By contrast, secondary microplastics emerge when macroplastics experience a loss in their structural integrity (i.e., from abiotic and biotic processes), leading to fragmentation (Costa et al., 2017). Hence, secondary microplastics include any small, irregularly shaped fragments that have partitioned from macroplastic degradation, such as plastic bags, crates, bottles, ropes, and fishing nets (Costa et al., 2017; Hermabessiere et al., 2017; Crawford & Quinn, 2019). Of the two types, secondary microplastics tend to be the more common form in the marine environment, with fibers from synthetic clothing, tire remnants, fish netting and other single use plastics being the largest contributors (DFO, 2021).

1.4. Adverse Effects of Microplastics on Aquatic Wildlife

Regardless of the source, albeit noteworthy, both primary and secondary microplastics are now acknowledged as one of the greatest challenges marine environments presently face. Many aquatic organisms end up ingesting microplastics as food, either from not possessing a feeding mechanism capable of discriminating between prey and anthropogenic material, mistaking the microplastic as planktonic prey, or from ingesting prey containing microplastics, indirectly (i.e., trophic transfer) (Moore, 2008; Lusher, 2015; Gallo et al., 2018; Luan et al., 2019; Alava, 2020; Mahara et al. 2022). In some species, like shore crabs (*Carcinus maenas*) and blue mussels (*Mytilus edulis* L.), microplastics can also be drawn into the body via gill cavity inhalation (Browne et al., 2008; van Moos et al., 2012; Watts et al., 2014; Lusher, 2015; Miller et al., 2017; Gallo et al., 2018). In effect, uptake of microplastics through different mechanisms has been documented in more than 300 marine species, including zooplankton, benthic invertebrates, fish, sea reptiles, seabirds, and marine mammals (Gallo et al., 2018; Luan et al., 2019; Alava, 2020; Savoca et al., 2021). Because there are no metabolic pathways specific to synthetic polymer breakdown in most aquatic organisms, the assimilation of microplastics can inflict a variety of adverse physical effects, depending on the size, shape, volume, density, roughness, polymer composition and additive/associated chemicals, and leaching pollutants. Adverse effects include gut obstruction and ulcerative lesions; weight loss from decreased food and nutrient intake; reduced respiration rates from microplastic entrapment in the gills; interference with other tissues or organs (i.e., lysosomal, circulatory, hemolymph) via translocation; impaired development, metabolic parameters, or cellular function; reduced mobility, brain function and fecundity; or reduced life expectancy (Browne et al., 2008; Teuten et al., 2009; Andrady, 2011; Besseling et al., 2013; Lambert et al., 2013; Wright et al., 2013b; Costa et al., 2017; Law, 2017; Nelms et al., 2019; Hale et al., 2020). Additionally, microplastics bring the risk of exposing aquatic organisms to toxic chemicals associated with the plastic (Koelmans et al., 2014; Espinosa et al., 2016; Adam et al., 2019).

Though plastic polymers are regarded as biochemically inert due to their large molecular size, hazardous non-polymeric substances, such as unreacted residual monomers, oligomers, low molecular weight polymer fragments, catalyst remnants, polymerization solvents, and various chemical additives (e.g., flame retardants,

plasticizers, antioxidants, ultraviolet radiation stabilizers, pigments, etc.) are intentionally incorporated during processing to enhance the inherent properties and prevent 'aging' of the plastic (Lithner et al., 2011; Olabisi & Adewale, 2016; Gallo et al., 2018). In most instances, these substances are of low molecular weight, and are either weakly or not completely bound to the polymer matrix (OECD, 2004; Lithner et al., 2011). This increases their likelihood of leaching out of the plastic and into the surrounding medium until the appropriate octanol/water partition coefficient (K_{ow}) is reached (Andrady, 2011). Moreover, it is rare and quite unlikely for organisms to be exposed to only one chemical in isolation, raising the prospect of co-contaminants interacting with one another and potentially inducing additive or synergistic effects (Rochman, 2015; Baztan et al., 2017). For instance, persistent organic pollutants (POPs), such as alkylbenzenes, organochlorinated compounds, and polychlorinated biphenyls, as well as polycyclic aromatic hydrocarbons (PAHs) and inorganic contaminants like silver, titanium dioxide nanoparticles, barium, sulphur, and zinc from the environment have been known to absorb or concentrate in microplastics (Teuten et al., 2009; Andrady, 2011; Fries et al., 2013; Khan et al., 2015). Once released from the polymer matrix, such contaminants can become absorbed within an organism, and may consequently provoke changes in molecular and cellular pathways, inhibit growth, delay maturity, induce morphological deformations, affect mobility, and in some cases, cause death (Lambert et al., 2013; Costa et al., 2017). Since many additives and POPs are lipophilic, they also have the potential to diffuse across cell membranes and subsequently become involved in biochemical reactions (Costa et al., 2017). Ultimately, this can result in severe behavioural effects and reproductive consequences (Costa et al., 2017; Crawford & Quinn, 2019).

Commercially important plasticizers (e.g., dibutyl phthalate), or trace monomers in plastics, such as bisphenol A (BPA) and alkylphenols, have also been shown to readily leach out of microplastics, become absorbed, and disrupt endocrine functionality of exposed organisms (Carlisle et al., 2009; ECHA, 2014; ECCO, 2018; Gallo et al., 2018). In sensitive species, such as molluscs, crustaceans, amphibians, and fish, chronic interference of the endocrine system from plasticizers even at low concentrations (i.e., ng/L or µg/L range) can inflict developmental and reproductive impairments (Koelmans et al., 2014; Plahuta et al., 2014; Gallo et al., 2018). Comparably, other additives like phthalates, chlorinated paraffins, and brominated flame

retardants have also been acknowledged as endocrine disruptors, carcinogenic, mutagenic, and toxic to reproduction in different aquatic species (Lithner et al., 2011; Bridson et al., 2021). Even some synthetic phenolic antioxidants and related transformation products, which are normally used to impede oxidative reactions and extend plastic shelf-life, can exert hepatic toxicity, endocrine disrupting effects, and carcinogenicity (Liu & Mabury, 2020). In this respect, the likelihood of organisms suffering adverse toxicological effects following chronic intake of microplastics becomes probable as microplastics not only constitute a physical obstacle to aquatic life, but also a dynamic vector and potential reservoir of inherent additives and adsorbed hydrophobic anthropogenic contaminants. Not to mention, microplastics can also serve as a physical vector of microorganisms and invasive species from the environment (Crawford & Quinn, 2019). Accordingly, 'plastic microbeads' and 'plastic manufactured items' have been added to the list of toxic substances under Schedule 1 of the Canadian Environmental Protection Act as part of the Government of Canada's efforts to achieve zero plastic waste and eliminate plastic pollution by 2030 (ECCC, 2020; ECCC, 2021; Plastic Soup Foundation, 2021). Furthermore, the composition and properties of many plastic additives have been revealed to public consumers (Espinosa et al., 2016). However, this is not the case for all as gaps in knowledge remain for some compounds (Espinosa et al., 2016). As a case in a point, and the focus of this study, limited information exists on the antioxidant Cyanox®53.

1.5. Cyanox®53

Originally developed by Cytec Industries Inc., Cyanox®53 is chemically characterized as a white powdered alkylated bisphenol derivative, more specifically a primary (phenolic) antioxidant, with a specific gravity density of 1.74 (van Alphen & van Turnhout, 1973; McEntee, 1990; AccuStandard, 2018; Wang et al., 2019; Wiley, 2021). By and large, phenolic compounds protect organic substances during storage, processing, or conversion by participating in reactions through resonance-stabilized free-radical forms, or by acting as free radical scavengers, to inhibit the rate of oxidation (Keck-Antoine et al., 2010; Gijsman, 2012; Ammar et al., 2016; Mankar & Mankar, 2020). Because of this, phenolic antioxidants are often used in rubber and plastic processing, fuel and lubricant fabrication, pharmaceutical and personal care products, or in food as preservatives. The integration of Cyanox®53 is intended to enhance the

stability of polymers (i.e., PE, PP, PS and ABS) by providing protection against thermo-oxidative degradation that would otherwise weaken structural integrity or cause discolouration during thermal processing (Bolgar et al., 2016; Bendell et al., 2020; Solvay, 2020). As such, Cyanox®53 can be added into a wide range of products including rubbers, PE wiring and cable resins, or even in the packaging of feminine hygiene products (e.g., wrapper in organic cotton tampons) (Flick, 2001; Bolgar et al., 2016; Greenpeace Research Laboratories, 2019).

Little is known about the physiochemical properties of Cyanox®53 because experimental data and model-based predictions are lacking. In fact, while information on other Cyanox® variants (e.g., Cyanox®2246, Cyanox®425, and Cyanox®1790) has been disclosed in an assortment of documents, information regarding the physiochemical properties, toxicological implications, or prevalence of Cyanox®53 in the environment remains almost non-existent. In the few times that the presence of Cyanox®53 has been recorded in the environment, this antioxidant has been found to be disassociated from its inert carrier and abnormally presented as a white fibrous particle. For example, following a microplastic composition survey at inner Kongsfjord, Svalbard, the Norwegian Geotechnical Institute in collaboration with the Geographical Survey of Norway recovered white fragments of Cyanox®53, at a frequency 27-64% of total microplastics, in beach surface sediments at two sampling sites (Knutsen et al., 2019). Given that the objective of the survey was to gather data on the distribution and presence of microplastics near the Arctic, no further comments, other than its relative abundance, were made for Cyanox®53. Similarly, Bendell et al. (2020) found fibrous particles of Cyanox®53, in addition to a high volume of microplastic fragments and spheres, in the digestive tracts of 26 varnish clams (*Nuttallia obscurata*) during a microplastic biomonitoring survey in Burrard Inlet, British Columbia (BC). Clams were also collected from the Baynes Sound, BC, for comparison, however, no fragments of Cyanox®53 were recovered. Based on their findings, Bendell et al. (2020) proposed that Burrard Inlet, BC could be geographically a unique source of Cyanox®53.

1.6. Polymer Analysis Techniques

Growing interest has been drawn to the driving forces and impacts of microplastic emissions in the environment. In response, an acceleration in the development of methods to quantify the sources and pathways of microplastics, as well

as to gain insight on the mechanisms behind microplastics acting as a sink for POPs and contaminants, has occurred in the scientific community. However, despite these efforts, the majority of microplastic research continues to be conducted under laboratory conditions and often lacks ecological relevance (Rozman & Kalčíková, 2022). As variations in microplastic sampling, quantification, and characterization continue to persist, there is still no universally accepted methodology in the analysis and measuring of microplastics and associated additives from environmental samples. For instance, unlike many contaminants found in aquatic settings, microplastics embody as a solid particle rather than as a dissolved chemical, and thus vary in mass, volume, density, and in the amount and types of additives adhered to them. Ultimately, such variation makes it very challenging, if not almost impossible, to generate standard concentrations of microplastics required for analysis and for inter-study or regulatory comparisons (Hanvey et al., 2017). Such a predicament also prevails for Cyanox®53 where only a few studies have been able to identify and record its presence in the environment (Knutsen et al. 2019; Bendell et al., 2020).

Recently, researchers have quantified and chemically identified microplastics using a suite of techniques, including fluorescent staining, density separation and attenuated total reflectance-Fourier transform infrared (ATR-FTIR) spectroscopic imaging (Maes et al., 2017; Olesen et al., 2018; Rodrigues et al., 2020). Other sensitive tools like proton nuclear magnetic resonance ($^1\text{H-NMR}$) and electrospray ionization-liquid chromatography/mass spectrometry (ESI-LC/MS) have been employed in addition to FTIR to provide more details on the structural make-up and dynamics of complex compounds. Less costly and non-invasive approaches, such as Quantitative Structure-Activity Relationship (QSAR) modelling, have also been utilized more frequently over traditional *in vivo* experiments in the identification of physiochemical properties, and toxicological mechanism and structure–activity relationship for specific chemicals (Lapenna et al., 2010; Hayes & Kruger, 2014; OECD, n.d.). Even global regulations, including European Chemical Agency REACH initiative, U.S. Toxic Substances Control Act, and the Canadian Environmental Protection Act, that once mandated *in vivo* toxicity testing, now encourage an increased reliance on *in silico* approaches to predict the intrinsic activity and potential absorption, distribution, metabolism, and excretion characteristics of chemicals (Madden et al., 2020; Zhou et al., 2021). Together, these

techniques offer complementary data and enhance the likelihood of fully characterizing poorly understood or unknown compounds.

Numerous studies have demonstrated the use of different bivalve species (i.e., mussels, oysters, and clams) as sentinels or biomonitors to track the distribution of microplastic pollution in marine environments (Browne et al., 2008; van Moos et al., 2012; Avio et al., 2015; Li et al., 2015; Baechler et al., 2019; Covernton et al., 2019; Bendell et al., 2020). The infaunal sediment-dwelling varnish clam have been used previously as a biomonitor for microplastics (Bendell et al., 2020). Varnish clams are both suspension and deposit feeders that exploit food from within the water interface and sediment, despite being sessile (Gillespie et al., 2001). This trait grants varnish clams the ability to be non-selective, opportunistic feeders and thus are beneficial in the tracking of microplastic pollution from the water column to surface sediments on beaches. Additionally, as an invasive species, varnish clams have become well-established in the southern coastal regions of BC like the Strait of Georgia and Barkley Sound, and thus represent a vital food source for a variety of tertiary consumers, including humans (Gillespie et al., 1999, 2001; Chan & Bendell, 2013; Bendell et al., 2020).

1.7. Research Objectives

Currently, there is a paucity of literature on the environmental prevalence, physiochemical properties, and toxicological implications of Cyanox®53. Thus, the purpose of this present investigation was to examine the abundance and distribution of Cyanox®53 in Burrard Inlet, BC, and to explore its toxicological implications. To accomplish the first objective, an environmental survey that involved the collection of marine surface sediments and adult varnish clams from seven intertidal beaches throughout Burrard Inlet, BC was conducted to detect the presence of Cyanox®53. For the second objective, prediction of environmental fate and potential adverse effects was performed via QSAR modelling. Being that a distinct chemical structure for Cyanox®53 has yet to be revealed in the literature, ATR-FTIR, ESI-LC/MS and ¹H-NMR were employed to generate a feasible structure for the operation of QSAR modelling. We predicted that Cyanox®53 would be the most abundant near the First Narrows strait (mouth of outer and inner harbour) in Burrard Inlet, BC where majority of the Port of Vancouver is centralized. Secondly, we hypothesized that, akin to other bisphenol

related compounds, Cyanox®53 may possess some degree of toxicity towards aquatic organisms. Through this approach, it is expected that the results generated will provide information on environmental concentrations, environmental fate, and toxicological properties of Cyanox®53 for risk assessments, as well as model a novel protocol that could be adopted in future investigations.

2. Materials & Methods

2.1. Study Sites

Sampling of adult *Nutallia obscurata* and marine surface sediments was conducted in Burrard Inlet, BC (49.3174° N, 123.1913° W) (with permission from the Department of Fisheries and Oceans Canada Permit # XMCFR 16 2020). Seven coastal sites between the outer and central harbours of Burrard Inlet were selected. These included: Spanish Banks Beach (SB), Jericho Beach (J), English Bay Beach (EB), Third Beach (TB), Ambleside Park Beach (AP), Cates Park Beach (CP), and Barnet Marine Park Beach (BMP). A complete map showing the seven sampling sites is shown in Figure 2.1. The site description, impact level, substrate type, and GPS coordinates of the seven intertidal study sites are provided in Table 2.1. An impact level of low (i.e., recreational boating with minimal commercial marine traffic), medium (i.e., moderate industrial and commercial marine traffic), or high (i.e., heavily industrial, and high commercial marine traffic) was assigned to each site based on local anthropogenic marine traffic.

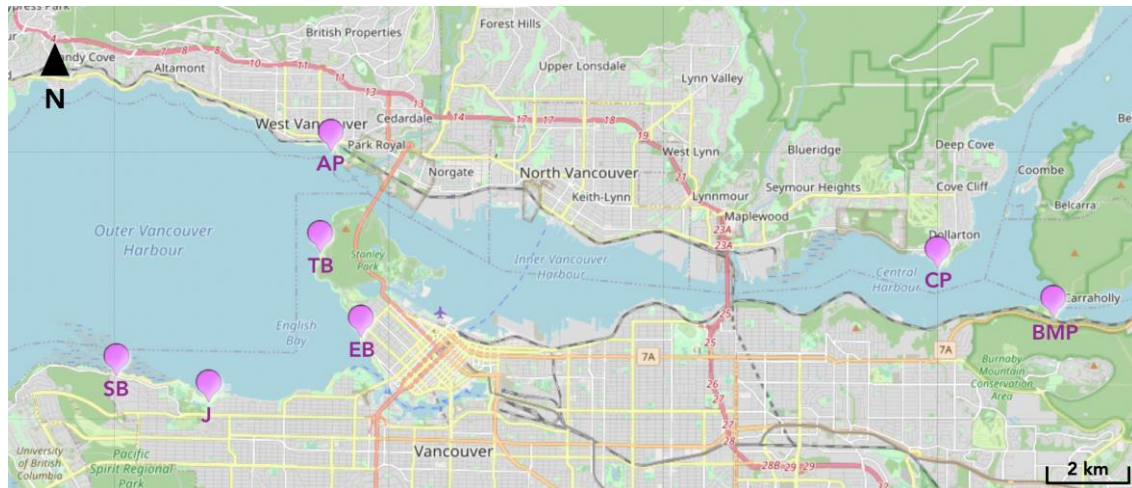


Figure 2.1. Locations of seven designated sampling sites in Burrard Inlet, BC involved in surface sediment and varnish clam (*Nutallia obscurata*) collections for environmental survey. Purple markers indicate sampling sites at Ambleside Park Beach (AP), Barnet Marine Park Beach (BMP), Cates Park Beach (CP), English Bay Beach (EB), Jericho Beach (J), Spanish Banks Beach (SB), and Third Beach (TB). Map courtesy of the U.S. Geological Survey (USGS, 2022).

Table 2.1. Characteristics and GPS coordinates for the seven intertidal study sites found in Burrard Inlet.

| Site Name | Site Description | Impact Level | Substrate Type | GPS |
|--------------------------------|--|--------------|--|-------------------------|
| Ambleside Park Beach (AP) | Outer harbour near the Lion's Gate Bridge and mouth of First Narrows waterway. Main waterfront district park in West Vancouver. | Medium | Mostly cobble beach with some sandy portions; loose and big granule sandy texture. | 49.3234° N, 123.1500° W |
| Barnet Marine Park Beach (BMP) | Central harbour towards the Port Moody Arm. Near oil refinery, with effluent discharge from authorized industrial, combined and sanitary sewer, and several stormwater outfalls. | High | Mostly cobble beach with some sandy portions; a hard, large granule texture. | 49.1725° N, 122.5530° W |
| Cates Park Beach (CP) | Central harbour along the north side of the inlet. A district park with a playground, picnic area, and space to boat, swim, and trail hike. | Low | Mostly cobble beach with some sandy portions; hard, large granule rocky texture. | 49.3030° N, 122.9553° W |
| English Bay Beach (EB) | Outer harbour along downtown Vancouver facing the Strait of Georgia. Base of highest density urban regions within Vancouver. | Medium | Sandy beach; loose and hard, large granule sandy texture. | 49.2872° N, 123.1614° W |
| Jericho Beach (J) | Outer harbour along the south-west portion of Vancouver near West Point Grey. Close to sailing club, tennis courts, and fields. | Low | Mostly cobble beach with some sandy portions; loose and hard, small granule sandy texture. | 49.2722° N, 123.1985° W |
| Spanish Banks Beach (SB) | Outer harbour along the south-west portion of Vancouver near West Point Grey. A part of a series of beaches with volleyball courts, BBQ areas, and boating fronts. | Low | Sandy beach; a loose and soft, small granule silt texture. | 49.2765° N, 123.2133° W |
| Third Beach (TB) | Outer harbour at the northern tip of Stanley Park. Near the Lion's Gate Bridge and Vancouver Seawall walkway. | Medium | Sandy beach; loose and soft, small granule sandy texture. | 49.3040° N, 123.1568° W |

2.2. Sediment Analysis

2.2.1. Sample Collection and Preparation

Sampling was conducted in late May to early June during a period of maximum low tides. Approximately 3.5 kg of surficial sediment was collected via 'grab sampling' technique at a depth of 10 cm from each site and placed into a labelled plastic bucket and sealed for prevention of contamination. Following collection, the seven sediment samples were transported back to the laboratory and sieved separately for particles < 5 mm into a pre-weighed aluminum tray using CE Tyler Canadian Standard 4.75 mm sieve. Cross-contamination between the seven samples was minimized by rinsing the sieve with de-ionized water and drying it with a paper towel. Once in the tray, 3 kg of the newly sieved sediment was subdivided into three 1 kg samples per study site. Each subsample was homogenized, and the wet weight was taken before the trays were placed into a Precision® Gravity Convection Incubator at 60°C for 48 hr or until completely dried. A temperature of 60°C was used in lieu of the suggested 110°C to prevent the potential melting of microplastics in the samples. Once dried, the dry weights were obtained for each subsample and then the samples were set aside for particle extraction.

2.2.2. Nile Red Fluorescent Tagging of Particles

As described in Maes et al. (2017), a stock solution of zinc chloride (ZnCl_2) (granular ACS reagent with a purity of > 97%) at a density of 1.38 g/mL was prepared gravimetrically at room temperature by combining 420 g ZnCl_2 with 700 mL analytical-grade water. Concurrently, Nile Red dye ($\geq 98.0\%$ purity) stock solution in acetone ($\geq 99.5\%$ purity) was prepared to a final concentration of 10 $\mu\text{g/mL}$ in a tinted vial and stored in a dark refrigerator at 4°C, to prevent chemical degradation and microbial growth, until tagging was conducted. Approximately 20 g of dry sediment was suspended in 30 mL ZnCl_2 stock solution and 2 mL Nile Red stock solution within a 50 mL centrifuge tube. Samples were shaken for 30 min on a Precision® Scientific Dubnoff Metabolic Shaking Incubator at 100 rpm. These steps of solution prep and staining were repeated for all sediment subsamples.

2.2.3. Density Separation of Particles

Recovery of particles from sediment samples was based on the procedures laid out in Maes et al. (2017), with some minor modifications. Like Maes et al. (2017), particles were separated by centrifuge. Each centrifuge tube filled with the sediment mixture was centrifuged in a Beckman Allegra 64R centrifuge at 3900 g for 8 min with a braking speed of 9. The supernatant containing the stained particles was collected using a 5 mL glass Pasteur pipette and decanted through a Whatman™ 1001-090 Grade 1, Pore Size, 9 µm qualitative cellulose nitrate filter paper under vacuum filtration. This procedure of density suspension was repeated for each subsample. Dried filter papers were placed into labelled petri dishes and sealed with Parafilm® M all-purpose laboratory tape until visual inspection could be conducted.

2.3. Bivalve Analysis

2.3.1. Sample Collection and Preparation

Nutallia obscurata was selected as a suitable biomonitor for the analysis of the abundance and distribution of microplastics and Cyanox®53. Twenty-five adult varnish clams varying in size were collected at each site in late May to early June from a depth of approximately 10 cm in the mid to high intertidal zones, particularly in brackish waters near freshwater streams or groundwater seepage per site (N = 175). All collected bivalves were secured with a thick rubber band around their shell to prevent the loss of any particle contents and then placed into their respective site labelled Ziploc® bag for ease of transportation. At the laboratory, biometric data of internal tissue weight, shell dimensions (length, height, width) and weight of each bivalve was measured, and a corresponding condition indices value was determined using equation 2.1 (Benali et al., 2015). Until needed, the bivalves were frozen at -4°C to preserve their internal tissues.

$$\text{Condition Index (g/cm}^3\text{)} = \frac{\text{Tissue Wet Weight (g)}}{\text{Body Length} \times \text{Height} \times \text{Width (cm}^3\text{)}} \times 100\% \quad (2.1)$$

2.3.2. Staining and Isolation of Particles

Whole-organism tissues were removed from each bivalve shell using a sterilized stainless-steel scoopula and forceps, and immediately placed into separate 100 mL

glass Erlenmeyer flasks. To minimize cross-contamination, dissection instruments were cleaned with 70% ethanol and wiped with a clean paper towel between each bivalve tissue removal. No pooling of the samples was conducted to allow for the determination of microplastics and Cyanox®53 particles per individual bivalve. Tissue digestion was carried out by incubating the removed tissue samples in freshly prepared 10% potassium hydroxide (KOH) (4 times the tissue volume) for 48 hr at 60°C within a Precision® Gravity Convection Incubator. At the 24 hr mark, 2.5 mL of Rit Dye More® was added into the digestion mixture to stain any synthetic polymer particles a periwinkle colour for identification. Following incubation, each sample was vacuum filtered through a Whatman™ 1001-090 Grade 1, Pore Size, 9 µm qualitative cellulose nitrate filter paper and rinsed with 30% hydrogen peroxide (H₂O₂) to remove any biofilm or fat membrane remnants that would interfere with particle identification. Any remaining particles within the flask were rinsed with de-ionized water and scooped into the filter paper with a rubber policeman. Dried filter papers were placed into labelled petri dishes and sealed with Parafilm® M all-purpose laboratory tape until visual inspection could be conducted.

2.4. Filtrate Inspection and ATR-FTIR

Extracted filtrates from bivalve samples were visually observed through a digital dissection microscope (Jiusion 40-1000x Magnification Endoscope 8 LED USB 2.0 Digital Microscope Mini Camera) and compared to the images captured by Bendell et al. (2020) as a reference. Fluorescent tagged filtrates found in the sediment samples were visually inspected using the same digital dissection microscope through an orange filter under blue excitation (420–495 nm). Any white fragmented/frayed particles suspected of being Cyanox®53 were submitted to ATR-FTIR spectroscopy for verification. Infrared spectra between 550 cm⁻¹ and 4000 cm⁻¹ were measured on a PerkinElmer FTIR Microscope Spotlight 200i, with the focus being set on a 10 µm area of the particle using a diamond crystal. Before examination, filter papers were sprayed with methanol (≥ 99.5% purity) ACS reagent (purchased from Sigma-Aldrich) to prevent loss of particles from static electricity or movement. Each ATR-FTIR spectra was assigned a polymer identify based on “best match” according to molecular bond vibrations and a “confidence” score ranging from 0-100%; a value of ≥ 70% was deemed as an acceptable level of confidence to account for weathering. For validation, all obtained ATR-FTIR spectra were compared with accessible online spectral databases, including

Bio-Rad® Laboratories, Knowitall®, and SpectraBase™. In addition, known samples of high-density polyethylene (HDPE), low-density polyethylene (LDPE), PP, PETE, PVC, PS, and extruded polystyrene (XPS) foam were submitted to ATR-FTIR spectroscopy to create a database to help identify common plastic polymer ATR-FTIR spectra of the field-collected particles (Figure C-1). If a positively matched Cyanox®53 ATR-FTIR spectra was recovered (assigned a confidence score $\geq 70\%$), the sample was reserved for follow-up chemical analyses (i.e., mass spectrometry and nuclear magnetic resonance) to identify key chemical properties. Once verified, total numbers of recovered microplastics and Cyanox®53 per bivalve and sediment sample were converted to number of particles per g of wet tissue weight (particles/g ww) and number of particles per kg of sediment dry weight (particles/kg dw), respectively. Adapted from the approach suggested by Alava (2021), biota-sediment accumulation factor (BSAF) ratios were calculated to assess the bioaccumulation potentials of mean Cyanox®53 and/or microplastic concentrations in the bivalve tissue against that deposited in the surface sediments on a kg weight basis for each site (equation 2.2). If the BSAF ratio was > 1 , bioaccumulation from the sediment was deemed probable, but if the BSAF ratio was ≤ 1 , then a lack bioaccumulation from the sediment was concluded.

$$BSAF = \frac{\text{Mean Particle Concentration in Biota (particles/kg ww)}}{\text{Mean Particle Concentration in Sediment (particles/kg dw)}} \quad (2.2)$$

2.5. Statistical Analyses

All statistical analyses were carried out in JMP®, Version 16 (SAS Institute Inc., 2021). Altogether, 21 replicates of sediment and 175 bivalves across seven sites were evaluated. Normal distribution and outliers in particle concentrations (from sediment and bivalves) and biometric data was visually inspected via frequency distribution and normal quartile-quantile plots. Correlations between wet tissue weight (g) and shell volume (cm^3) were analyzed for each bivalve with Pearson's coefficients, linear mixed-effects model, and subsequent effects test and Tukey's Honesty Significance Difference (HSD) post-hoc analyses. Normality in each dataset was assessed via Shapiro-Wilk's test. If a dataset failed the normality test, a logarithmic (i.e., $\log(x+1)$) transformation was applied and then retested for normality. Potential outliers were determined by plotting studentized residuals and were removed if an individual observation strayed outside the 95% simultaneous confidence limits (Bonferroni) at a ± 3 score, unless otherwise stated.

Homogeneity of variance for each dataset was also assessed via Levene's test. A one-way Analysis of Variance (ANOVA) followed by Tukey's HSD post-hoc analysis was used to determine the statistical significance of the microplastics and Cyanox®53 particle concentrations, respectively, across the sites in the different mediums (i.e., sediment, bivalves). If transformed data could not meet parametric assumptions, then a Kruskal-Wallis followed by a Steel-Dwass post-hoc analysis was performed to determine the significant difference in microplastics and Cyanox®53 particle concentrations, respectively, across the sites in the different mediums. For all statistical tests, a p-value < 0.05 was used for the significance determination.

2.6. Molecular Structure Identification of Cyanox®53 Particles

2.6.1. Single-Batch Equilibrium Leaching

Deuterated dimethyl sulfoxide (DMSO-d₆) (99.9%) solvent utilized during the extraction was supplied by the Chemistry Department at Simon Fraser University. Single-batch equilibrium leaching was carried out by placing equal parts (approximately 0.5 mg each) of the recovered Cyanox®53 and Cyanox®53-PVDF particles into two separate 1 mL Pyrex® glass test tubes and immersing them in 200 µL DMSO-d₆ for 10 days without exchange of the solution. To promote maximum partitioning, the samples were incubated in a Sybron Thermolyne™ Dri-bath heat block at 70°C while being shaken at 200 rpm on a Fisher Scientific™ Multi-Platform shaker during the 10 d leaching period.

2.6.2. ¹H-NMR and ESI-LC/MS

Prior to ¹H-NMR measurements, a calibration standard of tetramethylsilane (0.01%) was used to evaluate the signal-to-noise ratio (between the 3 to 7 ppm range) and to ensure a linear calibration curve was produced. ¹H-NMR measurements of the leached Cyanox®53-PVDF and Cyanox®53 samples were recorded on a Bruker Avance II 600 MHz spectrometer, equipped with a cryoprobe. Both ¹H-NMR spectra were acquired with 1024 scans at 298 K, between -1 ppm and 14 ppm, and referenced to the residual DMSO resonance at 2.50 ppm. As references, 10 mg of dry extract 2,2'-methylenebis(4-ethyl-6-tert-butylphenol) (≥ 98.0% purity), 2,2'-methylenebis(6-tert-butyl-

4-methylphenol) ($\geq 99.0\%$ purity), 4,4'-isopropylidenediphenol ($\geq 99.0\%$ purity), respectively, were dissolved into 2 mL of 99.9% DMSO- d_6 separately. Their $^1\text{H-NMR}$ spectra were acquired on a Bruker Avance II 600 MHz spectrometer equipped with a cryoprobe at 298 K, between -1 ppm and 14 ppm, with a relaxation delay of 5 secs for 128 scans. Produced spectra were used in the structural identification of Cyanox®53. Following $^1\text{H-NMR}$ analysis, high-resolution liquid chromatography mass spectrometry was performed on an Agilent 6210 TOF LC/MS using electrospray ionization mass spectrometry. Each sample concurrently ran on a C18 LC gradient from water-acetonitrile (0-100%) for 8 min. All obtained m/z values were background corrected to account for the water-acetonitrile mobile phase (~ 18 Da). All proposed chemical properties of Cyanox®53 following NMR and MS data collection were analyzed in MestReNova, Version 14.2.1 (Mestrelab Research S.L., 2021).

2.7. QSAR Modelling

Data collected from ATR-FTIR, $^1\text{H-NMR}$, and ESI-LC/MS analyses were used to create a chemical structure for Cyanox®53. Before QSAR modelling, conversion of Cyanox®53's proposed structure into Simplified Molecular Input Line Entry System (SMILES) notation was conducted in JChem for Office, Version 21.11.10 (ChemAxon, 2021). Estimated physical/chemical and environmental fate properties of Cyanox®53 were predicted using EPA and Syracuse Research Co.'s Windows®-based screening level tool Estimation Program Interface (EPI) Suite™ Version 4.11 (US EPA, 2021). Within the suite, the estimation programs KOWWIN™, WSKOWWIN™, WATERNT™, BIOWIN™, KOCWIN™ and BCFBAF™ and fate model LEV3EPI™ were implemented to obtain an estimated $\log K_{ow}$, melting and boiling point, water solubility (based on $\log K_{ow}$ or chemical fragments), rapid biodegradability probability, organic carbon to water partition coefficient (K_{oc}), fish bioconcentration factor (BCF) and bioaccumulation factor (BAF), biotransformation half-life, and partitioning time in air, soil, sediment, and water (under steady state conditions) for Cyanox®53. Potential acute and chronic toxicity values of Cyanox®53 to aquatic organism surrogates, such as fish, aquatic invertebrates (*Daphnia magna*), and aquatic plants (green algae), were predicted with the ecotoxicity model ECOSAR™ embedded in EPI Suite™ Version 4.11 (US EPA, 2021). If the $\log K_{ow}$ of Cyanox®53 was greater than the endpoint specific cut-off established, then no effects at saturation (NES) were expected for that endpoint. Additionally, if the predicted effect

level exceeded the water solubility of Cyanox®53 by ≥ 10 -fold, then NES was reported. Finally, the relative mammalian health hazards of Cyanox®53, based on its molecular structure and physiochemical properties, were estimated within Toxtree, Version 3.1.0 (Patlewicz et al., 2008). The specific plugins used included: Cramer rule decision tree, Verhaar scheme, START biodegradability and persistence, Benigni/Bossa rule-base for mutagenicity and carcinogenicity, SMARTCyp - Cytochrome P450-mediated drug metabolism and metabolite prediction, protein and DNA binding alert, *in vitro* mutagenicity (Ames test) alerts by ISS, and *in vivo* micronucleus assay in rodents (ISSMIC). Default settings were used to run all QSAR software, and no changes were made to the developers' programming.

2.8. Quality Assurance and Contamination Control

All procedures involving chemical materials during the study were performed within a biological safety cabinet unless stated otherwise. In the laboratory, a cotton lab coat and latex gloves were worn at all times. Tools and glassware in direct contact with the tissue, sediment, or chemicals were rinsed thoroughly with de-ionized water before use and disinfected with soap and de-ionized water afterwards. All workspaces were wiped down with 70% ethanol and paper towel both prior to and after use. All reagents were covered with aluminum foil and stored in clean glass containers before use. Samples were covered with either aluminum foil or lids whenever possible to reduce loss of samples and contamination from airborne or artificial sources. A face wash containing PE (Neutrogena® Oil-Free Acne Wash) was used as a positive control to ensure the KOH-tissue digestion process didn't degrade plastic products during microplastic extraction. Additionally, procedural blanks were processed and analysed alongside each batch during microplastic extraction procedures, FTIR, NMR and MS analyses to account for potential ambient or processing contamination of samples.

3. Results

3.1. Abundance and Distribution of Particles

3.1.1. Microplastics in Sediment

Microplastic particle concentrations were detected in surface sediments from all seven sites. Particle concentrations ranged from 4 to 18 particles/kg dw per site. The highest mean particle concentration of microplastics was reported at EB (15.7 ± 0.33 particles/kg dw) while the lowest mean concentration was found at J (6.67 ± 1.33 particles/kg dw). A summary of mean microplastic particle concentrations from each site is shown in Table A-1. Further categorization of these mean particle concentrations into micro-spheres, micro-fragments, micro-fibers, and micro-film per site can be seen in the Table A-2. Recovered particle concentrations demonstrated normality at all sites via normal quartile-quantile plotting and Shapiro-Wilk's test ($W = 0.94$, $p = 0.27$) with no major outliers being detected by studentized residual plotting. Nevertheless, no significant effect in mean particle concentrations between sites ($p = 0.124$) was observed in the one-way ANOVA (Figure 3.1).

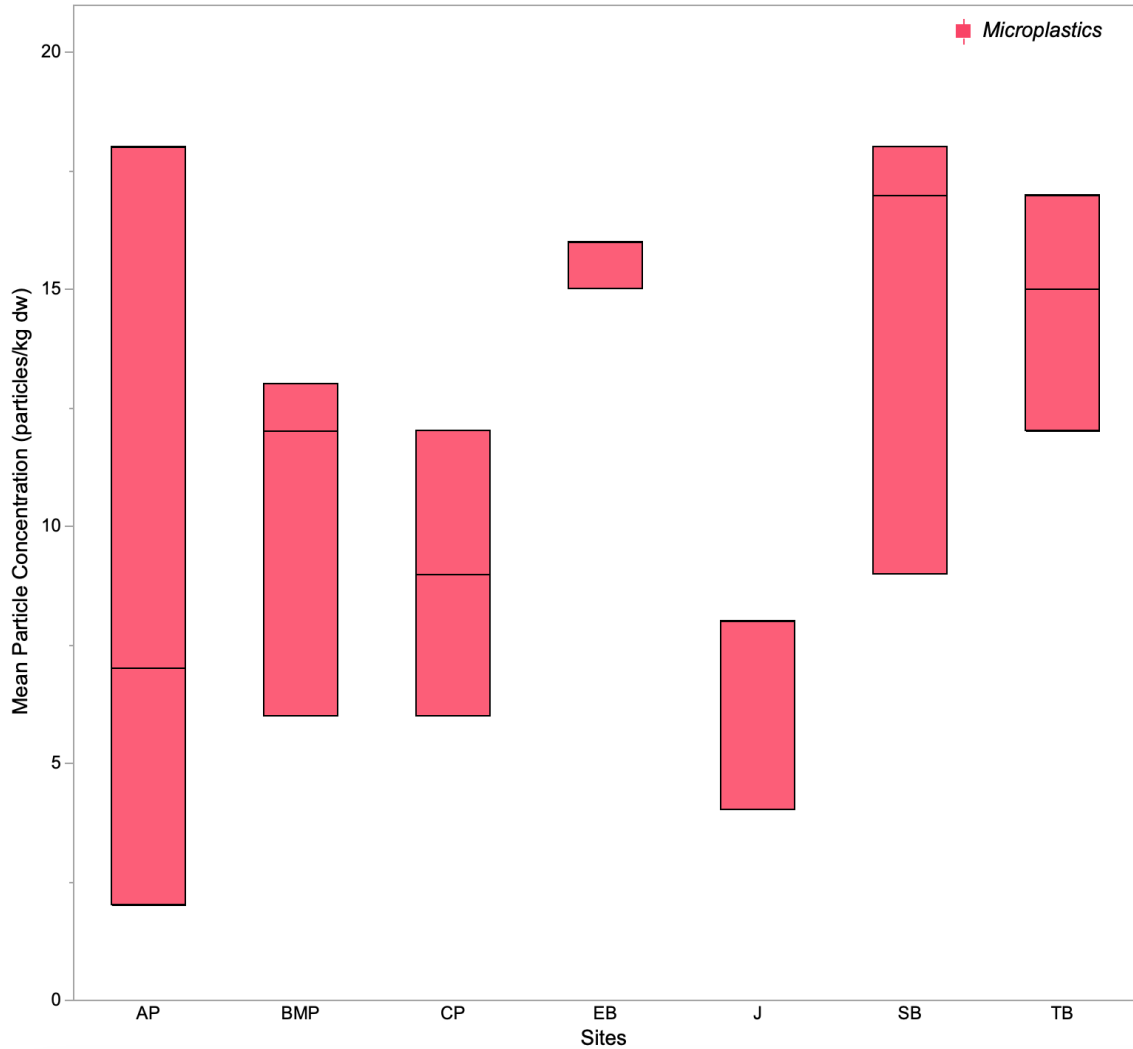


Figure 3.1 Microplastic concentrations recovered from surface sediment sampled at seven intertidal sites in Burrard Inlet. Boxplots demonstrating the median values (thick horizontal black line within box) and the lower and upper 25th and 75th percentiles (upper and lower boundaries of box) are presented. A total of N = 21 replicates were analyzed (n = 3 sample size per site). Sites (left to right): Ambleside Park (AP), Barnet Marine Park (BMP), Cates Park (CP), English Bay (EB), Jericho Beach (J), Spanish Banks (SB), and Third Beach (TB). A One-Way ANOVA followed by Tukey's HSD post-hoc analysis was used to determine significant difference between particles concentrations (particles/kg dw) across the sites. No significant difference between the sites ($p = 0.124$) was observed.

3.1.2. Cyanox®53 in Sediment

Cyanox®53 particle concentrations were only detected in surface sediments from AP, BMP, EB, and SB. Amongst these four sites, particle concentrations ranged from 1 to 5 particles/kg dw per site. The highest mean particle concentration of Cyanox®53 was observed at both AP (1.67 ± 0.88 particles/kg dw) and EB (1.67 ± 1.67 particles/kg dw), while the lowest detectable mean concentration was found at SB (0.33 ± 0.33 particles/kg dw). A summary of mean Cyanox®53 particle concentrations from each site is shown in Table A-1. Regardless of transformation, Cyanox®53 particle concentration data failed to comply with parametric assumptions (i.e., $p \leq 0.05$ in Shapiro-Wilk's test). Skewness in the normality of Cyanox®53 concentrations was attributed to non-detectable measurements at CP, J, and TB. As a result, data was analyzed via non-parametric Kruskal-Wallis and Steel-Dwass post-hoc analysis. No significant difference in mean particle concentrations between sites ($chi\text{-squared} = 5.84$, $df = 6$, $p = 0.442$) was observed in the Kruskal-Wallis analysis (Figure 3.2).

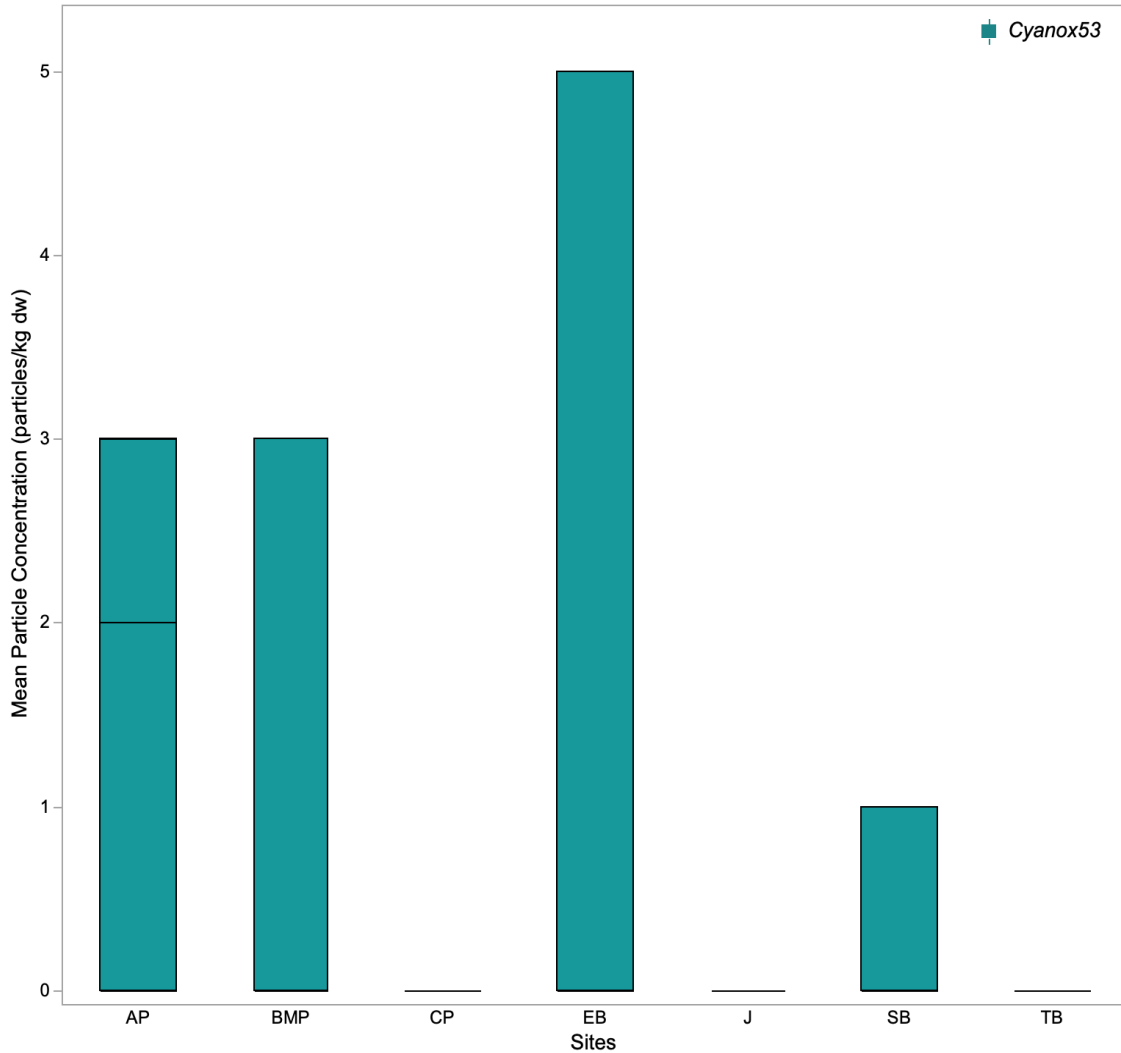


Figure 3.2 Cyanox®53 concentrations recovered from surface sediment sampled at seven intertidal sites in Burrard Inlet. Boxplots demonstrating the median values (thick horizontal black line within box), and the lower and upper 25th and 75th percentiles (upper and lower boundaries of box) are presented. A total of N = 21 replicates were analyzed (n = 3 sample size per site). Sites (left to right): Ambleside Park (AP), Barnet Marine Park (BMP), Cates Park (CP), English Bay (EB), Jericho Beach (J), Spanish Banks (SB), and Third Beach (TB). A Kruskal-Wallis followed by Steel-Dwass post-hoc analysis was used to determine significant difference between particles concentrations (particles/kg dw) across the sites. No significant difference between the sites (*chi-squared* = 5.84, df = 6, p = 0.442) was observed.

3.1.3. Bivalve Biometric Data

Compiled bivalve biometric data did not require transformation for any of the seven bivalve populations as shell width (cm), height (cm), length (cm), volume (cm³), and tissue weight (g) were all found to be normally distributed following frequency distribution, normal quartile-quantile plotting, and Shapiro-Wilk normalcy tests ($p > 0.05$; Table B-1). No outliers were observed based on studentized residual plotting; hence no individuals were omitted from the dataset. Overall, the largest individuals were collected at EB (mean shell volume of 507 ± 23 cm³) while the smallest were collected from SB (mean shell volume of 214 ± 7.8 cm³). A summary of mean biometric data for each site is shown in Table B-2. Relative condition indices (g/cm³) were calculated by dividing the wet tissue weight (g) from the shell volume (cm³) (product of shell width (cm), height (cm), length (cm)) of *Nutallia obscurata*, multiplied by 100% (equation 2.1; Benali et al., 2015). Mean condition indices were as followed: 2.87 ± 0.16 g/cm³ % (AP), 2.88 ± 0.041 g/cm³ % (BMP), 3.05 ± 0.036 g/cm³ % (CP), 2.66 ± 0.048 g/cm³ % (EB), 2.99 ± 0.035 g/cm³ % (J), 3.19 ± 0.18 g/cm³ % (SB), and 2.82 ± 0.041 g/cm³ % (TB).

The relationship between bivalve wet tissue weight (g) and shell volume (cm³) was presented for each site in a linear mixed-effects model (Figure 3.3). Respective linear regression equations and r^2 coefficients for each site are summarized in Figure 3.3. The following Pearson's correlation values were calculated for each site: 0.94 (AP), 0.87 (BMP), 0.95 (CP), 0.93 (EB), 0.98 (J), 0.30 (SB), and 0.92 (TB). Effect tests followed by Tukey's HSD post-hoc analysis was used to determine significance differences between the main effects (site and shell volume) and interaction between main effects. A significant effect of site ($p = 0.010$), shell volume ($p < 0.0001$), and an interactive effect ($p = 0.019$) was observed. Pairwise comparison observed a significant difference in wet tissue weights between J and SB.

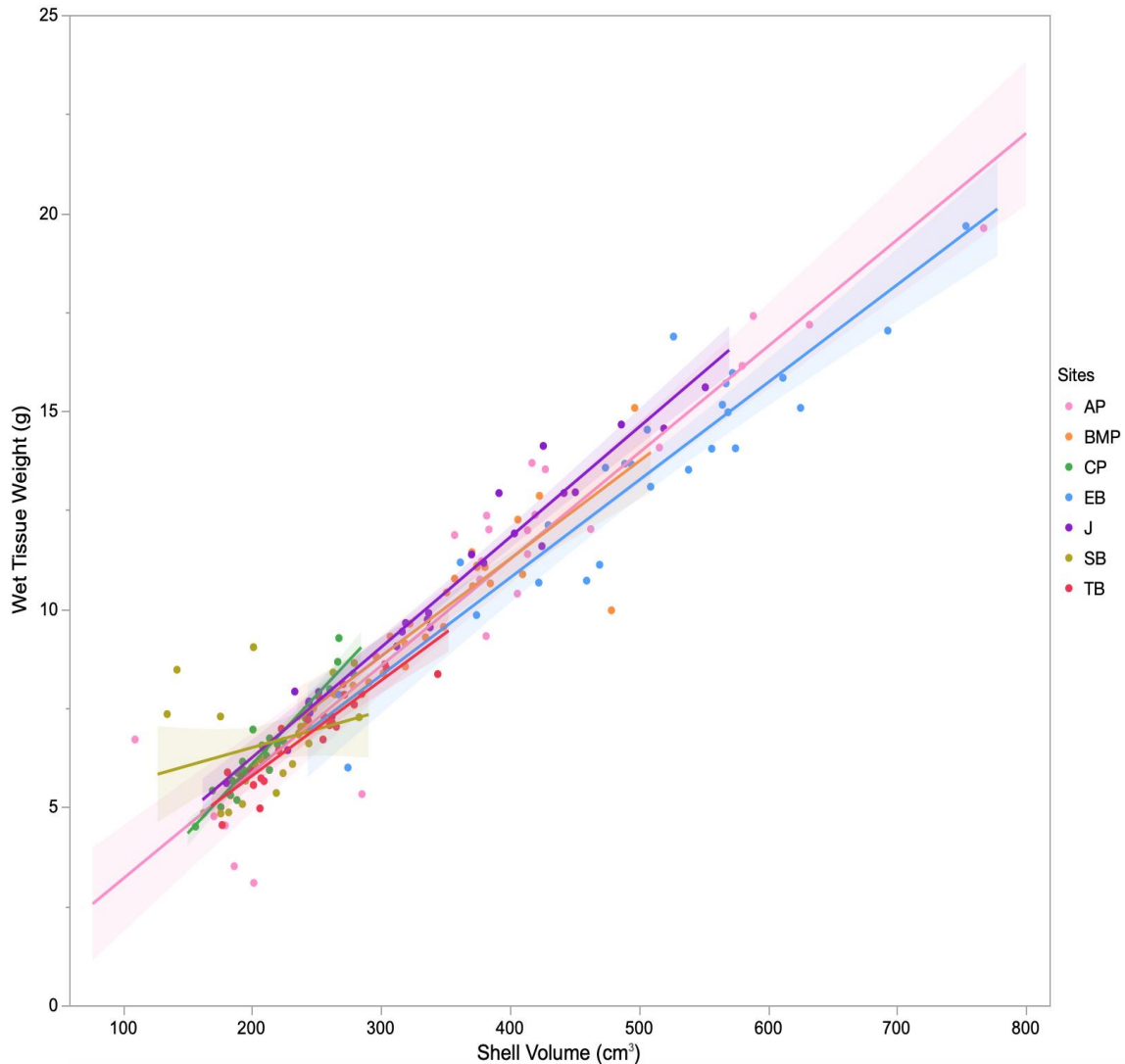


Figure 3.3 Relationship of wet tissue weight (g) to shell volume (cm³) of *Nutallia obscurata* sampled at seven intertidal sites in Burrard Inlet. Linear mixed-effects model demonstrating linear regressions (coloured lines), fitted confidence regions (transparent shading beneath regression lines), and plotted individuals (colourful dots) from each site are presented. A total of N = 175 bivalves were collected at a sample size of n = 25 per site. Sites: AP (pink), BMP (orange), CP (green), EB (blue), J (purple), SB (gold), and TB (red). The following linear equations and r² values were obtained for each site: AP (wet tissue weight = 0.027*shell volume + 0.050, r² = 0.89); BMP (wet tissue weight = 0.025*shell volume + 1.4, r² = 0.75); CP (wet tissue weight = 0.035*shell volume - 0.90, r² = 0.91); EB (wet tissue weight = 0.025*shell volume + 0.93, r² = 0.87); J (wet tissue weight = 0.028*shell volume + 0.69, r² = 0.96); SB (wet tissue weight = 0.0092*shell volume + 4.7, r² = 0.09); and TB (wet tissue weight = 0.024*shell volume + 0.98, r² = 0.84).

3.1.4. Microplastics in Bivalves

The majority, if not all, of the bivalves sampled from each of the seven sites accumulated microplastic within their digestive tract, resulting in frequency levels ranging between 80-100% (Table B-3). The highest mean particle concentration of microplastics was observed at AP (0.80 ± 0.21 particles/g ww), while the lowest were recorded at EB (0.19 ± 0.040 particles/g ww). A summary of mean microplastic particle concentrations at each site is shown in Table B-3. Further categorization of these concentrations into mean particles/g ww of micro-spheres, micro-fragments, micro-fibers, micro-film is shown in Table B-4.

Microplastics particle concentrations failed to comply with parametric assumptions (i.e., $p \leq 0.05$ in Shapiro-Wilk's test) regardless of transformation, hence a non-parametric Kruskal-Wallis and Steel-Dwass post-hoc analysis was performed. A significant difference in particle concentrations between sites ($chi\text{-squared} = 35.8$, $df = 6$, $p < 0.0001$) was observed in the Kruskal-Wallis analysis (Figure 3.4). Pairwise comparisons amongst the sites showed that AP significantly differed in mean microplastic particle concentrations from BMP ($p = 0.022$), EB ($p = 0.0031$), and J ($p = 0.0019$) (Figure 3.4). In addition, TB was observed to significantly differ from BMP ($p = 0.035$), EB ($p = 0.0058$), and J ($p = 0.0059$) in mean microplastic concentrations (Figure 3.4).

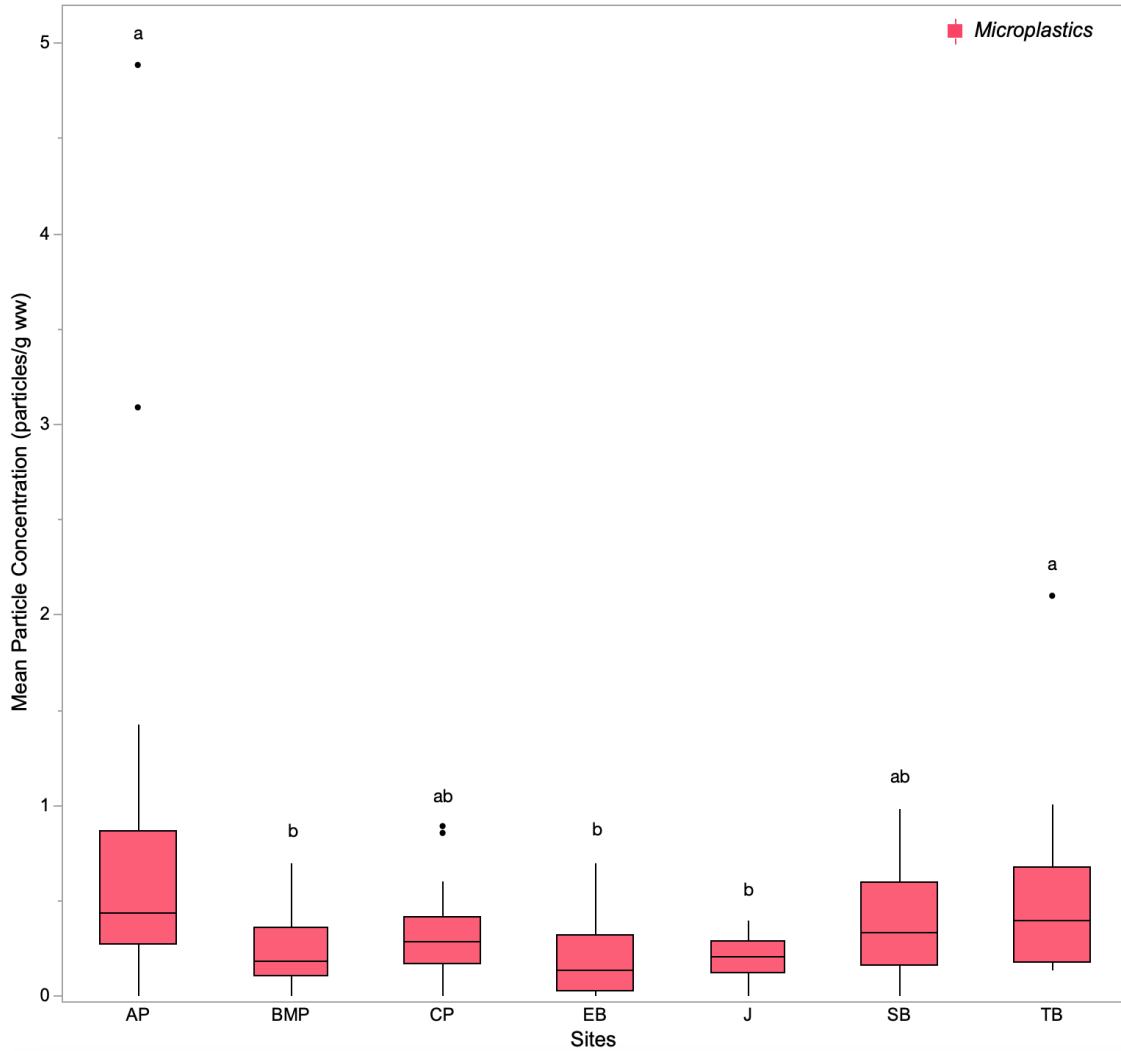


Figure 3.4 Microplastic concentrations recovered from *Nutallia obscurata* sampled at seven intertidal sites in Burrard Inlet. Boxplots demonstrating the median values (thick horizontal black line within box), the lower and upper 25th and 75th percentiles (upper and lower boundaries of box), the minimum and maximum values (whiskers) and any outliers (black dots) are presented. A total of N = 175 bivalves were collected at a sample size of n = 25 per site. Sites (left to right): Ambleside Park (AP), Barnet Marine Park (BMP), Cates Park (CP), English Bay (EB), Jericho Beach (J), Spanish Banks (SB), and Third Beach (TB). A Kruskal-Wallis followed by Steel-Dwass post-hoc analysis was used to determine significant difference between particles concentrations (particles/g ww) across the sites. A significant effect between the sites ($\chi^2 = 35.8$, $df = 6$, $p < 0.0001$) was observed. Different superscript letters indicate significant differences ($p < 0.05$).

3.1.5. Cyanox®53 in Bivalves

Particle concentrations of Cyanox®53 were recovered in bivalves from four out of the seven surveyed sites (AP, BMP, EB, and SB). Between 4-44% of the individuals possessed Cyanox®53 within their digestive tract (Table B-5). Among these four sites, the highest mean particle concentration of Cyanox®53 was observed at AP (0.25 ± 0.21 particles/g ww), while the lowest were detected at BMP (0.0048 ± 0.0048 particles/g ww). A summary of mean Cyanox®53 particle concentrations at each site is shown in Table B-5.

Cyanox®53 particle concentrations failed to comply to parametric assumptions (i.e., $p \leq 0.05$ in Shapiro-Wilk's test) regardless of transformation. Skewness in the normality of Cyanox®53 concentrations was attributed to non-detectable measurements at CP, J, and TB. As a result, a non-parametric Kruskal-Wallis and Steel-Dwass post-hoc analysis was performed. A significant difference in particle concentrations between sites (*chi-squared* = 40.7, *df* = 6, $p < 0.0001$) was observed in the Kruskal-Wallis analysis (Figure 3.5). In pairwise comparisons amongst the sites, EB significantly differed in mean Cyanox®53 particle concentrations from BMP ($p = 0.015$), CP ($p = 0.0046$), J ($p = 0.0046$), and TB ($p = 0.0046$) (Figure 3.5).

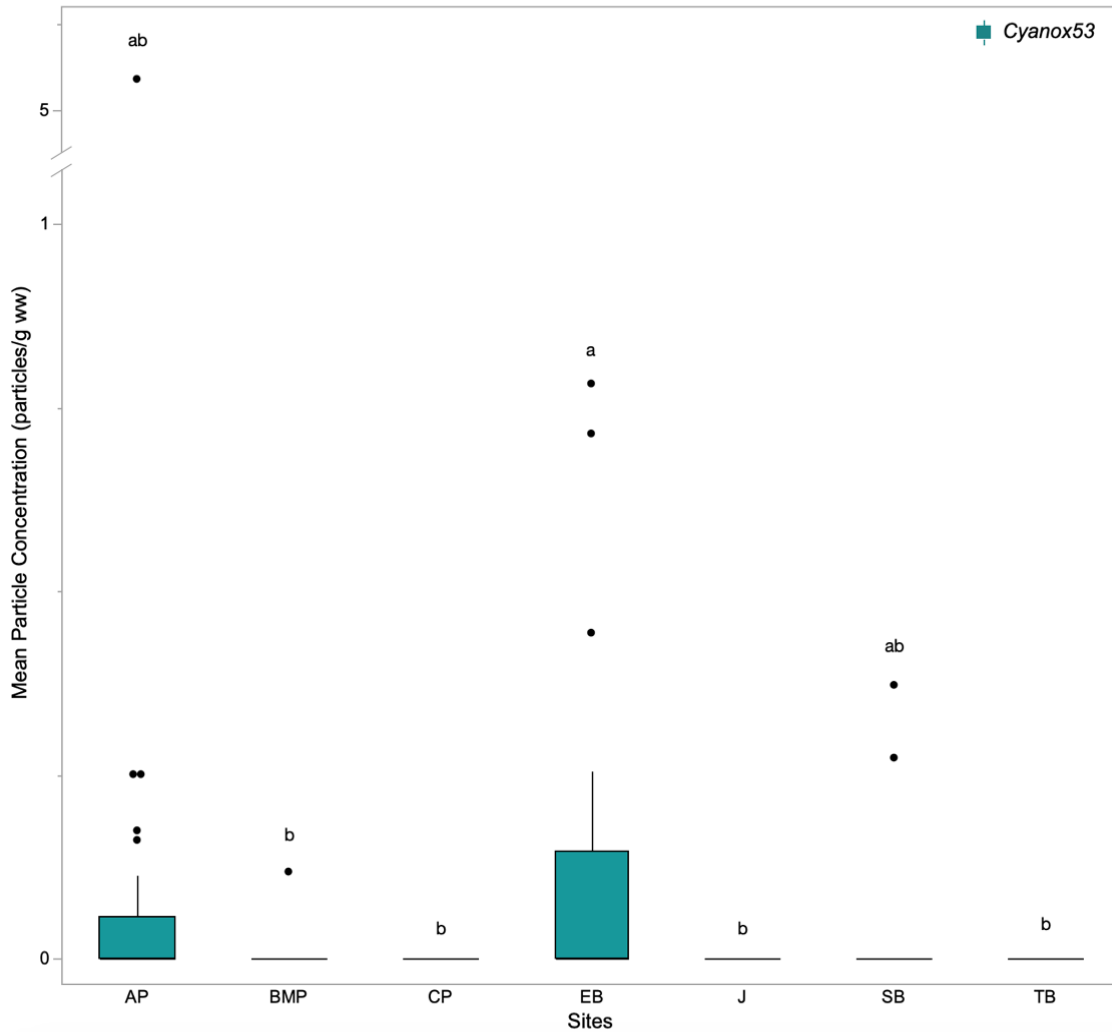


Figure 3.5 Cyanox®53 concentrations recovered from *Nutallia obscurata* sampled at seven intertidal sites in Burrard Inlet. Boxplots demonstrating the median values (thick horizontal black line within box), the lower and upper 25th and 75th percentiles (upper and lower boundaries of box), the minimum and maximum values (whiskers) and any outliers (black dots) are presented. Note the break indicated by slashed lines on the y axis. A total of N = 175 bivalves were collected at a sample size of n = 25 per site. Sites (left to right): Ambleside Park (AP), Barnet Marine Park (BMP), Cates Park (CP), English Bay (EB), Jericho Beach (J), Spanish Banks (SB), and Third Beach (TB). A Kruskal-Wallis followed by Steel-Dwass post-hoc analysis was used to determine significant difference between particles concentrations (particles/g ww) across the sites. A significant effect between the sites ($\chi^2 = 40.7$, $df = 6$, $p < 0.0001$) was observed. Different superscript letters indicate significant differences ($p < 0.05$).

3.1.6. Biota-Sediment Accumulation Factor Ratios

Collectively, particle concentrations concentrated in bivalve tissue exceeded concentrations deposited in surface sediment samples. Ratios ranging from 12.2 to 88.7 were calculated for microplastics, while Cyanox®53 demonstrated ratios between 0 and 147. A summary of these ratios is shown in Table 3.1.

Table 3.1 Biota-Sediment Accumulation Factor ratios based on mean microplastic and Cyanox®53 concentrations recovered from bivalves and sediment sampled at seven intertidal regions in Burrard Inlet.

| Site | Microplastic | Cyanox®53 |
|------|--------------|-----------|
| AP | 88.7 | 147 |
| BMP | 23.1 | 4.8 |
| CP | 35.7 | - |
| EB | 12.2 | 76.3 |
| J | 29.3 | - |
| SB | 27.7 | 77.7 |
| TB | 34.9 | - |

3.2. ATR-FTIR, ESI-LC/MS, and ¹H-NMR

3.2.1. ATR-FTIR

In total, 92 fragments (< 5 mm in size) were recovered from bivalve and sediment samples and positively associated with Cyanox®53 at a good level of confidence (≥ 70%). The majority of these fragments were identified as a chemical mixture of Cyanox®53 with either PVDF (49) or PE (8), while the remaining 35 fragments were assigned the distinct chemical identity of Cyanox®53. Following background noise removal, clean ATR-FTIR spectra were obtained for Cyanox®53-PVDF, Cyanox®53-PE and Cyanox®53. Photographs of field-collected fragments pertaining to these chemical identities, along with their ATR-FTIR spectrum, are shown in Figure 3.6.

Through evaluation of Cyanox®53's ATR-FTIR spectra, notably, 10 absorbance peaks were detected between 3600-600 cm⁻¹. More precisely, these peaks were observed at wavelengths indicative of hydroxyl alcohols (at 3600-3300 cm⁻¹ and 950-800 cm⁻¹), in-plane, out-of-plane and radical alkyls (at 3450-3300 cm⁻¹, 2850-2750 cm⁻¹, 1250-1000 cm⁻¹, and 790-600 cm⁻¹), and two aromatic rings (at 3100-2750 cm⁻¹, 2600-

2450 cm^{-1} , 1800-1700 cm^{-1} , and 1600-1250 cm^{-1}). The resultant sorption peaks and their accompanying functional group assignments is shown in Table 3.2.

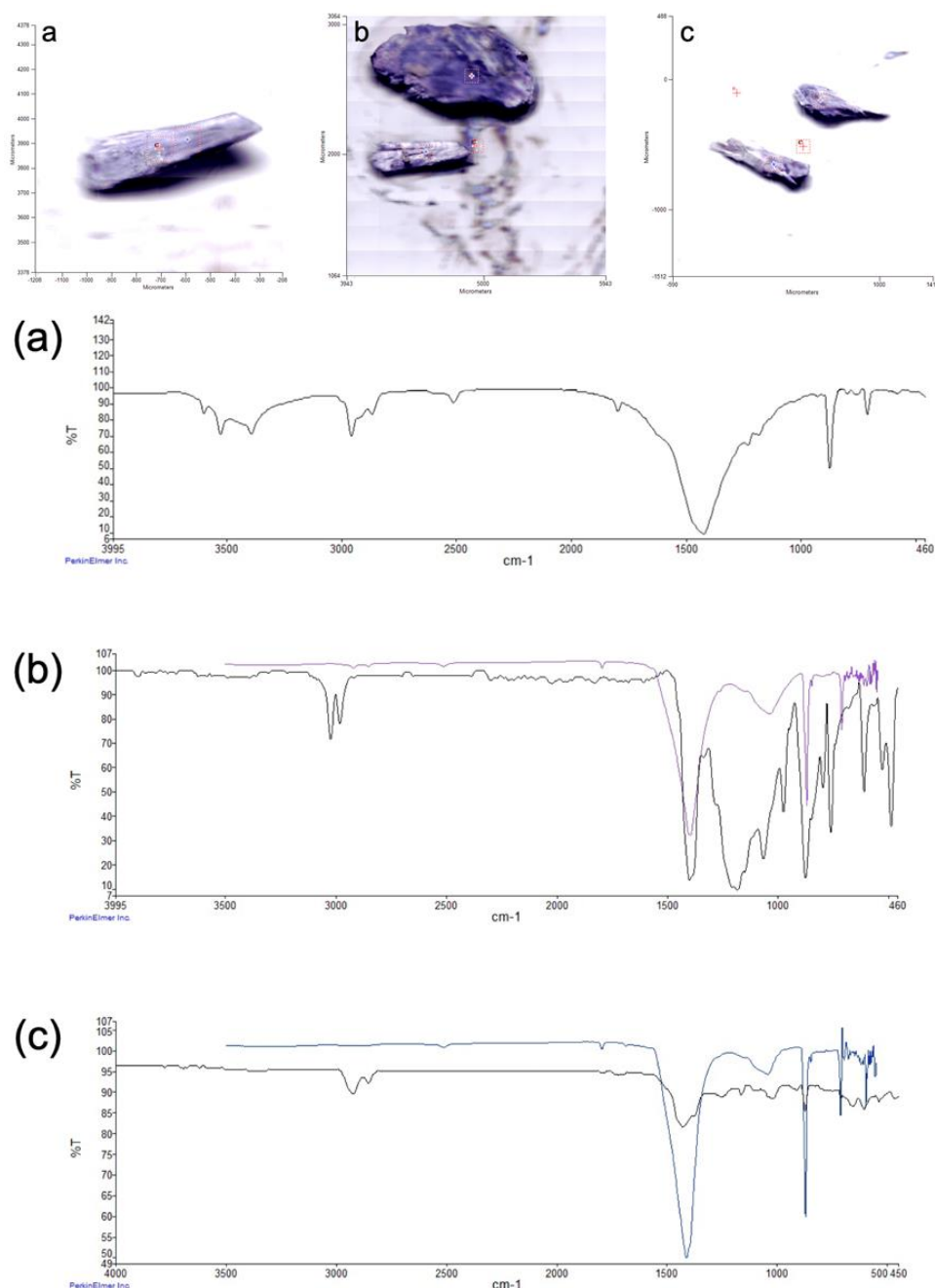


Figure 3.6 Fragments recovered from Burrard Inlet along with their matching ATR-FTIR spectra. (a) Cyanox®53, (b) Cyanox®53-PVDF, and (c) Cyanox®53-PE. Absorption band intensities in the ATR-FTIR spectra were measured based on transmittance (%) against wavenumbers (cm^{-1}) between 4000 cm^{-1} to 450 cm^{-1} .

Table 3.2 ATR-FTIR sorption peaks of Cyanox®53 based on leached Cyanox®53 and Cyanox®53-PVDF samples.

| IR Peak | Wavelength Range (cm ⁻¹) | Intensity Shape | Functional Group |
|---------|--------------------------------------|-----------------|---|
| 1 | 3600-3300 | weak, broad | O-H stretch (free; overlaps C-H stretch) |
| 2 | 3450-3300 | weak | C-H bend (radical on aromatic; overlapped by O-H stretch) |
| 3 | 3100-2750 | weak | C-H stretch (aromatic ring) |
| 4 | 2850-2750 | weak | C-H bend (in-plane alkyl on aromatic) |
| 5 | 2600-2450 | weak | Overtone band (aromatic) |
| 6 | 1800-1700 | weak | Overtone band (aromatic) |
| 7 | 1600-1250 | strong, sharp | C=C stretch (in aromatic ring) |
| 8 | 1250-1000 | weak | C-H bend (in-plane alkyl on aromatic) |
| 9 | 950-800 | medium, sharp | O-H bend |
| 10 | 790-600 | weak | C-H bend (out-of-plane on aromatic) |

3.2.2. ESI-LC/MS

As expected, all three reference chemicals produced spectra that aligned with literature measurements (Figure C-2). Specifically, the m/z values of 228.2 Da, 340.3 Da, and 368.3 Da were obtained with 100% certainty for BPA, Cyanox®2246, and Cyanox®425, respectively. In the Cyanox®53-PVDF sample, four individual intensity peaks were observed at retention times 5.26, 6.75, 7.16 and 7.46 min (Figure 3.7). Similarly, in the Cyanox®53 sample five distinct intensity peaks were observed at retention times 5.31, 6.06, 6.75, 7.14, and 7.46 min (Figure 3.7). Through process of elimination, the intensity peak that was detected at retention times 7.14 and 7.16 min in Cyanox®53 and Cyanox®53-PVDF, respectively, had equivalent molar masses of 358.4

Da with 100% certainty. Accordingly, the m/z value of 358.4 Da was deemed the authentic molecular mass for Cyanox®53.

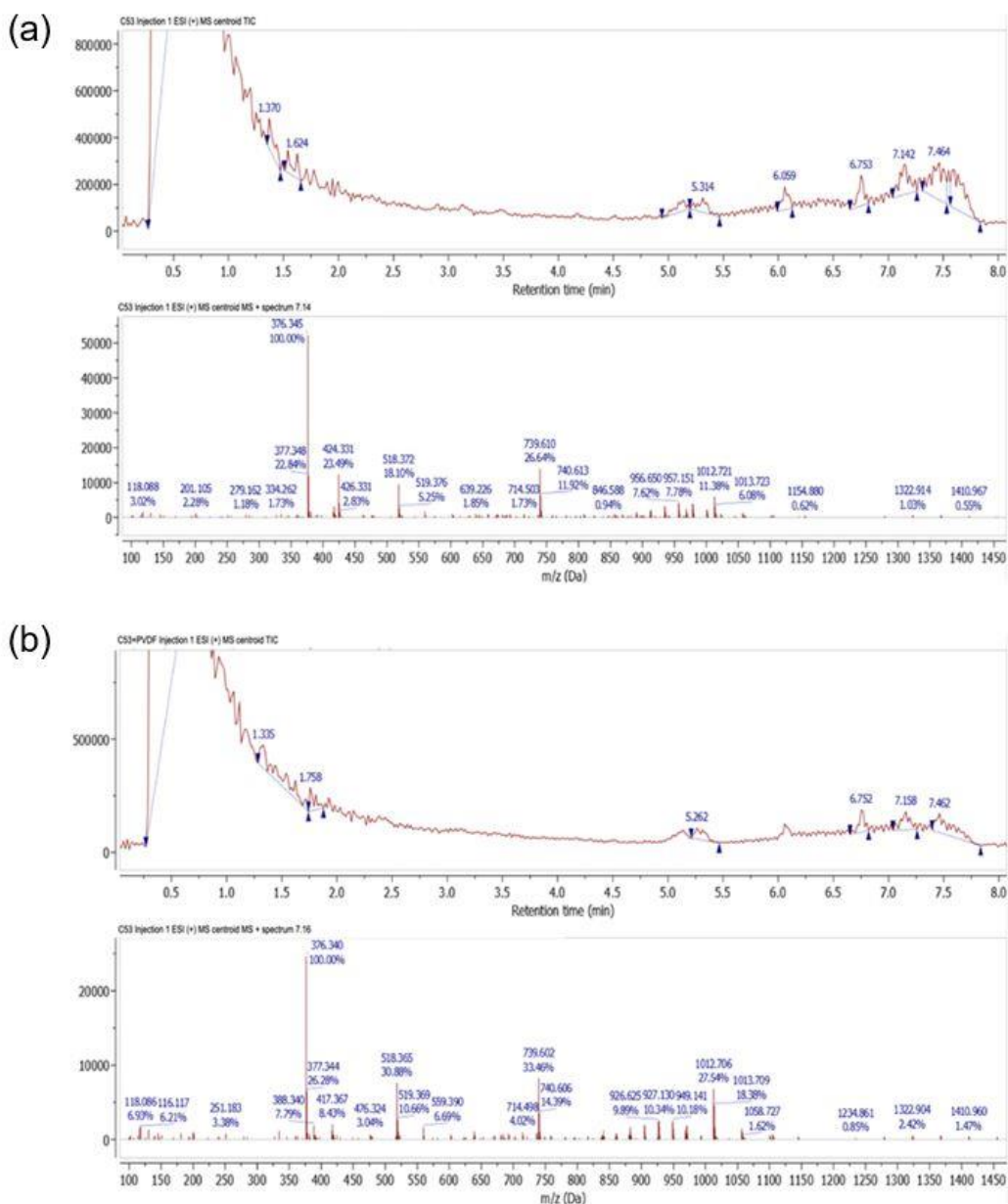


Figure 3.7 ESI-LC/MS spectra of leached Cyanox®53 fragments. (a) Cyanox®53 and (b) Cyanox®53-PVDF. ESI-LC/MS intensities were measured in positive ion mode against retention time (min) and m/z values (Da). Most relevant ion intensities are shown at retention times 7.14 for (a) Cyanox®53, and 7.16 for (b) Cyanox®53-PVDF.

3.2.3. ¹H-NMR

¹H-NMR spectra were obtained for leached Cyanox®53-PVDF and Cyanox®53 (Figure 3.8) and reference chemicals BPA, Cyanox®2246, and Cyanox®425 (Figure C-3). Peaks corresponding to water (3.50 ppm) and DMSO-d₆ (2.50 ppm) were considered as negligible background and hence ignored. Predictably, four distinct peaks were detected in BPA at 9.14, 6.98, 6.64 and 1.53 ppm and directly translated to integration values of 1.02 (hydroxyl), 2.08 (hydrogen), 2.06 (hydrogen), and 3.12 (methyl), respectively (Table C-2). For Cyanox®2246, chemical shifts at 8.25, 6.84, 6.64, 3.82, 2.13, and 1.35 ppm were observed and correlated to the integrations of 1.01 (hydroxyl), 1.06 (hydrogen), 1.05 (hydrogen), 1.07 (methylene bridge), 3.22 (methyl), and 9.78 (*tert*-butyl), respectively (Figure C-3). Similarly, chemical shifts at 8.24, 6.87, 6.67, 3.85, 2.42, 1.36, and 1.08 ppm were observed in Cyanox®425, which evidently coincided with the integrals of 0.98 (hydroxyl), 1.02 (hydrogen), 1.02 (hydrogen), 1.01 (methylene bridge), 2.09 (methylene), 9.51 (*tert*-butyl), and 3.16 (methyl), respectively (Table C-2). In the case of Cyanox®53-PVDF and Cyanox®53, identical chemical shifts and integral values were obtained (Figure 3.8). Peaks appeared at 8.47, 5.91, 5.86, 1.24 and 0.86 ppm, and corresponded to the integral values of 1.00 (hydroxyl), 1.08 (hydrogen), 1.08 (hydrogen), 9.52 (*tert*-butyl) and 3.36 (methyl), respectively. A summary of these ¹H-NMR measurements and structural assignments for each chemical is shown in Table 3.3.

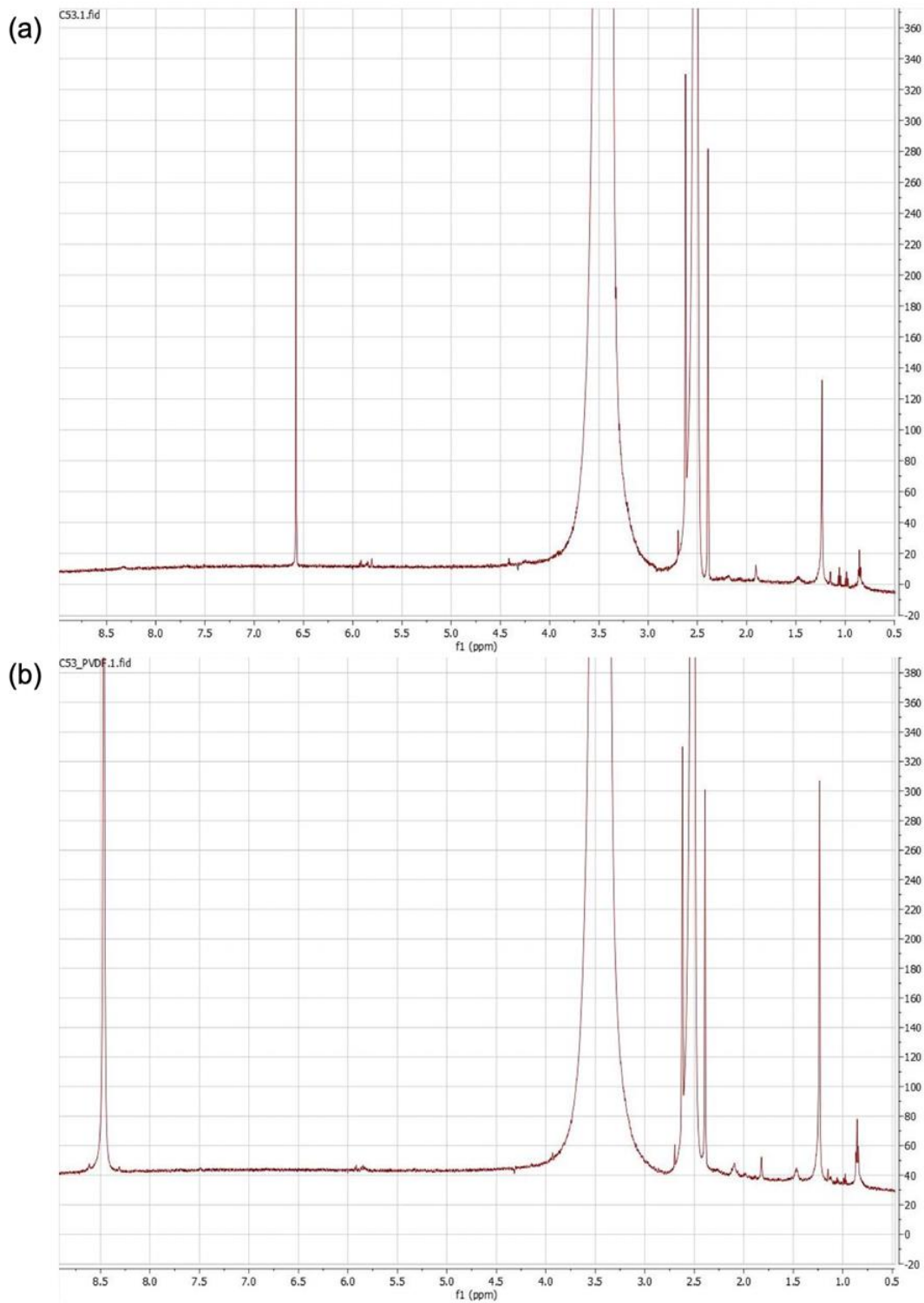
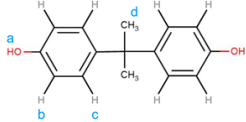
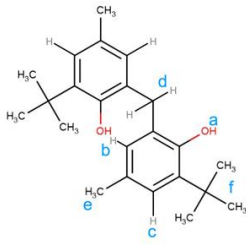
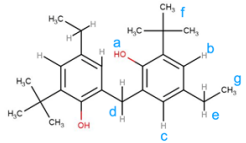
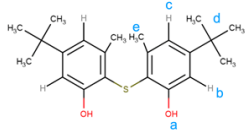


Figure 3.8 ¹H-NMR spectra of leached Cyanox®53 fragments. (a) Cyanox®53 and (b) Cyanox®53-PVDF. Proton peaks are measured based on intensity (ranging from 0 to 380) against chemical shift values (ppm) between 0.5 and 8.75 ppm.

Table 3.3 $^1\text{H-NMR}$ measurements and structural assignment of Bisphenol A, Cyanox®2246, Cyanox®425, and Cyanox®53. For each chemical, the notation, shift (ppm), integral label, hydrogen type and visual assignments are provided.

| Chemical | Notation | Shift (ppm) | Integral Label | Hydrogen Type | Assignment |
|-------------|----------|-------------|----------------|---|---|
| Bisphenol A | a | 9.14 | 1.02 | hydroxyl (OH) |  |
| | b | 6.98 | 2.08 | H on ring | |
| | c | 6.64 | 2.06 | H on ring | |
| | d | 1.53 | 3.12 | methyl (CH ₃) | |
| Cyanox®2246 | a | 8.25 | 1.01 | hydroxyl (OH) |  |
| | b | 6.84 | 1.06 | H on ring | |
| | c | 6.64 | 1.05 | H on ring | |
| | d | 3.82 | 1.07 | methylene bridge (CH ₂) | |
| | e | 2.13 | 3.22 | methyl (CH ₃) | |
| | f | 1.35 | 9.78 | <i>tert</i> -butyl (C ₄ H ₉) | |
| Cyanox®425 | a | 8.24 | 0.98 | hydroxyl (OH) |  |
| | b | 6.87 | 1.02 | H on ring | |
| | c | 6.67 | 1.02 | H on ring | |
| | d | 3.85 | 1.01 | methylene bridge (CH ₂) | |
| | e | 2.42 | 2.09 | methylene (CH ₂) | |
| | f | 1.36 | 9.51 | <i>tert</i> -butyl (C ₄ H ₉) | |
| | g | 1.08 | 3.16 | methyl (CH ₃) | |
| Cyanox®53 | a | 8.47 | 1.00 | hydroxyl (OH) |  |
| | b | 5.91 | 1.08 | H on ring | |
| | c | 5.86 | 1.08 | H on ring | |
| | d | 1.24 | 9.52 | <i>tert</i> -butyl (C ₄ H ₉) | |
| | e | 0.86 | 3.36 | methyl (CH ₃) | |

3.3. Structure and QSAR Modelling

3.3.1. Proposed Molecular Structure

Collected ATR-FTIR, ¹H-NMR, and ESI-LC/MS data allowed for the elucidation of a feasible chemical formulation for Cyanox®53 as C₂₂H₃₀O₂S, more specifically 2,2'-thiobis(3-methyl-5-tert-butylphenol). Application of JChem Office directly translated 2,2'-thiobis(3-methyl-5-tert-butylphenol) to the SMILES notation of CC1=C(SC2=C(C)C=C(C=C2O)C(C)(C)C)C(O)=CC(=C1)C(C)(C)C. A two-dimensional and three-dimensional software rendering of Cyanox®53's molecular structure is shown in Figure 3.9. Interestingly, a chemical search by SMILES notation in PubChem, ChemSpider and CompTox Dashboard databases returned no known CAS registry number for this structure. The proposed SMILES notation was used to obtain QSAR-based estimations of physical/chemical and environmental fate properties, aquatic toxicity, and relative toxicology hazard for Cyanox®53.

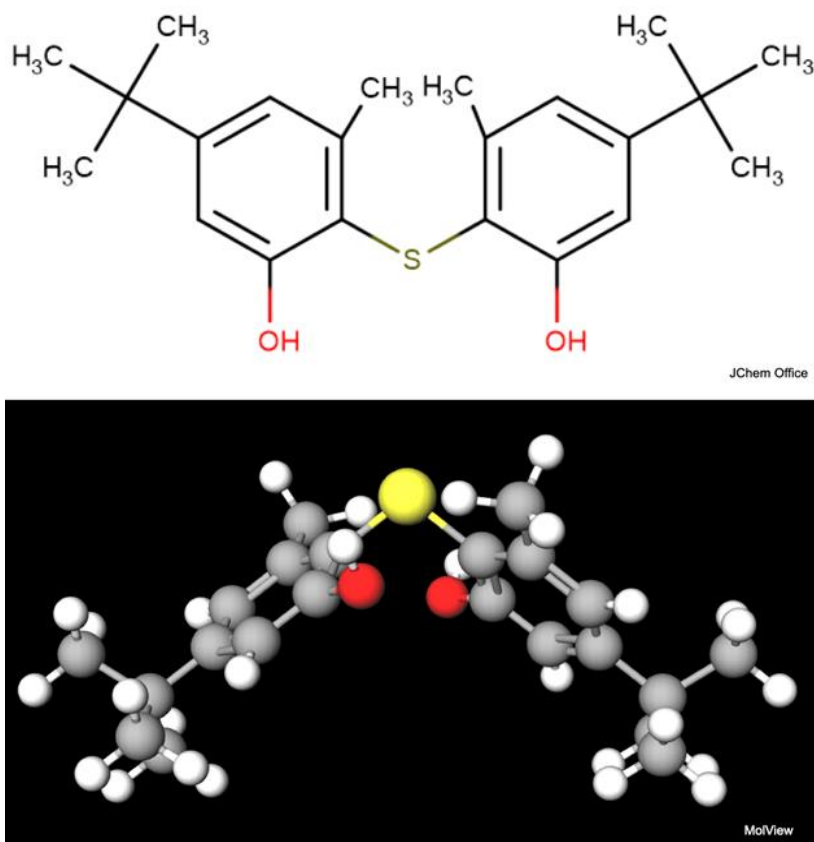


Figure 3.9 Proposed molecular structure of Cyanox®53. Two-dimensional (top) and three-dimensional (bottom).

3.3.2. EPI Suite™

Predictions of physical/chemical environmental fate and aquatic toxicity properties were successfully made for Cyanox®53 (Table 3.4). Based on the atom/fragment contribution, a log K_{ow} value of 8.24 was estimated. In addition, the melting and boiling point for Cyanox®53 were estimated at 196°C and 466°C, respectively. Water solubility estimates (at 25 °C) of 0.00191 mg/L (based on log K_{ow}) and 0.0568 mg/L (based on chemical fragments) were calculated for Cyanox®53 by WSKOWWIN™ and WATERNT™, respectively.

To estimate the BCF and BAF in fish, BCFBAF™ invokes two models, the first being a traditional regression based on log K_{ow} , and the second being the Arnot-Gobas upper trophic method. The following BCF and BAF estimations were acquired: BCF = 3,270 L/kg wet-wt (regression), BCF = 28.22 L/kg wet-wt (Arnot-Gobas upper trophic), and BAF = 308 L/kg wet-wt (Arnot-Gobas upper trophic). With respect to the predicted biotransformation half-life in fish, BCFBAF™ estimated Cyanox®53 to have a half-life equivalent to 2.5 days (normalized to a 10 g fish).

Calculated rapid biodegradability estimates were simulated under aerobic and anaerobic conditions. An ultimate survey and primary survey timeframe of 1.946 (months) and 2.966 (weeks), respectively, and a MITI linear model value of 0.0274 were estimated in the evaluation of rapid biodegradability. Accordingly, the BIOWIN™ model criteria for rapid biodegradation was not satisfied. Moreover, log K_{oc} estimates of 6.30 (based on MCI method) and 5.82 (based on K_{ow}) were obtained by KOCWIN™. Partitioning half-life times of Cyanox®53 in air, water, soil, and sediment under steady state conditions were estimated to be 1.27 hr, 60 d, 120 d, and 540 d, respectively. An estimated maximum half-life persistence of 189 d was computed.

ECOSAR™ was used to estimate acute toxicity endpoints at 50% lethal concentration (LC_{50}) for fish and *D. magna*, and 50% effective concentration (EC_{50}) for green algae. For fish, a simulated 96 hr exposure predicted a LC_{50} value of 0.0040 mg/L with a log K_{ow} maximum of 7.0. A LC_{50} value of 0.0020 mg/L with a log K_{ow} maximum of 5.5 was predicted for *D. magna* in a simulated 48 hr exposure. In the case of the green algae, a 96 hr exposure manifested a EC_{50} value of 0.058 mg/L with a maximum log K_{ow} of 6.4. Chronic toxicity effect endpoints were also predicted for fish, *D. magna* and green

algae based on a geometric mean between the lowest observed effects concentration (LOEC) and no observed effect concentration (NOEC) of the study. A maximum log K_{ow} cut-off was set to 8.0 (indicative of a poorly soluble chemical) as a baseline for comparison in fish, *D. magna* and green algae. Chronic effect concentrations of 0.00078 mg/L, 0.00062 mg/L, and 0.020 mg/L were predicted for fish, *D. magna*, and green algae, respectively.

3.3.3. Toxtree

Relative mammalian health hazards were predicted for Cyanox®53 (Table 3.4). Cyanox®53 was categorized as being not readily hydrolyzed and found not to contain toxicophoric groups (e.g., aromatic amine, amides, carboxyl, reactive oxygens, etc.). Based on its molecular structure, a Cramer class III (high hazard) toxicological level of concern designation and the lowest threshold of toxicological concern (TTC) value of 90 ug/day (1.5 ug/kg/bw/d) when administered orally were assigned. Regarding biodegradability and persistence, Cyanox®53 was assessed as a class II (persistent chemical) because of its terminal *tert*-butyl groups. No alerts of potentially causing DNA lesions, including nucleophilic substitution (SN1) reactions, Schiff base formation, acyl transfer agents, or nucleophilic aliphatic substitution (SN2) reactions, were indicated during the protein and DNA binding predictions. However, Cyanox®53 was identified as a Michael acceptor, an electrophilic agent with the potential to covalently bind to the nucleophilic sites of proteins and DNA in organisms. Model simulation of an *in vitro* test (i.e., Ames test) for mutagenicity based on the ISS model reported no alerts for strain *S. typhimurium* and therefore deemed a non-mutagenic classification. Similarly, a model simulation of an *in vivo* micronucleus assay in rodents based on the ISS model did not identify Cyanox®53 as a substance that could cause cytogenetic damage (class II). By discriminant analyses and structural rules, Cyanox®53 was negative for genotoxic and non-genotoxic carcinogenicity. Cytochrome P450 mediated drug metabolism was simulated. The model predicted that Cyanox®53 was potentially capable of undergoing S-oxidation at the primary site of metabolism, as well as aliphatic hydroxylation at the secondary site of metabolism and aromatic hydroxylation at the tertiary site of metabolism. The toxic mode of action (MOA) could not be predicted at this point according to the rules laid out in the Verhaar scheme.

Table 3.4 Comprehensive summary of estimated physiochemical, ecotoxicity and relative hazard properties of Cyanox®53 via QSAR modelling.

| QSAR Model | Profile Pluggin | Endpoint | Prediction |
|------------|---------------------|---|---|
| | KOWWIN™ | Log K _{ow} | 8.24 |
| | MPBPVP™ | Melting and boiling points | 196°C, 466°C |
| | WSKOWWIN™, WATERNT™ | Water solubility (at 25 °C) | 0.00191 mg/L (K _{ow} method), 0.0568 mg/L (chemical fragments method) |
| | BCFBAF™ | BAF | 308 L/kg wet-wt (Arnot-Gobas upper trophic method) |
| | - | BCF | 3,270 L/kg wet-wt (regression method), 28.22 L/kg wet-wt (Arnot-Gobas upper trophic method) |
| | - | Biotransformation half-life in fish | 2.5 days (normalized to a 10 g fish) |
| | BIOWIN™ | Biodegradability prediction | Not readily biodegradability |
| EPI Suite™ | KOCWIN™ | Log K _{oc} | 6.30 (MCI method), 5.82 (K _{ow} method) |
| | LEV3EPI™ | Partitioning half-life in air, water, soil, and sediment (under steady conditions); persistence time (max half-life in environment) | 1.27 hr (air), 60 d (water), 120 d (soil), and 540 d (sediment); 189 d (persistence time) |
| | ECOSAR™ | Fish, LC ₅₀ (96 hr) | 0.0040 mg/L, max log K _{ow} at 7.0 |
| | - | Daphnia magna, LC ₅₀ (48 hr) | 0.0020 mg/L, max log K _{ow} at 5.5 |
| | - | Green algae, EC ₅₀ (96 hr) | 0.058 mg/L, max log K _{ow} at 6.4 |
| | - | Fish, chronic | 0.00078 mg/L, max log K _{ow} at 8.0 |
| | - | Daphnia magna, chronic | 0.00062 mg/L, max log K _{ow} at 8.0 |
| | - | Green algae, chronic | 0.020 mg/L, max log K _{ow} at 8.0 |

| QSAR Model | Profile Pluggin | Endpoint | Prediction |
|------------|---|---|--|
| | Cramer rule decision tree | Toxicological level of concern (when administered orally) | Cramer class III (high hazard); 90 ug/day (1.5 ug/kg/bw/d) TTC value |
| | START biodegradability and persistence | Biodegradability and persistence | Class II (persistent chemical) |
| | Benigni/Bossa rule-base | Carcinogenicity and mutagenicity | Negative for genotoxic and non-genotoxic carcinogenicity |
| Toxtree | SMARTCyp | CYP 450 mediated drug metabolism | S-oxidation (primary), aliphatic hydroxylation (secondary) and aromatic hydroxylation (tertiary) |
| | Protein and DNA binding alert | Protein and DNA binding ability | Michael acceptor |
| | ISS <i>in vitro</i> mutagenicity (Ames test) alerts | Mutagenicity | Non-mutagenic |
| | ISSMIC | Rodent micronucleus assay (<i>in vivo</i>) | Does not cause cytogenetic damage (class II) |
| | Verhaar scheme | Toxicity MOA | Could not be classified |

4. Discussion

The purpose of this present investigation was two-fold: i) detect the presence of Cyanox®53 in Burrard Inlet, BC; and ii) estimate the environmental persistence, bioaccumulation potential and toxicity of Cyanox®53 using accepted model simulations based on a proposed molecular structure. Expanding upon Bendell et al. (2020), the environmental survey conducted in this study successfully recovered Cyanox®53 concentrations, along with microplastic concentrations, in both the surface sediments and varnish clams sampled from several sites in Burrard Inlet, BC. In addition, this study was the first to apply ATR-FTIR, ESI-LC/MS and ¹H-NMR to identify a plausible chemical structure for Cyanox®53. It was from this proposed structure that the environmental fate and potential toxicity of Cyanox®53 were predicted in EPI Suite™ and Toxtree. Most notably, Cyanox®53 was predicted to be a persistent chemical unlikely to bioaccumulate; however, it is uncertain if it can elicit toxicity to aquatic organisms.

4.1. Environmental Survey and Potential Sources

4.1.1. Cyanox®53 Concentrations

As predicted, Cyanox®53 concentrations were found to be the most abundant near the First Narrows strait (mouth of outer and inner harbour) in Burrard Inlet, BC where majority of the Port of Vancouver is centralized. The highest levels of Cyanox®53 were presented at AP and EB in both sediments and bivalves, yet no significant difference was seen between these elevated sites in either sampling mediums. Although levels of Cyanox®53 from AP did not differ significantly from the sediments or bivalves from the other sites, concentrations from EB did significantly differ from BMP, CP, J, and TB in the collected bivalves. The differences between EB and CP, J, or TB are not surprising as those latter three sites did not record detectable concentrations of Cyanox®53 in either surface sediments or bivalves. Thus, the only true significant difference in Cyanox®53 concentrations within bivalves between sites worth acknowledging would be between EB and BMP. The high abundance of Cyanox®53 at EB seen in this study coincides with recent reports of Cyanox®53 concentrations being found in field-collected varnish clams during a survey near False Creek and English Bay (Achiluzzi, 2022). Moreover, the results in this present study congruent with those of

Bendell et al. (2020), who found Cyanox®53 concentrations in bivalves sampled from AP, BMP, CP, EB, and J. However, unlike the previous survey, concentrations of Cyanox®53 were not detected at CP or J.

A possible reason for the lack of Cyanox®53 concentrations at CP and J could be that temporal factors, such as seasonality or heavy precipitation, influenced the distribution of the surveyed concentrations. In most instances microplastics, and alike particles, are carried into the marine-coastal environment either by atmospheric deposition (i.e., wind), urban runoff (i.e., wastewater treatment plants, storm drains and combined sewer overflows), oceanic or river currents, bioturbation, or wildlife (Espinosa et al., 2016; Gallo et al., 2018; Braig et al., 2019; Crawford & Quinn, 2019). Of these dynamics, however, arguably the biggest contributors to fluctuations in environmental microplastic abundances and distribution over short periods of time are hydroclimatic and hydrodynamic factors (Talbot & Chang, 2022). Indeed, it has been suggested that precipitation may serve to transport land-based microplastics into aquatic environments (Talbot & Chang, 2022). According to Schmidt et al. (2018), microplastic levels in aquatic environments tend to be significantly higher after a long-lasting dry period (e.g., several weeks) and subsequent rain event (e.g., flash flood), as opposed to samples collected during a dry period. In Burrard Inlet, the frequency and magnitude of rainfall events varies significantly throughout the year and have only become more pronounced as climate change continues to be an issue (BCMOE, 2015). Though the wettest months in Vancouver, BC, take place during the Fall season (mid-September to late November), rainfall events are still prevalent in the Spring (mid-March to early June), ranging from light drizzles to flash floods after a dry period. In this study, sampling took place during late May to early June, meaning the occurrence of rainfall was probable. On average, 65 mm of precipitation over 13 days of the month is expected during May in Vancouver, BC (World Weather & Climate Information, 2022). Similarly, in June an average of 53 mm of precipitation over a total of 12 days can be expected (World Weather & Climate Information, 2022). Against this background, it is possible that any Cyanox®53 particles dispersed along the beach could have been transported from the surface sediments to the oceanic water column by rainfall before the time of sampling. It is also worth noting that varnish clams are typically found in the mid to high intertidal zones, particularly in brackish waters near freshwater streams or groundwater seepage that connect with the incoming tide. Thus, the likelihood of any Cyanox®53 particles being washed away and

carried towards the water column increases. Given these points, it can be assumed that the distribution of Cyanox®53 concentrations were influenced by environmental factors.

4.1.2. Potential Source(s) of Cyanox®53

Like Knutsen et al. (2019) and Bendell et al. (2020), a key characteristic of the field-collected Cyanox®53 particles in this study were their disassociation from its inert carrier and abnormal presentation as a separate entity with a white fibrous, fragmented exterior. It is unknown why this alleged powdered additive continues to emerge as a solid at beaches. Moreover, there is little information available on how Cyanox®53 fragments are being discharged into the environment. While the literature may not be able to offer definitive answers to these questions, perhaps a clue may come from the physical results. Namely, the fact that field-collected Cyanox®53 continue to emerge as white fibrous fragments in locations with high anthropogenic activity.

Burrard Inlet has an extensive industrial history with the logging of old growth forests, use as a route for commercial trade and different maritime activities (e.g., shipbuilding, wood creosoting, manufacturing, boating), and offers space for the urbanization and development of residential areas (Bendell et al., 2020). While these assets and uses make the inlet a vital marine system of considerable ecological and economic importance, simultaneously such anthropogenic pressures also negatively impact ecologically rich habitats, as well as many marine species (i.e., salmon, whales, clams, crab, and waterfowl), and have made the shallow costal fjord become a hotspot for legacy contaminants and microplastic pollution (Environment Canada, 1998; Braig et al., 2019; Morin & Evans., 2022). According to Taft et al. (2022), intense shoreline alterations and colonial development has removed 1,214 ha of intertidal and subtidal areas, with the most severe changes occurring at False Creek Flats (> 99% intertidal area lost), the Capilano River Estuary (80% intertidal area lost), and the Seymour-Lynn Estuary (56% intertidal area lost). Taking this into account, one can speculate that a link exists between Cyanox®53 particles and these alterations in the inlet's landscape, particularly construction and engineering applications. Such a claim is reasonable because Cyanox®53 can be integrated into cable resins, coating liners of PE wiring and thermally insulated piping, and that some Cyanox® variants (i.e., Cyanox®2246 and Cyanox®425) provide processing and thermal stability in rubbers products, acrylics, and

polyolefins marketed to the pharmaceutical and construction industries (Flick, 2001; Solvay, 2022). To explore this speculation, further investigation is required.

Another plausible source of Cyanox®53 is through pyrotechnics. Every year, Vancouver, BC hosts several fireworks events including New Year's, Canada Day, Halloween, and most notoriously the "Honda Celebration of Light", a three-night off-shore international fireworks competition held in English Bay annually at the end of July. Fireworks are a significant source of microplastic debris that contribute to atmospheric, terrestrial, freshwater, and marine pollution (Devereux et al., 2022). Though it depends on the type of firework involved, a pyrotechnic mixture contains roughly 10% of a polymeric binder, either made from a natural material (e.g., starch), synthetic material (e.g., novolac), or a synthetic polymer (e.g., PVC) (Naik and Patil, 2015; Toader et al., 2017; Devereux et al., 2022). In certain circumstances, fireworks may also include plastic attachments, such as a mortar/tube on the bottom end to boost their momentum at launch, or a cone at the top to aid their flight pattern, in which case additional plastic debris is likely to discharge upon denotation (Naik and Patil, 2015; Devereux et al., 2022). From this perspective, it is therefore possible that antioxidants, like Cyanox®53, would be incorporated either directly into the pyrotechnic composition, or indirectly in the outer plastic attachments if equipped, to offer stability. Coupled with the fact that the fragmented nature of Cyanox®53 particles were comparable in appearance to frayed firework shrapnel, there is reasonable ground to the suggestion that Cyanox®53 may be connected to pyrotechnics; however, further investigation (e.g., inspection of firework product ingredients) is warranted to confirm this.

4.1.3. Microplastic Concentrations

Apart from Cyanox®53, a high abundance of microplastics (most commonly HDPE, LDPE, PP, PS, and PVC, and PVDF) was also recovered in sediments and clam tissue, with concentrations being more abundantly prevalent than Cyanox®53 at all assessed sites in both sampling mediums. Expressed BSAF ratios demonstrated that bivalves accumulated higher mean particle concentrations, more frequently microplastics (80-100%), in their guts and gills than the intertidal sediment samples. Compared to other studies, the compiled microplastic concentrations in this study were consistent with the abundance ranges expressed in infaunal bivalves of other worldwide environments (Baechler et al., 2019; Hermabessiere et al., 2019; Gedik & Eryasar, 2020; Wakkaf et

al., 2020; Ding et al., 2021; Truchet et al. 2021). The higher abundance of microplastics than Cyanox®53, especially in the bivalves, comes as no surprise given that bivalves species, (e.g., *Venerupis philippinarum*, *Siliqua patula*, *Mytilus edulis*, and even *Crassostrea gigas*) have a history of use as biomarkers of microplastic contamination levels, as well as pollutants, hypoxia, and algal toxins, occupying the water column and surrounding sediments (Baechler et al., 2019; Hermabessiere et al., 2019; Bendell et al., 2020; Cho et al., 2021; Huffman Ringwood, 2021). Moreover, bivalves from areas with intensive anthropogenic activities, like Burrard Inlet, tend to contain a significantly higher number of microplastics than those with fewer human activities (Li et al., 2016; Ding et al., 2021). Sediments act as a sink of microplastics negatively buoyant from weathering or biological interactions (i.e. plankton-formed aggregation or biofouling), hence bivalves, to varying degrees, will inevitably accumulate suspended microplastics as they pull particles (i.e. diatoms, bacteria, phytoplankton, etc.) into their incurrent siphons from the water column, or collect organic detritus from the sediment with their foot (Gillespie et al., 1999, 2001; Hidalgo-Ruz et al., 2012; Cho et al., 2021; Ding et al., 2021). If not discharged immediately from the body, microplastics ultimately end up permeating in the foot, mantle, gills, and digestive glands of the bivalve through adherence (Wang et al., 2021). In the case of this present study, the largely sessile, sediment dwelling varnish clams functioned as both suspension and deposit feeders, thereby increasing their likelihood of accumulating any marine debris and xenobiotic particles within the water interface and sediment (Gillespie et al., 2001). For this reason, it is hardly surprising that the bivalves bioaccumulated more particles than the surrounding sediment samples at each site. These results support the notion that bivalves, more specifically opportunistic feeding species, are suitable bioindicators of microplastic pollution. Moreover, it demonstrates that opportunistic bivalves could be used as indicators of microplastics bioaccumulation, perhaps based on the function of retention time and/or elimination rate of the microplastics in the bivalve, to support the categorization and screening of potentially bioaccumulative microplastics and nanoplastics in bioaccumulation assessments (Alava, 2021).

4.2. Compound Identification

Despite undergoing minor weathering degradation, recovered Cyanox®53 fragments successfully returned clean ATR-FTIR spectra at a $\geq 70\%$ level of confidence.

Relative intensities of the respective peaks were indicative of hydroxyl alcohols, in-plane, out-plane and radical alkyls, and two aromatic rings. When compared to other Cyanox® phenolic antioxidants, namely Cyanox®2246 and Cyanox®425, the functional groups observed in the obtained spectra comply with the key structural features of a bifunctional phenolic antioxidant compound. Interestingly, a prominent number of the analyzed Cyanox®53 fragments demonstrated chemical associations with other polymer forms, most chiefly PE and PVDF.

It is no accident that chemical signatures of PE and PVDF were reported by ATR-FTIR. The versatility of both thermoplastics, in terms of durability and tolerance to aggressive chemicals and mechanical impacts, has allowed them to be used in a multitude of applications, such as household goods, packaging, electronics, medical equipment, and structural and construction materials (Britannica, 2010; Dobbin, 2017; PVC Pipe Supplies, 2022). In the context of Cyanox®53, a convergence in practical applications materializes. To be exact, Cyanox®53 is also used in plastic packaging and construction materials (e.g., industrial wiring and cable resins, thermally insulated pipelines) (Flick, 2001; Cruce et al., 2014; Bolgar et al., 2016; Solvay, 2022). Provided this, it is highly likely that Cyanox®53 would be integrated into thermoplastics, such as PE and PVDF, which are commonly employed in industrial or packaging applications. This connection backs earlier deliberations of Cyanox®53 particles being linked to construction materials or pyrotechnics since PE and PVDF are used in such applications, either explicitly or implicitly.

The combined efforts of ESI-LC/MS and ¹H-NMR generated acceptable spectra such that a likely chemical structure for Cyanox®53 was determined. Leachates of Cyanox®53 and Cyanox®53-PVDF both returned equivalent molar masses of 358.4 Da with 100% certainty, and equivalent ¹H-NMR spectra with identical shifts and integral values, despite the diluted concentrations. The respective ¹H-NMR peaks for Cyanox®53 were deduced as hydroxyl hydrogen, *tert*-butyl, and methyl groups. There is currently no literature about MS and NMR data for Cyanox®53 for comparison. Alternatively, inspection of spectra from the SpectraBase™ database, as well as comparison to real-time spectra, of BPA, Cyanox®2246 and Cyanox®425 as standards as reference chemicals were utilized in the assessment of Cyanox®53's chemical structure. Analysis of reference BPA, Cyanox®2246, and Cyanox®425 produced molar masses of 228.148 Da, 340.268 Da, and 368.305 Da, respectively, and integral signals

proportional to the number of resonant protons in their respective molecular structures. When arranged side by side, the molar mass obtained for Cyanox®53 evidently lies within the range of the references, and by extension further supports past patent assertions of Cyanox®53 being an alkylated bisphenol (McEntee, 1990; Cruce et al., 2014; Wang et al., 2019). Moreover, the chemical shifts noted in the Cyanox®53 and Cyanox®53-PVDF ¹H-NMR spectra conform to the key hydrogen features of the reference chemicals. It is worth noting that no cross contamination by PVDF was observed in the Cyanox®53-PVDF leachate ESI/LC-MS and ¹H-NMR spectra. Presumably, the incubation temperature of 70°C during the 10 d single batch equilibrium extraction did not induce dissolution of PVDF (melting point of 177°C) in the DMSO-d₆. Thus, the results obtained from the Cyanox®53-PVDF leachate belong to Cyanox®53.

In the final analysis, 2,2'-thiobis(3-methyl-5-tert-butylphenol) was concluded to be a feasible chemical structure for Cyanox®53. As stated above, because this is one of first studies to investigate Cyanox®53 extensively, no direct comparisons through literature were possible. Other NMR analyses, including ¹³C-NMR and two-dimensional NMR (e.g., correlation spectroscopy (COSY) or nuclear Overhauser effect spectroscopy (NOESY), and heteronuclear single-quantum correlation spectroscopy (HSQC)), that are knowingly employed in the structural determination of complex compounds, also could not be performed for the Cyanox®53 leachates because a sufficient concentration for such testing could not be acquired from the field-collected particles. Thus, further analytical analyses are required to verify the structure proposed here. For the purpose of this study, 2,2'-thiobis(3-methyl-5-tert-butylphenol) was carried forward into the QSAR modelling to estimate the environmental fate and potential toxicity of Cyanox®53.

4.3. Persistence, Bioaccumulation, and Toxicity Predictions

4.3.1. Persistence

Though there are several questions that need to be addressed concerning Cyanox®53, chief among them is the inquiry of whether it imposes as an environmental threat. In this study, EPI Suite™ was used to predict such criteria for Cyanox®53. Based on the proposed chemical structure of 2,2'-thiobis(3-methyl-5-tert-butylphenol), a log K_{ow} of 8.24 with a water solubility of 0.00191 mg/L (0.0568 mg/L based on chemical fragments) at 25°C were predicted for Cyanox®53. Generally, chemicals with high log

K_{ow} values (≥ 5) are deemed to be poorly water soluble and tend to partition to organic matter in soils and sediments within their surroundings (CEPA, 2013; Chi et al., 2018). The predicted estimates for Cyanox®53 were a high $\log K_{oc}$ (> 5), indicative of low mobility in sediment because of a strong adsorption to organic particulates; a low biodegradability rate equivalent to 2 months before complete mineralization; and partitioning half-lives of 120 and 540 days in soil and sediment, respectively. Based on these estimates, a max half-life of 189 days in the environment was predicted. A similar conclusion was drawn in Toxtree where Cyanox®53 was classified as a class II persistent chemical because it has structural features associated with chemicals that are known to be persistent (e.g., terminal *tert*-butyl branches). Together, these model predictions suggest that Cyanox®53 is likely to persist in its chemical form via adsorption to organic matter and thus have a prolonged fate in the environment.

4.3.2. Bioaccumulation and Biomagnification

Bioaccumulation potential is another important parameter to consider in the risk assessment of environmental pollutants. Bioaccumulation is the process by which a chemical is absorbed into the tissue of an organism from all possible exposure routes, namely by ambient medium (water, sediment, soil, or air) or diet, with internal concentration higher than those observed in abiotic environmental compartments (Gobas et al., 2009; CEPA, 2013; EPA, 2021). It is important to identify the bioaccumulation potential of chemicals because toxicity often tends to increase with the amount accumulated (CEPA, 2013). Highly bioaccumulative chemicals are of particular concern to biota given the potential to cause direct adverse health effects (i.e., physiological damage) or indirect toxicity in higher trophic level organisms or/and apex predators at the top of the foodweb (i.e., biomagnification) regardless of the ambient concentration (CEPA, 2013). In the simplest model, $\log K_{ow}$ can be used to screen the bioaccumulation potential of a chemical based on the assumption that the absorption of an organic substance is driven by its hydrophobicity (ECHA, 2022). However, bioaccumulation potential is not solely dependent on hydrophobicity, rather other underlying mechanisms and physiological properties of an organism can affect the bioconcentration and bioaccumulation potentials of organic substances. For instance, many organic substances can undergo metabolism (biotransformation) and depuration, resulting in a decrease in the bioaccumulation potential of the parent compound

(ECETOC, 1998; CEPA, 2013). Moreover, in scenarios where organisms are exposed to very hydrophobic substances (i.e., $\log K_{ow} > 7.5$), a reduction in bioavailability (and therefore bioaccumulation/bioconcentration potentials) can be expected because the chemical will be largely absorbed to any dissolved or particulate organic carbon suspended in the diet (Gobas & Morrison, 2000; Gobas, 2001; Arnot & Gobas, 2003; CEPA, 2013). By this logic, while the predicted $\log K_{ow}$ of Cyanox®53 appears to exceed the threshold set by Environment Canada ($\log K_{ow} > 5$), its measurement cannot provide a definite answer for bioaccumulation potential of Cyanox®53 in its chemical form. Alternatively, BAF and BCF were used as they provide a more realistic interpretation of bioaccumulation potential of a substance (CEPA, 2013; CEPA, 2013). In Canada, a criterion of 5000 for BAFs or BCFs are recommended as the threshold to address lipophilic substances with the potential to bioaccumulate and biomagnify (CEPA, 2013). Concerning Cyanox®53, the predicted BAF (308 L/kg wet-wt Arnot-Gobas method) and BCF (3,270 L/kg wet-wt regression method; 28.22 L/kg wet-wt Arnot-Gobas method) values fell below the benchmarks set by Environment Canada. Therefore, based on the predicted bioaccumulation potential, Cyanox®53 would appear unlikely to bioaccumulate in its chemical form, and thus would not be considered a chemical of concern in this capacity. Although bioaccumulation and biomagnification tend to increase with the K_{ow} in range of medium to high lipophilicity, both predicted water solubility values for Cyanox®53 are indicative of low mobility, which in turn can limit its uptake rate in aquatic organisms, as well as inhibit its kinetics to bioaccumulate and biomagnify in the food-chain (ECETOC, 2000). In this respect, the likelihood that Cyanox®53 would transfer up the trophic levels in chemical form lessens based on the predicted water solubility and $\log K_{ow}$ values.

4.3.3. Toxicity

Many studies have published information on the toxicological significance of phenolic antioxidants in plastics (Liu & Mabury, 2020). For instance, Cyanox®425 is classified as an irritant to the skin, eyes, and respiratory tract, and may cause long lasting harmful effects to aquatic species, including changes in motor activity and reproduction (Kim et al., 2019; Wypych & Wypych, 2020; ECHA, 2022). Similarly, exposure to Cyanox®2246 has been shown to cause irritation to the eyes and respiratory tract (Kim et al., 2019; Wypych & Wypych, 2020; ECHA, 2022). It can also

impair fertility or unborn offspring through reproductive toxicity, making it especially hazardous to aquatic life (Kim et al., 2019; Wypych & Wypych, 2020; ECHA, 2022). Irganox 1081, an isomer of the proposed structure in this study (C₂₂H₃₀O₂S), is associated with skin sensitization and inducing chronic effects in aquatic species (Kim et al., 2019; ECHA, 2022). In the case of Cyanox®53, however, predictions by EPI Suite™ and Toxtree models were inconclusive on whether significant toxicity would be elicited.

According to the ECOSAR™ model, the proposed chemical structure of this study was found to be insufficiently water soluble to elicit toxicological effects at saturation in the acute and chronic exposure scenarios for fish, *D. magna*, or green algae when the predicted log K_{ow} of 8.24 was used as the determinant. However, when the predicted water solubility values were applied as the determinants of toxicity, different results were seen. Specifically, if the predicted water solubility of 0.00191 mg/L (based on the predicted log K_{ow} of 8.24) was used for comparison, potential toxicological effects were simulated in the acute and chronic exposure scenarios for *D. magna* and fish surrogates, with NES being noted in the green algae. But, if the predicted water solubility of 0.0568 mg/L (based on chemical fragments) was used, potential toxicological effects were observed in acute and chronic exposure scenarios for *D. magna*, fish and green algae. Clearly, there is a discrepancy between the predicted log K_{ow} and water solubility values. It is because of this disconnect that a definitive answer cannot be given on the toxicological effects of Cyanox®53 based on the EPI Suite™ results.

In Toxtree, Cyanox®53 was predicted to be non-mutagenic and non-carcinogenic based on the ISS *in vitro* Ames test and Benigni/Bossa rule-base test models. In addition, the structure was not associated with enhanced toxicity, nor could a distinct toxicological MOA be predicted. Nevertheless, the suggested Cyanox®53 structure was identified as a high hazard (Cramer Class III chemical) with a conservative TTC of 90 ug/day (1.5 ug/kg/bw/d) for dietary intake in mammalian species because of its extended persistence and inability to hydrolyze or biodegrade readily. Interestingly, the proposed structure was also identified as having the potential to act as a Michael acceptor or precursor for Michael reactions. Michael acceptors function as electrophilic agents, giving them the potential to covalently bind to the nucleophilic sites of proteins and DNA in organisms (Mulliner et al., 2011). In excess, the binding of Michael acceptors to either protein or DNA can result in the development of diseases in aquatic organisms, including allergic contact dermatitis, cancer, or other toxicological effects (Mulliner et al., 2011).

Because of this, the structural identification of Michael acceptors has been used as a determinant of toxicity (Mulliner et al., 2011). In the context of Cyanox®53, one could argue that its potential to act as a Michael acceptor contradicts model estimates of low toxicity, mutagenicity, and carcinogenicity potential predicted by Toxtree. Even so, the likelihood that an excessive amount of Cyanox®53 particles would leach out a high enough concentration to induce significant toxicity within a short period of time before being discharged is considerably low. In addition, given that frank toxicity was not observed in the varnish clams containing Cyanox®53 particles in this study, the potential of Cyanox®53 causing toxicological effects appears to lessen. All the same, it cannot be said for certain that a toxicological effect would not have eventually taken place on some level in the clams from chronic exposure. Indeed, rather than exert acute toxicity, perhaps the hazardous nature of Cyanox®53 particles stem from their ability to bioaccumulate as a solid and potential to cause physical harm at the organ level, either directly in an organism or indirectly when predatory species unknowingly ingest contaminated prey (i.e., trophic transfer) (Gallo et al., 2018; Nelms et al., 2019). The only way to verify this theory would be to perform chronic *in vitro* or *in vivo* toxicity tests. For instance, prospective research could perform OECD test guidelines No. 201, 204, 210, 211, or 230 with Cyanox®53 particles (OCED, 1984; 2009; 2011; 2012; 2013).

4.3.4. EPI Suite™ and Toxtree Model Limitations

Although QSAR analyses have been deemed an accepted method in the screening of environmental risk and hazard of poorly understood or unknown chemicals, different levels of uncertainty and variability exist within each model and measured parameter. Indeed, there are different ways to assess toxicity (e.g., *in vitro* and *in vivo* toxicity testing, *in silico* approaches, etc.) and depending on the approach used, different answers are generated. Therefore, it is relevant to consider uncertainty in individual predictions when QSAR models are used in the assessment of chemical safety (Sahlin, 2013). For example, it is known that log K_{ow} predictions in EPI Suite™ are derived from experimental K_{ow} values of the nearest chemical analogs (Do et al., 2022). Because of this, it increases the probable of inaccurately predicting certain descriptors for a chemical. The simple solution to this issue would be to compare the predicted results to experimental data collected in model-based or laboratory-based research for verification. However, in the case of Cyanox®53, there are no model-based or experimental data for

comparison in the literature, therefore making it very challenging to decisively measure its toxicological significance. Coupling this with the fact that the predictions seen in this present study, albeit valuable, are merely based on a feasible structure (as further verification via laboratory experimentation could not be performed), the likelihood that uncertainty may exist in the predictions from EPI Suite™ and Toxtree arises. Even so, it should not be implied that the results observed in this study are completely invaluable or inaccurate. Instead, these results represent a baseline for comparison in future studies and should be validated with OECD test guidelines. In fact, prospective research could perform the following OECD test guidelines to verify the log K_{ow} , water solubility, and biodegradation values of Cyanox®53 predicted in this study: No. 105, 107, 117, 123, and 301 (OECD, 1992; 1995; 1995; 2004; 2006)

Another plausible explanation as to why the toxicological predictions of this study were inconclusive could be related to the assumptions of the two models. Namely, the assumption that all compounds exist as neatly dissolved chemicals, and not the solid particulate by which Cyanox®53 has been recently appearing in the environment. In EPI Suite™, its chemical domain of applicability does not cover the full range of substances, and it does not currently produce accurate estimates for inorganic substances, organometallic substances, some ionizable organic compound, large molecular weight (> 500 Da) substances, nanomaterials, perfluorinated and other halogenated compounds, compounds without functional groups, and compound containing significant organic functional groups (Card et al., 2017). Similarly, only dissolved organic chemicals are considered in Toxtree. When it comes to Cyanox®53, it evidently does not adhere to the above chemical profiles. Neither EPI Suite™ nor Toxtree models include polymer particles in their chemical domains, meaning any predictions procured for Cyanox®53 falsely assumed that the organic additive existed as a dissolved chemical, instead of a solid particle. Such a misinterpretation can ultimately reduce the overall accuracy and predictive powers of said QSAR models. Not to mention, in assuming that Cyanox®53 only exists as a dissolved chemical in the environment, it neglects the possibility that Cyanox®53 particles could bioaccumulate within the tissue of an organism as a solid particulate and elicit eventual toxicity through chronic exposure. To correct this oversight, consideration needs to be given to the inclusion of polymer particles like Cyanox®53 in QSAR models. In addition, further investigation needs to be conducted on the leachability and retention time of accumulated Cyanox®53 particles in clams. As a

future study, one could analyze the retention time and depuration of Cyanox®53 particle accumulated in field-collected varnish clams at different time points (e.g., 1, 2, 4 and 8 d) post collection.

4.4. Conclusions

Given the shortcoming of admissions in literature on Cyanox®53, the evidence uncovered in this work shows promise for forthcoming analyses. It was only recently that the presence of Cyanox®53 in the environment had been documented, making this study one of the first to successfully recover concentrations in surface sediments and bivalves from Burrard Inlet, BC. This is also the first study to chemically characterize Cyanox®53 with ATR-FTIR, ESI-LC/MS and ¹H-NMR, and predict its environmental fate and potential toxicity. We hypothesized that, akin to other bisphenol related compounds, Cyanox®53 potentially possessed some degree of toxicity towards aquatic organisms. Based on QSAR modelling, Cyanox®53 was predicted to be a persistent chemical unlikely to bioaccumulate; however, it was inconclusive on whether it could elicit toxicity. At present, QSAR models function on the assumption that organic compounds exist as neatly dissolved chemicals in the environment, and thus can only provide accurate predictions for “traditional” chemicals. This assumption ultimately became a limitation in this study because the QSAR models did not consider the possibility of Cyanox®53 bioaccumulating as a solid particulate within in an individual, leading to a possible disconnect in the predicted log K_{ow} and water solubility, and consequently, the toxicological significance. Still, the predictions estimated in this present study hold value as they represent a baseline for comparison in future works. If a definitive answer is ever to be obtained concerning the risk of Cyanox®53, however, consideration needs to be given to the inclusion of polymer particles like Cyanox®53 in QSAR models. In addition, further investigation into its potential toxicity, leachability, and retention time as a physical particle in marine organisms is required, most likely through *in vitro* and *in vivo* testing. Another challenge that existed in this research was that the collected Cyanox®53 concentrations could not be compared to standardized benchmarks due to a lack of model-based and experimental data in the literature. Because of this, it is unknown if the collected Cyanox®53 concentrations were within the regulatory range. In the future, establishment of a regulatory program that monitors microplastics and particles like Cyanox®53 would prove beneficial, especially in the determination of

environmentally relevant benchmark concentrations for inter-study or regulatory comparisons. Moreover, by monitoring Cyanox®53 concentrations in the environment, it would also aid in pinpointing the distinct source(s) of Cyanox®53. Despite all the challenges that were faced in this present study, valuable information on environmental concentrations, persistence, bioaccumulation potential, and toxicological implications of Cyanox®53 were determined in a novel protocol that can be used in future investigations.

References

- AccuStandard. (2018). Plastic Additive Standards Guide. Retrieved from <https://www.accustandard.com/plastic-additive-catalog-2nd-edition>
- Achiluzzi, E. (2022). *Risk Assessment: Role of microplastics through benthic invertebrate communities in False Creek, Vancouver*. [Master's thesis, Simon Fraser University]. SFU Summit Institutional Repository.
- Adam, V., Yang, T., & Nowack, B. (2019). Toward an ecotoxicological risk assessment of microplastics: Comparison of available hazard and exposure data in freshwaters. *Environmental Toxicology and Chemistry*, 38(2), 436-447. doi:10.1002/etc.4323
- Alava, J. J. (2020). Modeling the bioaccumulation and biomagnification potential of microplastics in a cetacean foodweb of the northeastern pacific: a prospective tool to assess the risk exposure to plastic particles. *Frontiers in Marine Science*, 7, 566101.
- Alava, J. J. (2021). Proposing a Bioaccumulation Metric Criteria Framework for Plastic Particles in Marine Biota and Foodwebs. In Abstracts Book: Society of Environmental Toxicology and Chemistry (SETAC) North America 42nd Annual Meeting (SETAC SciCon4). Solutions with Respect for Our Community and Environment. November 14-18, 2021. Virtual. Portland, Oregon. pp. 25. Retrieved from <https://scicon4.setac.org/wp-content/uploads/2021/11/SciCon4-abstract-book.pdf>
- Ali, S. S., Elsamahy, T., Al-Tohamy, R., Zhu, D., Mahmoud, Y. A., Koutra, E., Metwally, M. A., Kornaros, M., & Sun, J. (2021). Plastic wastes biodegradation: Mechanisms, challenges and future prospects. *Science of The Total Environment*, 780, 146590. doi:10.1016/j.scitotenv.2021.146590
- Aliotta, S., & Colley, J. (2013, January 8). Bioremediation. Retrieved from <https://www.geoengineer.org/education/web-class-projects/cee-549-geoenvironmental-engineering-winter-2013>
- Ammar, A., Alahmad, K., & Korma, S. A. (2016). Natural antioxidants, Phenolics compounds and their relationship to health. *International Journal of Research*. 3(3), 2348-3997.
- American Chemistry Council. (2021, July 19). Plastics: Uses, Benefits, and Chemical Safety Facts. Retrieved from <https://www.chemicalsafetyfacts.org/plastics/>
- Andrady, A. L., & Neal, M. A. (2009). Applications and societal benefits of plastics. *Philosophical transactions of the Royal Society of London. Series B, Biological sciences*, 364(1526), 1977–1984. <https://doi.org/10.1098/rstb.2008.0304>

- Andrady, A. L. (2011). Microplastics in the marine environment. *Marine Pollution Bulletin*, 62(8), 1596-1605. doi:10.1016/j.marpolbul.2011.05.030
- Arnot, J. A., & Gobas, F. A. (2003). A generic QSAR for assessing the bioaccumulation potential of organic chemicals in aquatic food webs. *QSAR & Combinatorial Science*, 22(3), 337-345.
- Avio, C. G., Gorbi, S., Milan, M., Benedetti, M., Fattorini, D., Derrico, G., d'Errico, G., Pauletto, M., Bargelloni, L., & Regoli, F. (2015). Pollutants bioavailability and toxicological risk from microplastics to marine mussels. *Environmental Pollution*, 198, 211-222. doi:10.1016/j.envpol.2014.12.021
- Baechler, B., Granek, E., Hunter, M., & Conn, K. (2019). Microplastic Concentrations in Two Oregon Bivalve Species: Spatial, Temporal, and Species Variability. *Environmental Science and Management Datasets*. doi:10.15760/esm-data.1
- Baechler, B. R., Stienbarger, C. D., Horn, D. A., Joseph, J., Taylor, A. R., Granek, E. F., & Brander, S. M. (2020). Microplastic occurrence and effects in commercially harvested North American finfish and shellfish: current knowledge and future directions. *Limnology and Oceanography Letters*, 5(1), 113-136.
- Baztan, J., Bergmann, M., Booth, A., Broglio, E., Carrasco, A., Chouinard, O., Clüsener-Godt, M., Cordier, M., Cozar, A., Devrieses, L., Enevoldsen, H., Ernsteins, R., Ferreira-da-Costa, M., Fossi, M. C., Gago, J., Galgani, F., Garrabou, J., Gerdt, G., Gomez, M., Gómez-Parra, A., Gutow, L., Herrera, A., Herring, C., Huck, T., Huvet, A., Ivar do Sul, J. A., Jorgensen, B., Krzan, A., Lagarde, F., Liria, A., Lusher, A., Miguelez, A., Packard, T., Pahl, S., Paul-Pont, I., Peeters, D., Robbins, J., Ruiz-Fernández, A. C., Rung, E. J., Sánchez-Arcilla, A., Soudant, P., Surette, C., Thompson, R. C., Valdés, L., & Wallace, N. (2017). Breaking Down the Plastic Age. *Fate and Impact of Microplastics in Marine Ecosystems*, 177-181. doi:10.1016/b978-0-12-812271-6.00170-8
- Benali, I., Boutiba, Z., Merabet, A., & Chevre, N. (2015). Integrated use of biomarkers and condition indices in mussels (*Mytilus galloprovincialis*) for monitoring pollution and development of biomarker index to assess the potential toxic of coastal sites. *Marine Pollution Bulletin*, 95(1), 385–394. <https://doi.org/10.1016/j.marpolbul.2015.03.041>
- Bendell, L. I., Lecadre, E., & Zhou, W. (2020). Use of sediment dwelling bivalves to biomonitor plastic particle pollution in intertidal regions; A review and study. *Plos One*, 15(5). doi:10.1371/journal.pone.0232879
- Besseling, E., Wegner, A., Foekema, E. M., van den Heuvel-Greve, M. J., & Koelmans, A. A. (2013). Effects of microplastic on fitness and PCB bioaccumulation by the Lugworm *Arenicola marina* (L.). *Environmental Science & Technology*, 47, 593–600.

- Bolgar, M., Hubball, J., Groeger, J., & Meronek, S. (2016). *Handbook for the chemical analysis of plastic and polymer additives*. Boca Raton, FL: CRC Press.
- Bose, P. (2021, June 15). Bioremediation: An Overview. Retrieved from <https://www.azolifesciences.com/article/Bioremediation-An-Overview.aspx>
- Braig, S., Delisle, K., & Noël, M. (2019). Water Quality Assessment and Proposed Objectives for Burrard Inlet: Microplastics Technical Report. Prepared for Tsleil-Waututh Nation and the Province of B.C. Retrieved from https://www2.gov.bc.ca/assets/gov/environment/air-land-water/water/waterquality/water-quality-objectives/2020-03-31_biwqos_mpsdoc.pdf
- Bridson, J. H., Gaugler, E. C., Smith, D. A., Northcott, G. L., & Gaw, S. (2021). Leaching and extraction of additives from plastic pollution to inform environmental risk: A multidisciplinary review of analytical approaches. *Journal of Hazardous Materials*, 414, 125571. doi:10.1016/j.jhazmat.2021.125571
- Britannica, T. Editors of Encyclopaedia (2010, December 17). *Polyvinylidene fluoride*. *Encyclopedia Britannica*. Retrieved from <https://www.britannica.com/science/polyvinylidene-fluoride>
- British Columbia Ministry of Environment. (2015). Indicators of Climate Change for British Columbia: 2016 Update. Ministry of Environment, British Columbia, Canada. Retrieved from <http://www.env.gov.bc.ca/soe/indicators/climate-change/precip.html>
- British Plastic Federation. (2021). Plastic Applications. Retrieved from <https://www.bpf.co.uk/plastipedia/applications/default.aspx>
- Browne, M. A., Dissanayake, A., Galloway, T. S., Lowe, D. M., & Thompson, R. C. (2008). Ingested Microscopic Plastic Translocates to the Circulatory System of the Mussel, *Mytilus edulis* (L.). *Environmental Science & Technology*, 42(13), 5026-5031. doi:10.1021/es800249a
- Canadian Environmental Protection Act. (2013). Ecological State of the Science Report on Decabromodiphenyl Ether (decaBDE). Retrieved from Canadian Environmental Protection Act website <https://www.ec.gc.ca/lcpe-cepa/default.asp?lang=En&n=B901A9EB&offset=3>
- Canadian Environmental Protection Act. (2013). Guidance Manual for the Risk Evaluation Framework for Sections 199 and 200 of CEPA 1999: Decisions on Environmental Emergency Plans. Retrieved from Government Canada website <https://www.canada.ca/en/environment-climate-change/services/canadian-environmental-protection-act-registry/historical/guidance-manual-risk-evaluation-framework-cepa-decisions-environmental-emergency-plans/process.html;%20https://www.ec.gc.ca/lcpe-cepa/default.asp?lang=En&n=B901A9EB&offset=3>

- Card, M. L., Gomez-Alvarez, V., Lee, W. H., Lynch, D. G., Orentas, N. S., Lee, M. T., Wong, E. M., & Boethling, R. S. (2017). History of EPI Suite™ and future perspectives on chemical property estimation in US Toxic Substances Control Act new chemical risk assessments. *Environmental Science: Processes & Impacts*, 19(3), 203-212.
- Carlisle, J., Chan, D., Golub, M., Henkel, S., Painter, P., & Wu, K. L. (2009, September). *Toxicological Profile for Bisphenol A* (Tech.). Retrieved http://www.opc.ca.gov/webmaster/ftp/project_pages/MarineDebris_OEHHA_ToxProfiles/Bisphenol A Final.pdf
- Chan, K., & Bendell, L.I. (2013). Potential effects of an invasive bivalve, *Nuttallia obscurata*, on select sediment attributes within the intertidal region of coastal British Columbia. *Journal of Experimental Marine Biology and Ecology*, 444, 1, 66-72.
- Chi, Y., Zhang, H., Huang, Q., Lin, Y., Ye, G., Zhu, H., & Dong, S. (2018). Environmental risk assessment of selected organic chemicals based on TOC test and QSAR estimation models. *Journal of Environmental Sciences*, 64, 23-31.
- Cho, Y., Shim, W. J., Jang, M., Han, G. M., & Hong, S. H. (2021). Nationwide monitoring of microplastics in bivalves from the coastal environment of Korea. *Environmental Pollution*, 270, 116175.
- Crawford, C. B., & Quinn, B. (2019). *Microplastic pollutants*. Amsterdam: Elsevier.
- Cruce, C. J., Giardello, M. A., Conley, B. L., Stephen, A. R. (2014). *CA Patent No. 2,915,486 A1*. Gatineau, Québec: Canadian Intellectual Property Office.
- Costa, J. P., Duarte, A. C., & Rocha-Santos, T. A. (2017). Microplastics – Occurrence, Fate and Behaviour in the Environment. *Characterization and Analysis of Microplastics Comprehensive Analytical Chemistry*, 1-24. doi:10.1016/bs.coac.2016.10.004
- Covernton, G. A., Pearce, C. M., Gurney-Smith, H. J., Chastain, S. G., Ross, P. S., Dower, J. F., & Dudas, S. E. (2019). Size and shape matter: A preliminary analysis of microplastic sampling technique in seawater studies with implications for ecological risk assessment. *Science of The Total Environment*, 667, 124-132. doi:10.1016/j.scitotenv.2019.02.346
- Department of Fisheries and Oceans Canada. (2021, March 29). Microplastics. Retrieved from <https://www.dfo-mpo.gc.ca/science/environmental-environnement/microplastics-microplastiques/index-eng.html>
- Devereux, R., Westhead, E. K., Jayaratne, R., & Newport, D. (2022). Microplastic abundance in the Thames River during the New Year period. *Marine Pollution Bulletin*, 177, 113534.

- Ding, J., Sun, C., He, C., Li, J., Ju, P., & Li, F. (2021). Microplastics in four bivalve species and basis for using bivalves as bioindicators of microplastic pollution. *Science of the Total Environment*, 782, 146830.
- Dobbin, C. (2017). An industrial chronology of polyethylene. In Spalding, M. A., & Chatterjee, A. (Eds.) *Handbook of industrial polyethylene and technology: Definitive guide to manufacturing, properties, processing, applications and markets set* (pp. 3-23). John Wiley & Sons.
- Do, A. T. N., Kim, Y., Ha, Y., & Kwon, J. H. (2022). Estimating the Bioaccumulation Potential of Hydrophobic Ultraviolet Stabilizers Using Experimental Partitioning Properties. *International journal of environmental research and public health*, 19(7), 3989.
- EPI SUITE™ for Microsoft® Windows, Version 4.11. US EPA. (2021). United States Environmental Protection Agency, Washington, DC, USA.
- Environment and Climate Change Canada (2018, June). *Canadian Environmental Protection Act, 1999 Federal Environmental Quality Guidelines* (Tech.). Retrieved <https://www.canada.ca/content/dam/eccc/documents/pdf/pded/bpa/20180626-BPA-EN.pdf>
- Environment and Climate Change Canada. (2020, October 15). *Canada Gazette, Part I, Volume 154, Number 41: Order Adding a Toxic Substance to Schedule 1 to the Canadian Environmental Protection Act, 1999* (Tech.). Retrieved from <https://gazette.gc.ca/rp-pr/p1/2020/2020-10-10/html/reg1-eng.html>
- Environment and Climate Change Canada. (2021, May 12). *Toxic substances list: schedule 1* (Tech.). Retrieved from <https://www.canada.ca/en/environment-climate-change/services/canadian-environmental-protection-act-registry/substances-list/toxic/schedule-1.html>
- Environment Canada. (1998). *Fraser River Action Plan: Burrard Inlet Technical Summary Report* (DOE-FRAP 1998-02). Retrieved from https://publications.gc.ca/collections/collection_2015/ec/En83-6-1998-2-eng.pdf
- Erni-Cassola, G., Zadjelovic, V., Gibson, M.I., & Christie-Oleza, J.A. (2019). Distribution of plastic polymer types in the marine environment; A meta-analysis. *Journal of Hazardous Materials*, 369, 691-698. doi:10.1016/j.jhazmat.2019.02.067
- Espinosa, C., Esteban, M. Á., & Cuesta, A. (2016). Microplastics in Aquatic Environments and Their Toxicological Implications for Fish. *Toxicology - New Aspects to This Scientific Conundrum*, 113–145. doi: 10.5772/64815

- European Centre for Ecotoxicology and Toxicology of Chemicals. (1998). *QSARs in the Assessment of Environmental Fate and Effects of Chemicals* (Tech. No. 74). Brussels, Belgium: European Centre for Ecotoxicology and Toxicology of Chemicals. Retrieved from <https://www.ecetoc.org/wp-content/uploads/2014/08/ECETOC-TR-074.pdf>. (ISSN-0773-8072-74).
- European Centre for Ecotoxicology and Toxicology of Chemicals. (2000). *Persistent Organic Pollutants (POPs) Response to UNEP/INC/CEG-I Annex 1* (Tech. No. 41). Brussels, Belgium: European Centre for Ecotoxicology and Toxicology of Chemicals. Retrieved from <https://www.ecetoc.org/wp-content/uploads/2014/08/DOC-0412.pdf>
- European Chemicals Agency. (2014, December 11). *Dibutyl phthalate (DBP)* (Support Document). Retrieved <https://echa.europa.eu/documents/10162/e4edaefa-84a4-4972-89f0-470cd64bc949>
- European Chemical Agency. (2022). Retrieved from <http://echa.europa.eu/>
- Evode, N., Qamar, S. A., Bilal, M., Barceló, D., & Iqbal, H. M. (2021). Plastic waste and its management strategies for environmental sustainability. *Case Studies in Chemical and Environmental Engineering*, 4, 100142. doi:10.1016/j.cscee.2021.100142
- Flick, E. W. (2001). *Plastics additives: An industrial guide* (3rd ed., Vol. 1). Norwich, NY: William Andrew Publishing.
- Fries, E., Dekiff, J. H., Willmeyer, J., Nuelle, M., Ebert, M., & Remy, D. (2013). Identification of polymer types and additives in marine microplastic particles using pyrolysis-GC/MS and scanning electron microscopy. *Environmental Science: Processes & Impacts*, 15(10), 1949. doi:10.1039/c3em00214d
- Gallo, F., Fossi, C., Weber, R., Santillo, D., Sousa, J., Ingram, I., Nadal, A., Romano, D. (2018). Marine litter plastics and microplastics and their toxic chemicals components: The need for urgent preventive measures. *Environmental Sciences Europe*, 30(1). doi:10.1186/s12302-018-0139-z
- Gedik, K., & Eryaşar, A. R. (2020). Microplastic pollution profile of Mediterranean mussels (*Mytilus galloprovincialis*) collected along the Turkish coasts. *Chemosphere*, 260, 127570.
- Geyer, R., Jambeck, J. R., & Law, K. L. (2017). Production, use, and fate of all plastics ever made. *Science Advances*, 3(7), e1700782. <https://doi.org/10.1126/sciadv.1700782>
- Gibb, B. C. (2019). Plastics are forever. *Nature Chemistry*, 11(5), 394–395. <https://doi.org/10.1038/s41557-019-0260-7>
- Gijsman, P. (2012). Polymer Stabilization. *Handbook of Environmental Degradation of Materials*, 673-714. doi:10.1016/b978-1-4377-3455-3.00023-7

- Gillespie, G. E., Parker, M., & Merilees, W. (1999). Distribution, Abundance, Biology and Fisheries Potential of the Exotic Varnish Clam (*Nuttallia obscurata*) in British Columbia. Canadian Science Advisory Secretariat [CSAS] Research Document, 2011/143. Fisheries and Oceans Canada, Ottawa (ONT).
- Gillespie, G., Rusch, B., Gormican, S. J., Marshall, R., & Munroe, D. (2001). Further Investigations of the Fisheries Potential of the Exotic Varnish Clam (*Nuttallia obscurata*) in British Columbia. CSAS Research Document, 2001/143. Fisheries and Oceans Canada, Ottawa (ONT).
- Gobas, F. A. P. C., & Morrison, H. A. (2000). Bioconcentration and biomagnification in the aquatic environment. *Handbook of property estimation methods for chemicals*, 189-231.
- Gobas, F. A. (2001). Assessing bioaccumulation factors of persistent organic pollutants in aquatic food-chains. In *Persistent organic pollutants* (pp. 145-165). Springer, Boston, MA.
- Gobas, F. A., de Wolf, W., Burkhard, L. P., Verbruggen, E., & Plotzke, K. (2009). Revisiting bioaccumulation criteria for POPs and PBT assessments. *Integrated Environmental Assessment and Management: An International Journal*, 5(4), 624-637.
- Gouin, T., Becker, R. A., Collot, A. G., Davis, J. W., Howard, B., Inawaka, K., Lampi, M., Serrano Ramon, B., Shi, J., & Hopp, P. W. (2019). Toward the development and application of an environmental risk assessment framework for microplastic. *Environmental Toxicology and Chemistry*, 38(10), 2087-2100.
- Government of Canada. (2020). Plastics challenge: In-situ sensing technology for monitoring microplastics in the marine environment. Retrieved from <https://www.ic.gc.ca/eic/site/101.nsf/eng/00091.html>
- Greenpeace Research Laboratories. (2019). *Identification of polymer type used for a selection of organic-certified tampon applicators and their packaging on sale in the UK* (pp. 1-9, Rep. No. GRL-AR-2019-04). England: Greenpeace Research Laboratories School of Biosciences.
- Hale, R. C., Seeley, M. E., La Guardia, M. J., Mai, L., & Zeng, E. Y. (2020). A Global Perspective on Microplastics. *Journal of Geophysical Research: Oceans*, 125. e2018JC014719. doi: 10.1029/2018JC014719
- Hanvey, J. S., Lewis, P. J., Lavers, J. L., Crosbie, N. D., Pozo, K., & Clarke, B. O. (2017). A review of analytical techniques for quantifying microplastics in sediments. *Analytical Methods*, 9(9), 1369-1383. doi:10.1039/c6ay02707e
- Haram, L. E., Carlton, J. T., Ruiz, G. M., & Maximenko, N. A. (2020). A plasticene lexicon. *Marine Pollution Bulletin*, 150, 110714.

- Hayes, A. (Ed.), & Kruger, C. (Ed.). (2014). *Hayes' Principles and Methods of Toxicology*. London: CRC Press; <https://doi.org/10.1201/b17359>
- Hermabessiere, L., Dehaut, A., Paul-Pont, I., Lacroix, C., Jezequel, R., Soudant, P., & Duflos, G. (2017). Occurrence and effects of plastic additives on marine environments and organisms: A review. *Chemosphere*, *182*, 781-793. doi:10.1016/j.chemosphere.2017.05.096
- Hermabessiere, L., Paul-Pont, I., Cassone, A. L., Himber, C., Receveur, J., Jezequel, R., El Rakwe, M., Rinnert, E., Rivièrè, G., Lambert, C., Huvet, A., Dehaut, A., Duflos, G., & Soudant, P. (2019). Microplastic contamination and pollutant levels in mussels and cockles collected along the channel coasts. *Environmental Pollution*, *250*, 807-819.
- Hidalgo-Ruz, V., Gutow, L., Thompson, R. C., & Thiel, M. (2012). Microplastics in the marine environment: a review of the methods used for identification and quantification. *Environmental Science & Technology*, *46*(6), 3060-3075.
- Hopewell, J., Dvorak, R., & Kosior, E. (2009). Plastics recycling: Challenges and opportunities. *Philosophical Transactions of the Royal Society B: Biological Sciences*, *364*(1526), 2115-2126. doi:10.1098/rstb.2008.0311
- Huffman Ringwood, A. (2021). Bivalves as Biological Sieves: Bioreactivity Pathways of Microplastics and Nanoplastics. *The Biological Bulletin*, *241*(2), 185-195.
- Jambeck, J. R., Geyer, R., Wilcox, C., Siegler, T. R., Perryman, M., Andrady, A., Narayan, R., & Law, K. L. (2015). Plastic waste inputs from land into the ocean. *Science*, *347*(6223), 768-771.
- JChem for Office, Version 21.11.10. ChemAxon. (2021). Retrieved from <http://www.chemaxon.com>.
- JMP®, Version 16. SAS Institute Inc., Cary, NC, (2021).
- Keck-Antoine, K., Lievens, E., Bayer, J., Mara, J., Jung, D., & Jung, S. (2010). Additives to design and improve the performance of multilayer flexible packaging. *Multilayer Flexible Packaging*, 37-56. doi:10.1016/b978-0-8155-2021-4.10004-8
- Khan, F. R., Syberg, K., Shashoua, Y., & Bury, N. R. (2015). Influence of polyethylene microplastic beads on the uptake and localization of silver in zebrafish (*Danio rerio*). *Environmental Pollution*, *206*, 73-79. doi:10.1016/j.envpol.2015.06.009
- Kim, S., Chen, J., Cheng, T., Gindulyte, A., He, J., He, S., Li, Q., Shoemaker, B. A., Thiessen, P. A., Yu, B., Zaslavsky, L., Zhang, J., & Bolton, E. E. (2019). PubChem in 2021: new data content and improved web interfaces. *Nucleic Acids Res.*, *49*(D1), D1388–D1395. <https://doi.org/10.1093/nar/gkaa971>

- Knutsen, H., Singdahl-Larsen, C., & Bonnevie Cyvin, J. (2019). *Microplastics in Svalbard fjords and Bjørnøy transect Sediments* (Rep. No. 20190263-01-R) (H. Eter Arp, Ed.). Norwegian Geotechnical Institute. Retrieved from https://www.ngu.no/upload/Publikasjoner/Rapporter/2019/2019_027.pdf.
- Koelmans, A. A., Besseling, E., & Foekema, E. M. (2014). Leaching of plastic additives to marine organisms. *Environmental Pollution*, *187*, 49–54. doi: 10.1016/j.envpol.2013.12.013
- Lambert, S., Sinclair, C., & Boxall, A. (2013). Occurrence, Degradation, and Effect of Polymer-Based Materials in the Environment. *Reviews of Environmental Contamination and Toxicology*, Volume 227, 1-53. doi:10.1007/978-3-319-01327-5_1
- Lapenna, S., Fuart-Gatnik, M., & Worth, A. (2010). *Review of QSAR models and software tools for predicting acute and chronic systemic toxicity* (Publication. No. JRC61930). Luxembourg (Luxembourg): Publications Office of the European Union. doi:10.2788/60766
- Laville, S. (2019, November 06). Dumped fishing gear is biggest plastic polluter in ocean, finds report. Retrieved from <https://www.theguardian.com/environment/2019/nov/06/dumped-fishing-gear-is-biggest-plastic-polluter-in-ocean-finds-report>
- Law, K. L. (2017). Plastics in the Marine Environment. *Annual Review of Marine Science*, *9*(1), 205-229. doi:10.1146/annurev-marine-010816-060409
- Lawson, E. (2018, July 27). Sustainability in the Workplace: 5 Major Benefits of Plastic Recycling. Retrieved from <https://blog.impactplastics.co/blog/sustainability-in-the-workplace-5-major-benefits-of-plastic-recycling>
- Li, J., Yang, D., Li, L., Jabeen, K., & Shi, H. (2015). Microplastics in commercial bivalves from China. *Environmental Pollution*, *207*, 190-195. doi:10.1016/j.envpol.2015.09.018
- Li, J., Qu, X., Su, L., Zhang, W., Yang, D., Kolandhasamy, P., Daoji, L., & Shi, H. (2016). Microplastics in mussels along the coastal waters of China. *Environmental Pollution*, *214*, 177-184.
- Lithner, D., Larsson, Å, & Dave, G. (2011). Environmental and health hazard ranking and assessment of plastic polymers based on chemical composition. *Science of The Total Environment*, *409*(18), 3309-3324. doi:10.1016/j.scitotenv.2011.04.038
- Lithner, D., Nordensvan, I., & Dave, G. (2011). Comparative acute toxicity of leachates from plastic products made of polypropylene, polyethylene, PVC, acrylonitrile–butadiene–styrene, and epoxy to *Daphnia magna*. *Environmental Science and Pollution Research*, *19*(5), 1763-1772. doi:10.1007/s11356-011-0663-5

- Liu, R., & Mabury, S. A. (2020). Synthetic Phenolic Antioxidants: A Review of Environmental Occurrence, Fate, Human Exposure, and Toxicity. *Environmental Science & Technology*, 54(19), 11706-11719. doi:10.1021/acs.est.0c05077
- Liu, Z., Wang, H., & Zhang, S. (2022). An enhanced risk assessment framework for microplastics occurring in the Westerscheldt estuary. *Science of The Total Environment*, 153006.
- Luan, L., Wang, X., Zheng, H., Liu, L., Luo, X., & Li, F. (2019). Differential toxicity of functionalized polystyrene microplastics to clams (*Meretrix meretrix*) at three key development stages of life history. *Marine Pollution Bulletin*, 139, 346-354. doi:10.1016/j.marpolbul.2019.01.003
- Lusher, A. (2015). Microplastics in the Marine Environment: Distribution, Interactions and Effects. In: Bergmann M., Gutow L., Klages M. (Eds) *Marine Anthropogenic Litter*. Springer, Cham. https://doi.org/10.1007/978-3-319-16510-3_10
- Madden, J. C., Enoch, S. J., Paini, A., & Cronin, M. T. (2020). A review of *in silico* tools as alternatives to animal testing: Principles, resources and applications. *Alternatives to Laboratory Animals*, 48(4), 146-172.
- Maes, T., Jessop, R., Wellner, N., Haupt, K., & Mayes, A. G. (2017). A rapid-screening approach to detect and quantify microplastics based on fluorescent tagging with Nile Red. *Scientific Reports*, 7(1). doi:10.1038/srep44501
- Mahara, N., Alava, J. J., Kowal, M., Grant, E., Boldt, J. L., Kwong, L. E., & Hunt, B. P. V. (2021). Assessing size-based exposure to microplastics and ingestion pathways in zooplankton and herring in a coastal pelagic ecosystem of British Columbia, Canada. *Marine Ecology Progam Series*, 683: 139–155. <https://doi.org/10.3354/meps13966>
- Mankar, V. H., & Mankar, C. (2020). Sterically Hindered Phenols as Antioxidant. *European Journal of Molecular & Clinical Medicine*, 7(07), 3481-3491. doi:10.31838/ejmcm.07.07
- McCartney, I. (2019, May 8). The Advantages and Disadvantages of Polyethylene. *Kempner*. Retrieved from <https://kempner.co.uk/2019/05/08/the-advantages-and-disadvantages-of-polyethylene-blog/>
- McEntee, T. C. (1990). *U.S. Patent No. 4,891,391*. Washington, DC: U.S. Patent and Trademark Office.
- MestReNova, Version 14.2.1. Mestrelab Research S.L. (2021). Feliciano Barrera 9B, Bajo, 15706 Santiago de Compostela, Spain.
- Miller, M. E., Kroon, F. J., & Motti, C. A. (2017). Recovering microplastics from marine samples: A review of current practices. *Marine Pollution Bulletin*, 123(1-2), 6-18. doi:10.1016/j.marpolbul.2017.08.058

- Moore, C.J. (2008). Synthetic polymers in the marine environment: A rapidly increasing, long-term threat. *Environmental Research*, 108(2), 131-139.
doi:10.1016/j.envres.2008.07.025
- Morin, J., and Evans, A.B. (2022) Historical Ecology in Burrard Inlet: Summary of Historic, Oral History, Ethnographic, and Traditional Use Information. Fisheries Centre Research Report 30 (2) 64 pp.
- Mulliner, D., Wondrousch, D., & Schüürmann, G. (2011). Predicting Michael-acceptor reactivity and toxicity through quantum chemical transition-state calculations. *Organic & Biomolecular Chemistry*, 9(24), 8400-8412.
- Naik, V., & Patil, K. C. (2015). High energy materials. *Resonance*, 20(5), 431-444.
- Nelms, S. E., Barnett, J., Brownlow, A., Davison, N. J., Deaville, R., Galloway, T. S., Lindeque, P. K., Santillo, D., & Godley, B. J. (2019). Microplastics in marine mammals stranded around the British coast: Ubiquitous but transitory? *Scientific Reports*, 9(1). doi:10.1038/s41598-018-37428-3
- OCED. (2004). Emission Scenario Document on Plastic Additives. Series on Emission Scenario Documents, No. 3. OECD Environmental Health and Safety Publications. Environment Directorate, Paris
- OCED. (n.d.). OECD Quantitative Structure-Activity Relationships Project [(Q)SARs]. Retrieved from <https://www.oecd.org/chemicalsafety/risk-assessment/oecdquantitativestructure-activityrelationshipsprojectqsars.htm>
- OCED. (1984). Test Guideline No. 204: Fish, Prolonged Toxicity Test: 14-Day Study. Retrieved from https://www.oecd-ilibrary.org/environment/test-no-204-fish-prolonged-toxicity-test-14-day-study_9789264069985-en
- OCED. (1992). Test Guideline No. 301: Ready Biodegradability. Retrieved from https://www.oecd-ilibrary.org/environment/test-no-301-ready-biodegradability_9789264070349-en
- OCED. (1995). Test Guideline No. 105: Water Solubility. Retrieved from https://www.oecd-ilibrary.org/environment/test-no-105-water-solubility_9789264069589-en
- OCED. (1995). Test Guideline No. 107: Partition Coefficient (n-octanol/water): Shake Flask Method. Retrieved from https://www.oecd-ilibrary.org/environment/test-no-107-partition-coefficient-n-octanol-water-shake-flask-method_9789264069626-en
- OCED. (2004). Test Guideline No. 117: Partition Coefficient (n-octanol/water), HPLC Method. Retrieved from https://www.oecd-ilibrary.org/environment/test-no-117-partition-coefficient-n-octanol-water-hplc-method_9789264069824-en

- OCED. (2006). Test Guideline No. 123: Partition Coefficient (1-Octanol/Water): Slow-Stirring Method. Retrieved from https://www.oecd-ilibrary.org/environment/test-no-123-partition-coefficient-1-octanol-water-slow-stirring-method_9789264015845-en
- OCED. (2009). Test Guideline No. 230: 21-day Fish Assay. *A Short-Term Screening for Oestrogenic and Androgenic Activity, and Aromatase Inhibition*. Retrieved from https://www.oecd-ilibrary.org/environment/test-no-230-21-day-fish-assay_9789264076228-en
- OCED. (2011). Test Guideline 201: Freshwater Alga and Cyanobacteria, Growth Inhibition Test. Retrieved from https://www.oecd-ilibrary.org/environment/test-no-201-alga-growth-inhibition-test_9789264069923-en
- OCED. (2012). Test Guideline No. 211: Daphnia magna Reproduction Test. Retrieved from https://www.oecd-ilibrary.org/environment/test-no-211-daphnia-magna-reproduction-test_9789264185203-en
- OCED. (2013). Test Guideline No. 210: Fish, Early-life Stage Toxicity Test. Retrieved from https://www.oecd-ilibrary.org/environment/test-no-210-fish-early-life-stage-toxicity-test_9789264203785-en
- Olesen, K., Van Alst, N., Simon, M., Vianello,, A., Liu, F., Vollertsen, J., & Kansiz, M. (2018). *Analysis of Microplastics using FTIR Imaging: Identifying and quantifying microplastics in wastewater, sediment and fauna* (Tech. No. 5991-8271EN). Santa Clara, CA: Agilent Technologies. Retrieved from https://www.agilent.com/cs/library/applications/5991-8271EN_microplastics_ftir_application.pdf.
- Patlewicz G., Jeliaskova N., Safford R. J., Worth A. P., & Aleksiev B. (2008) An evaluation of the implementation of the Cramer classification scheme in the Toxtree software. *SAR QSAR Environ Res.*;19(5-6):495-524.
- Plahuta, M., Tišler, T., Pintar, A., & Toman, M. J. (2015). Adverse effects of bisphenol A on water louse (*Asellus aquaticus*). *Ecotoxicology and Environmental Safety*, 117, 81-88. doi:10.1016/j.ecoenv.2015.03.031
- Plastic Soup Foundation. (2021, June 10). Canada declares plastic toxic and plans to ban SUP items. Retrieved from <https://www.plasticsoupfoundation.org/en/2021/06/canada-declares-plastic-toxic-and-plans-to-ban-sup-items/>
- PVC Pipe Supplies. (2022). *What is PVDF*. Retrieved from <https://pvcpipesupplies.com/what-is-pvdf>
- Reed, C. (2015). Dawn of the Plasticene age. *New Scientist*, 225(3006), 28-32.

- Rochman, C. M. (2015). The complex mixture, fate and toxicity of chemicals associated with plastic debris in the marine environment. In M. Bergmann, L. Gutow, & M. Klages (Eds.), *Marine anthropogenic litter* (pp. 117–140). Berlin: Springer.
- Rodrigues, M., Gonçalves, A., Gonçalves, F., & Abrantes, N. (2020). Improving cost-efficiency for MPs density separation by zinc chloride reuse. *MethodsX*, 7, 100785. doi:10.1016/j.mex.2020.100785
- Rozman, U., & Kalčíková, G. (2022). Seeking for a perfect (non-spherical) microplastic particle—The most comprehensive review on microplastic laboratory research. *Journal of Hazardous Materials*, 424, 127529.
- Sahlin, U. (2013). Uncertainty in QSAR predictions. *Alternatives to Laboratory Animals*, 41(1), 111-125.
- Savoca, M. S., Mcinturf, A. G., & Hazen, E. L. (2021). Plastic ingestion by marine fish is widespread and increasing. *Global Change Biology*, 27(10), 2188-2199. doi:10.1111/gcb.15533
- Schmidt, L. K., Bochow, M., Imhof, H. K., & Oswald, S. E. (2018). Multi-temporal surveys for microplastic particles enabled by a novel and fast application of SWIR imaging spectroscopy—Study of an urban watercourse traversing the city of Berlin, Germany. *Environmental pollution*, 239, 579-589.
- Sharma, B., Rawat, H., Ja, P., & Sharma, R. (2017). Bioremediation - A Progressive Approach toward Reducing Plastic Wastes. *International Journal of Current Microbiology and Applied Sciences*, 6(12), 1116-1131. doi:10.20546/ijcmas.2017.612.126
- Sheth, M. U., Kwartler, S. K., Schmaltz, E. R., Hoskinson, S. M., Martz, E. J., Dunphy-Daly, M. M., Schultz, T.F., Read, A.J., Eward, W.C., & Somarelli, J. A. (2019). Bioengineering a future free of marine plastic waste. *Frontiers in Marine Science*, 6, 624.
- Solvay. (2022). *CYANOX®*. Retrieved from <https://www.solvay.com/en/brands/cyanox>
- Solvay. (2022). *Cyanox®2246 Antioxidant*. Retrieved from <https://www.solvay.com/en/product/cyanox-2246-antioxidant>
- Solvay. (2022). *Cyanox®425 Antioxidant*. Retrieved from <https://www.solvay.com/en/product/cyanox-425>
- Taft, S., Oldford, G., Lilley, P.L., Oetterich, S.B., Morin, J., George, M., George, M., and Christensen, V. (2022). Reconstructing the pre-contact shoreline of Burrard Inlet (British Columbia, Canada) to quantify cumulative intertidal and subtidal area change from 1792 to 2020. Fisheries Centre Research Report 30(1) 48 pp.

- Talbot, R., & Chang, H. (2022). Microplastics in freshwater: a global review of factors affecting spatial and temporal variations. *Environmental Pollution*, 292, 118393.
- Teuten, E. L., Saquing, J. M., Knappe, D. R., Barlaz, M. A., Jonsson, S., Björn, A., Rowland, S. J., Thompson, R. C., Galloway, T. S., Yamashita, R., Ochi, D., Wantanuki, Y., Moore, C., Hung Viet, P., Seang Tana, T., Prudente, M., Boonyatumanond, R., Zaharia, M. P., Akkhavong, K., Ogata, Y., Hirai, H., Iwasa, S., Mizukawa, K., Hagino, Y., Imamura, A., Saha, M., & Takada, H. (2009). Transport and release of chemicals from plastics to the environment and to wildlife. *Philosophical Transactions of the Royal Society B: Biological Sciences*, 364(1526), 2027-2045. doi:10.1098/rstb.2008.0284
- Thompson, R. C. (2015). Microplastics in the Marine Environment: Sources, Consequences and Solutions. In: Bergmann M., Gutow L., Klages M. (Eds) *Marine Anthropogenic Litter*. Springer, Cham. Retrieved from https://doi.org/10.1007/978-3-319-16510-3_7
- Toader, G., Rotariu, T., Rusen, E., Tartiere, J., Esanu, S., Zecheru, T., Stancu, I., Serafim, A., & Pulpea, B. (2017). New solvent-free polyurea binder for plastic pyrotechnic compositions. *MAT. PLAS*, 54(1), 22-28.
- Truchet, D. M., López, A. F., Arduoso, M. G., Rimondino, G. N., Buzzi, N. S., Malanca, F. E., Spetter, C. V., & Severini, M. F. (2021). Microplastics in bivalves, water and sediments from a touristic sandy beach of Argentina. *Marine Pollution Bulletin*, 173, 113023.
- UNEP. (2018). Single-Use Plastics: A Roadmap for Sustainability. In United Nations Environment Programme; UNEP: Nairobi, Kenya,; p. 90. Available online: <https://www.unenvironment.org/resources/report/single-use-plastics-roadmap-sustainability>
- UNEP. (2021). From Pollution to Solution: A Global Assessment of Marine Litter and Plastic Pollution; UNEP: Nairobi, Kenya. Available online: <https://www.unep.org/resources/pollution-solution-global-assessment-marine-litter-and-plastic-pollution>
- United States Environmental Protection Agency. (2021). KABAM Version 1.0 User's Guide and Technical Documentation - Appendix F -Description of Equations Used to Calculate the BCF, BAF, BMF, and BSAF Values. Retrieved from United States Environmental Protection Agency website <https://www.epa.gov/pesticide-science-and-assessing-pesticide-risks/kabam-version-10-users-guide-and-technical-3#F1>

- United States Geological Survey. (2022). USGS The National Map: National Boundaries Dataset, 3DEP Elevation Program, Geographic Names Information System, National Hydrography Dataset, National Land Cover Database, National Structures Dataset, and National Transportation Dataset; USGS Global Ecosystems; U.S. Census Bureau TIGER/Line data; USFS Road Data; Natural Earth Data; U.S. Department of State Humanitarian Information Unit; and NOAA National Centers for Environmental Information, U.S. Coastal Relief Model.
- van Alphen, J., & van Turnhout, C. M. (1973). Rubber chemicals. Boston, MA: Dordrecht Reidel Publishing Company.
- van Franeker, J. A., & Meijboom, A. (2002). *Litter NSV; marine litter monitoring by northern fulmars (a pilot study)*. (Alterra-rapport; No. 401). Alterra. Retrieved from <https://edepot.wur.nl/45695>
- van Moos, N., Burkhardt-Holm, P., & Köhler, A. (2012). Uptake and Effects of Microplastics on Cells and Tissue of the Blue Mussel, *Mytilus edulis* L. after an Experimental Exposure. *Environmental Science & Technology*, *46*(20), 11327-11335. doi:10.1021/es302332w
- Wakkaf, T., El Zrelli, R., Kedzierski, M., Balti, R., Shaiek, M., Mansour, L., Tlig-Zouari, S., Bruzard, S., & Rabaoui, L. (2020). Microplastics in edible mussels from a southern Mediterranean lagoon: Preliminary results on seawater-mussel transfer and implications for environmental protection and seafood safety. *Marine Pollution Bulletin*, *158*, 111355.
- Wang, L., Stephen, A. R., Boothe, P. W., Schulze, T., Giardello, M. A., Trimmer, M. S., Cruce, C. J., Motamedi, F. J., & Edgecombe, B. (2019). *U.S. Patent No. 10,457,597*. Washington, DC: U.S. Patent and Trademark Office.
- Wang, R., Mou, H., Lin, X., Zhu, H., Li, B., Jiangyong, W., Junaid, M., & Wang, J. (2021). Microplastics in Mollusks: Research Progress, Current Contamination Status, Analysis Approaches, and Future Perspectives. *Frontiers in Marine Science*, 1671.
- Watts, A. J., Lewis, C., Goodhead, R. M., Beckett, S. J., Moger, J., Tyler, C. R., & Galloway, T. S. (2014). Uptake and Retention of Microplastics by the Shore Crab *Carcinus maenas*. *Environmental Science & Technology*, *48*(15), 8823-8830. doi:10.1021/es501090e
- Wiley, J. (2021). *CYANOX 53*. Retrieved from <https://spectrabase.com/spectrum/D4wMn8dQ8OL>.
- World Weather & Climate Information. (2022). Average weather May in Vancouver (British Columbia), Canada. Retrieved from <https://weather-and-climate.com/vancouver-May-averages>

- World Weather & Climate Information. (2022). Average weather in June in Vancouver (British Columbia), Canada. Retrieved from <https://weather-and-climate.com/vancouver-June-averages>
- Wright, S. L., Rowe, D., Thompson, R. C., & Galloway, T. S. (2013b). Microplastic ingestion decreases energy reserves in marine worms. *Current Biology*, *23*(23), R1031–R1033.
- Wright, S., Ulke, J., Font, A., Chan, K., & Kelly, F. (2020). Atmospheric microplastic deposition in an urban environment and an evaluation of transport. *Environment International*, *136*, 105411. doi:10.1016/j.envint.2019.105411
- Wypych, A., & Wypych, G. (2020). *Databook of Antioxidants*. Elsevier.
- Young, R. (2021, June 22). Canada's plastic problem: Sorting fact from fiction. Retrieved from <https://oceana.ca/en/blog/canadas-plastic-problem-sorting-fact-fiction/>
- Zhang, Y., Gao, T., Kang, S., & Sillanpää, M. (2019). Importance of atmospheric transport for microplastics deposited in remote areas. *Environmental Pollution*, *254*, 112953. doi:10.1016/j.envpol.2019.07.121
- Zhou, L., Fan, D., Yin, W., Gu, W., Wang, Z., Liu, J., Xu, Y., Shi, L., Liu, M., & Ji, G. (2021). Comparison of seven *in silico* tools for evaluating of daphnia and fish acute toxicity: case study on Chinese Priority Controlled Chemicals and new chemicals. *BMC Bioinformatics*, *22*(1), 1-31.

Appendix A

Sediment Analysis Data

Table A-1. Mean particle concentrations and standard error of microplastics and Cyanox®53 in sediment sampled from seven intertidal sites in Burrard Inlet.

| Site | Microplastics (particles/kg dw) | Cyanox®53 (particles/kg dw) |
|------|---------------------------------|-----------------------------|
| AP | 9.00 ± 4.73 | 1.67 ± 0.882 |
| BMP | 10.3 ± 2.19 | 1.00 ± 1.00 |
| CP | 9.00 ± 1.73 | 0.00 ± 0.00 |
| EB | 15.7 ± 0.33 | 1.67 ± 1.67 |
| J | 6.67 ± 1.33 | 0.00 ± 0.00 |
| SB | 14.7 ± 2.85 | 0.333 ± 0.00 |
| TB | 14.7 ± 1.45 | 0.00 ± 0.00 |

Table A-2. Mean particle concentrations and standard error of micro-spheres, micro-fragments, micro-fibers, and micro-films in sediment sampled from seven intertidal sites in Burrard Inlet.

| Site | Micro-spheres (particles/kg dw) | Micro-fragments (particles/kg dw) | Micro-fibers (particles/kg dw) | Micro-films (particles/kg dw) |
|------|---------------------------------|-----------------------------------|--------------------------------|-------------------------------|
| AP | 1.00 ± 1.00 | 3.33 ± 2.85 | 2.00 ± 1.15 | 2.67 ± 0.67 |
| BMP | 3.00 ± 1.41 | 5.00 ± 3.06 | 1.67 ± 0.88 | 0.67 ± 0.67 |
| CP | 0.00 ± 0.00 | 6.67 ± 1.45 | 1.67 ± 0.33 | 0.67 ± 0.67 |
| EB | 1.00 ± 1.00 | 10.33 ± 1.33 | 2.00 ± 0.00 | 2.33 ± 0.88 |
| J | 1.00 ± 1.00 | 3.00 ± 1.73 | 1.33 ± 0.67 | 1.33 ± 0.67 |
| SB | 3.00 ± 1.73 | 10.33 ± 0.88 | 1.00 ± 1.00 | 0.33 ± 0.33 |
| TB | 2.00 ± 1.00 | 9.00 ± 1.00 | 1.33 ± 0.67 | 2.33 ± 0.88 |

Appendix B

Bivalve Analysis Data

Table B-1. Tests of normality showing Shapiro Wilk's test value and p-values for wet tissue weight, and shell width, length, height and volume of bivalves sampled from seven sites regions in Burrard Inlet.

| Site | Wet Tissue Weight (g) | Width (cm) | Length (cm) | Height (cm) | Shell Volume (cm ³) |
|------|-------------------------|-------------------------|-------------------------|-------------------------|---------------------------------|
| AP | W = 0.964, p = 0.498 | W = 0.969, p = 0.622 | W = 0.963, p = 0.467 | W = 0.959, p = 0.351 | W = 0.953, p = 0.296 |
| BMP | W = 0.970, p = 0.639 | W = 0.987, p = 0.979 | W = 0.977, p = 0.821 | W = 0.944, p = 0.181 | W = 0.968, p = 0.604 |
| CP | W = 0.960, p = 0.405 | W = 0.951, p = 0.271 | W = 0.944, p = 0.182 | W = 0.934, p = 0.106 | W = 0.923, p = 0.061 |
| EB | W = 0.931, p = 0.092 | W = 0.964, p = 0.489 | W = 0.960, p = 0.412 | W = 0.969, p = 0.624 | W = 0.972, p = 0.687 |
| J | W = 0.971, p = 0.668 | W = 0.960, p = 0.411 | W = 0.955, p = 0.330 | W = 0.959, p = 0.389 | W = 0.965, p = 0.528 |
| SB | W = 0.936, p = 0.118 | W = 0.954, p = 0.307 | W = 0.953, p = 0.297 | W = 0.952, p = 0.285 | W = 0.920, p = 0.052 |
| TB | W = 0.972, p = 0.709 | W = 0.976, p = 0.787 | W = 0.985, p = 0.968 | W = 0.957, p = 0.368 | W = 0.956, p = 0.346 |

Table B-2. Mean and standard error of wet tissue weight, shell width, length, height and volume, and related condition indices of bivalves sampled from seven intertidal sites in Burrard Inlet.

| Site | Tissue Wet Weight (g) | Width (cm) | Length (cm) | Height (cm) | Shell Volume (cm ³) | Condition Index (g/cm ³ %) |
|------|-----------------------|--------------|--------------|--------------|---------------------------------|---------------------------------------|
| AP | 10.9 ± 0.89 | 1.86 ± 0.071 | 4.83 ± 0.13 | 4.07 ± 0.12 | 387 ± 31 | 2.87 ± 0.16 |
| BMP | 10.1 ± 0.35 | 1.84 ± 0.028 | 4.84 ± 0.060 | 3.92 ± 0.040 | 352 ± 12 | 2.88 ± 0.041 |
| CP | 6.39 ± 0.24 | 1.44 ± 0.019 | 4.23 ± 0.039 | 3.41 ± 0.039 | 209 ± 6.4 | 3.05 ± 0.036 |
| EB | 13.4 ± 0.60 | 2.08 ± 0.039 | 5.43 ± 0.081 | 4.41 ± 0.078 | 507 ± 23 | 2.66 ± 0.048 |
| J | 10.4 ± 0.56 | 1.81 ± 0.050 | 4.97 ± 0.087 | 3.77 ± 0.068 | 348 ± 20 | 2.99 ± 0.035 |
| SB | 6.64 ± 0.24 | 1.56 ± 0.026 | 4.18 ± 0.052 | 3.26 ± 0.038 | 214 ± 7.8 | 3.19 ± 0.18 |
| TB | 6.81 ± 0.23 | 1.54 ± 0.027 | 4.51 ± 0.050 | 3.45 ± 0.043 | 242 ± 8.7 | 2.82 ± 0.041 |

Table B-3. Mean particle concentration and standard error, and frequency of microplastics recovered in bivalves sampled at the seven intertidal sites in Burrard Inlet.

| Site | n | Individuals with Microplastics | Total Microplastics Recovered | Mean Microplastic Concentration (particles/g ww) | Bivalves with Microplastics (%) |
|------|----|--------------------------------|-------------------------------|--|---------------------------------|
| AP | 25 | 25 | 168 | 0.80 ± 0.21 | 100 |
| BMP | 25 | 22 | 64 | 0.24 ± 0.040 | 88 |
| CP | 25 | 24 | 49 | 0.32 ± 0.044 | 96 |
| EB | 25 | 20 | 66 | 0.19 ± 0.040 | 80 |
| J | 25 | 22 | 48 | 0.20 ± 0.023 | 88 |
| SB | 25 | 23 | 65 | 0.41 ± 0.058 | 92 |
| TB | 25 | 25 | 88 | 0.51 ± 0.085 | 100 |

Table B-4. Mean and standard error of micro-spheres, micro-fragments, micro-fibers, and micro-films in bivalves sampled at the seven intertidal sites in Burrard Inlet.

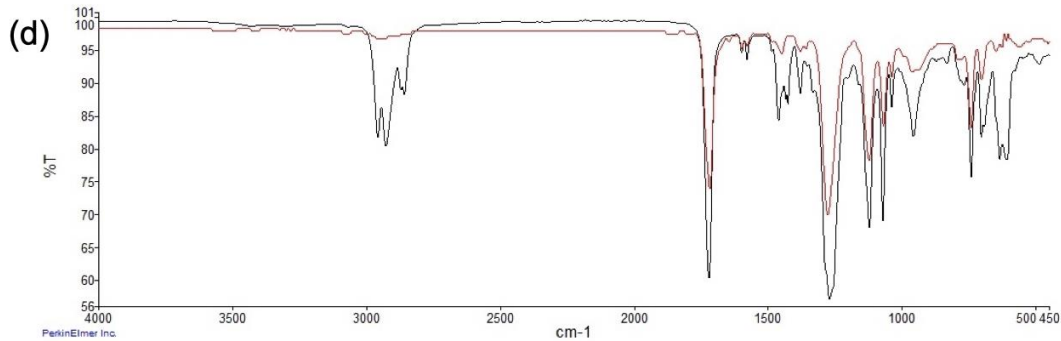
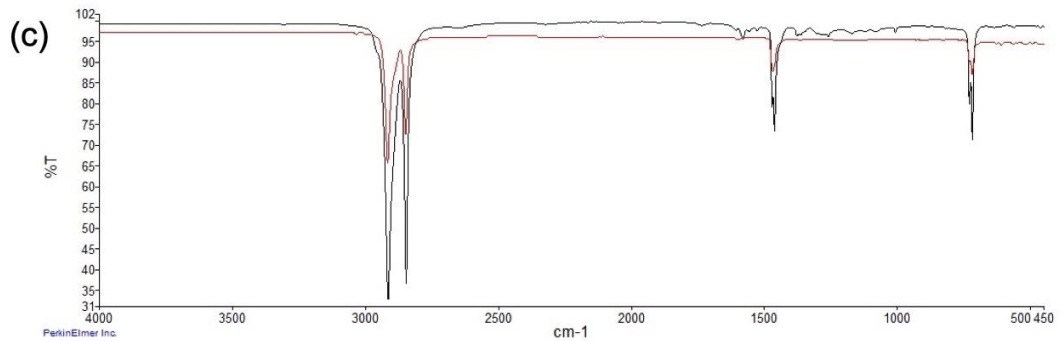
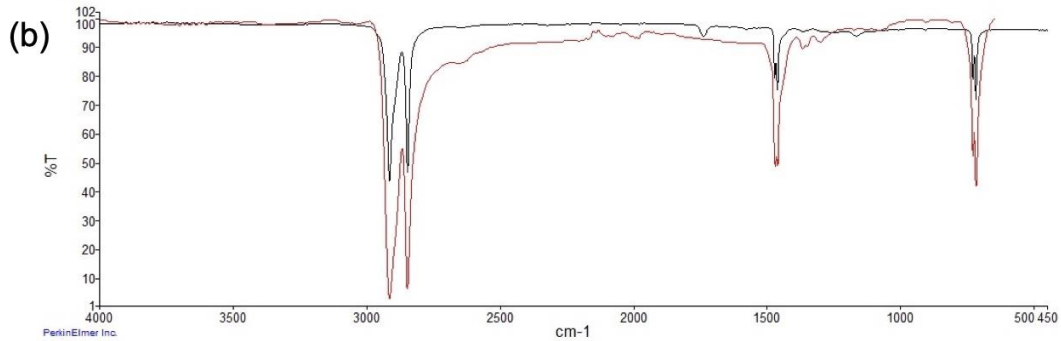
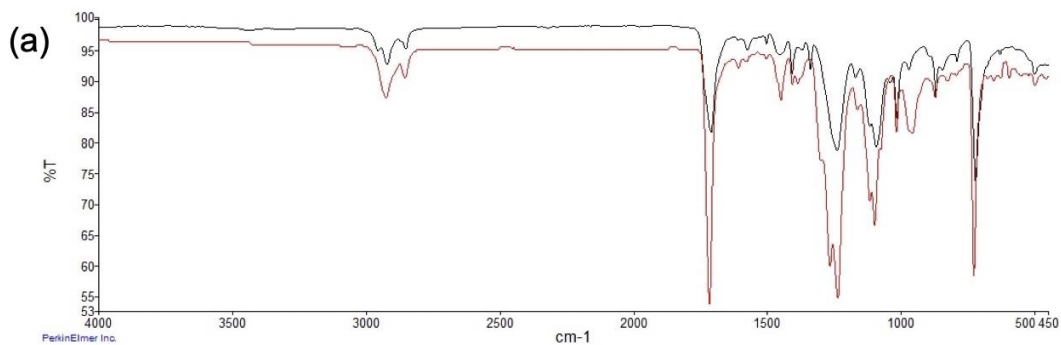
| Site | Micro-spheres (particle/g ww) | Micro-fragments (particles/g ww) | Micro-fibers (particles/g ww) | Micro-films (particles/g ww) |
|------|----------------------------------|-------------------------------------|----------------------------------|---------------------------------|
| AP | 0.013 ± 0.0070 | 0.65 ± 0.22 | 0.053 ± 0.015 | 0.086 ± 0.017 |
| BMP | 0.0087 ± 0.0061 | 0.20 ± 0.039 | 0.039 ± 0.014 | 0.061 ± 0.010 |
| CP | 0.0068 ± 0.0068 | 0.088 ± 0.027 | 0.075 ± 0.018 | 0.15 ± 0.021 |
| EB | 0.019 ± 0.0083 | 0.12 ± 0.034 | 0.015 ± 0.0072 | 0.037 ± 0.0090 |
| J | 0.022 ± 0.011 | 0.032 ± 0.015 | 0.049 ± 0.012 | 0.094 ± 0.013 |
| SB | 0.015 ± 0.010 | 0.10 ± 0.046 | 0.15 ± 0.037 | 0.14 ± 0.025 |
| TB | 0.046 ± 0.019 | 0.20 ± 0.077 | 0.087 ± 0.025 | 0.18 ± 0.015 |

Table B-5. Mean particle concentration and standard error, and frequency of Cyanox®53 recovered in bivalves sampled at the seven intertidal sites in Burrard Inlet.

| Site | n | Individuals with Cyanox®53 | Total Cyanox®53 Recovered | Mean Cyanox®53 Concentration (particles/g ww) | Bivalves with Cyanox®53 (%) |
|------|----|----------------------------------|---------------------------------|---|-----------------------------------|
| AP | 25 | 6 | 29 | 0.25 ± 0.21 | 24 |
| BMP | 25 | 1 | 1 | 0.0048 ± 0.0048 | 4 |
| CP | 25 | 0 | 0 | 0.00 ± 0.00 | 0 |
| EB | 25 | 11 | 44 | 0.13 ± 0.044 | 44 |
| J | 25 | 0 | 0 | 0.00 ± 0.00 | 0 |
| SB | 25 | 2 | 4 | 0.026 ± 0.018 | 8 |
| TB | 25 | 0 | 0 | 0.00 ± 0.00 | 0 |

Appendix C

Reference Spectra for Comparison



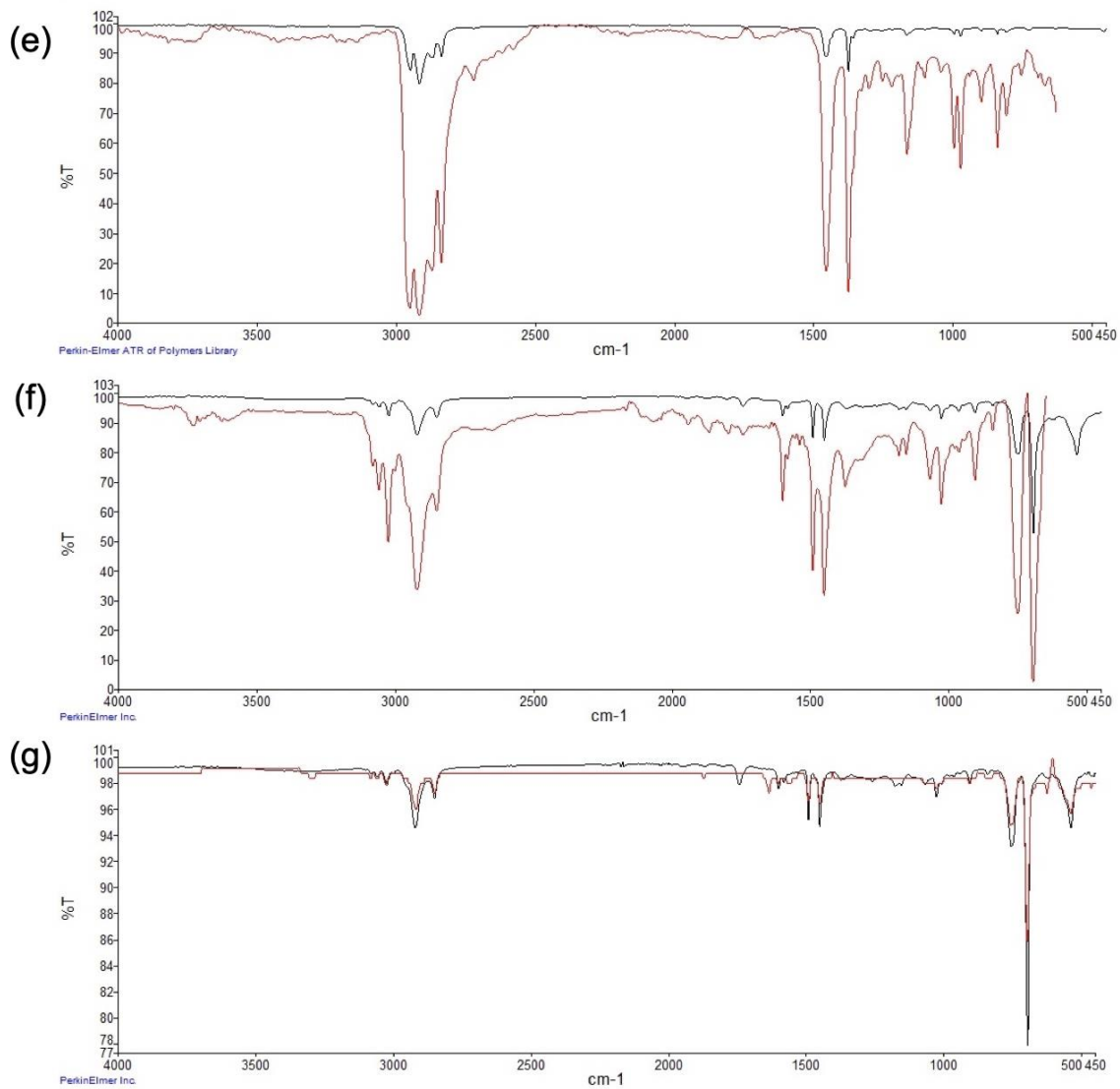


Figure C-1. Reference ATR-FTIR spectra of seven common polymers. (a) PETE, (b) HDPE, (c) LDPE, (d) PVC, (e) PP, (f) PS, and (g) XPS - Styrofoam™.

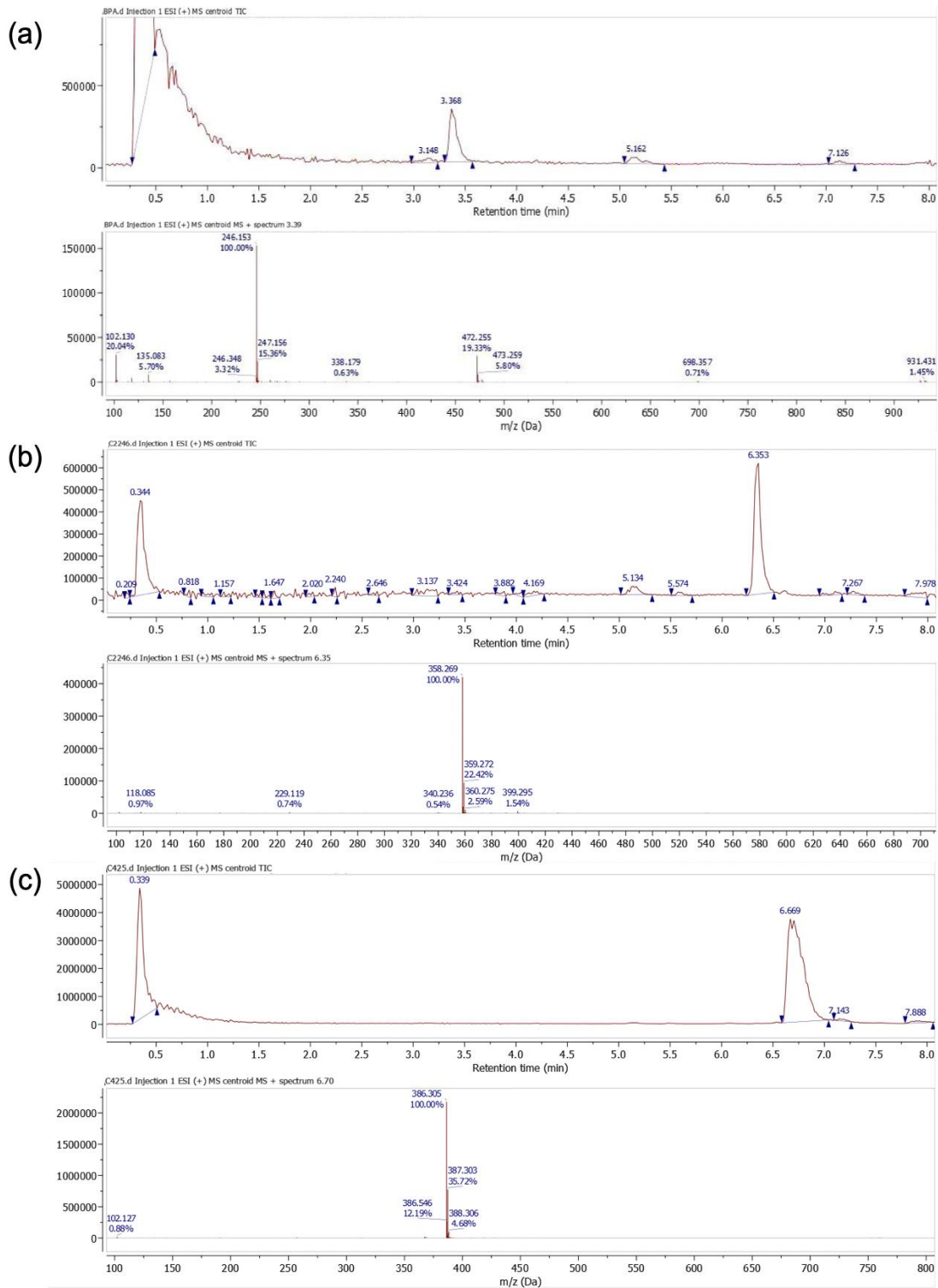


Figure C-2. ESI-LC/MS spectra of reference chemicals (a) BPA, (b) Cyanox®2246, and (c) Cyanox®425.

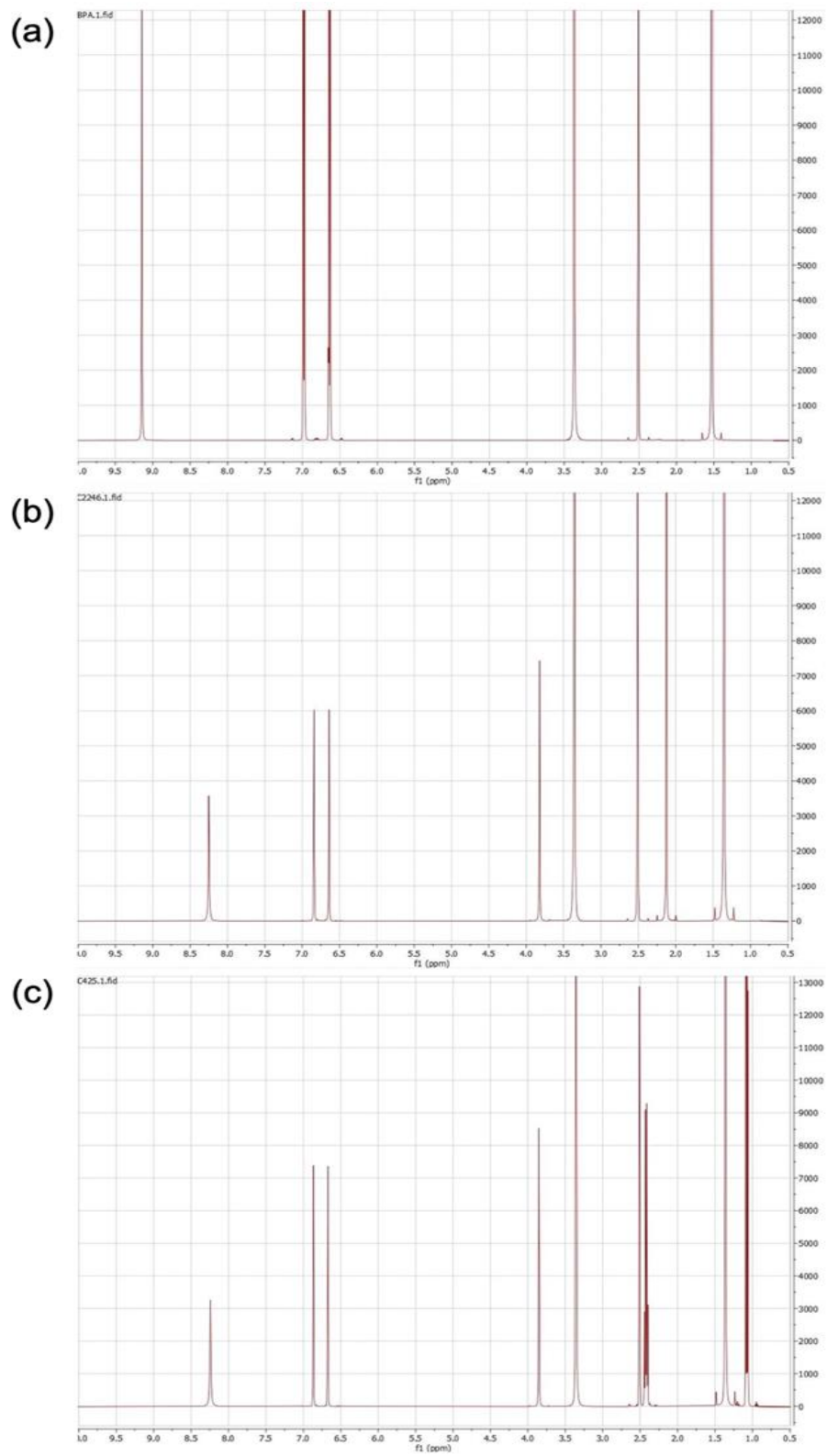


Figure C-3. ¹H-NMR spectra of reference chemicals (a) BPA, (b) Cyanox®2246, and (c) Cyanox®425.